Cerebral Blood Flow and Cerebrovascular Reactivity Measurement using Arterial Spin Labeling Magnetic Resonance Imaging: Data from The Irish Longitudinal Study on Ageing

A thesis submitted to Trinity College Dublin, The University of Dublin

for the degree of M.D. in Clinical Medicine

by Dr. Caoilfhionn Ní Leidhin MB BCh BAO MRCS FFRRCSI

under the supervision of Professor J.F. Meaney

Centre for Advanced Medical Imaging,
St. James's Hospital,
James's Street,
Dublin 8

January 2022

DECLARATION

I declare that this thesis has not been submitted as an exercise for a degree at this or any other university and that it is entirely my own work.

I agree to deposit this thesis in the university's open access institutional repository or allow the library to do so on my behalf, subject to Irish Copyright Legislation and Trinity College Library conditions of use and acknowledgement.

Signed: 

Student Number: 16332819

Date: 31/01/2022

ACKNOWLEDGEMENTS

I would like to sincerely thank the following people who contributed to this work:

Professor James Meaney for affording me the opportunity to undertake this research and for his invaluable mentorship over the past number of years.

Professor Rose Anne Kenny, for her unstinting determination and constructive feedback.

Dr. Jason McMorrow, for his unfailing belief, encouragement and support and for his help and expertise with data analysis.

Dr. Silvin Knight, for his invaluable mentorship and guidance and for technical support.

Dr. Michael Chappell, for his technical expertise and ready availability.

Professor Andrew Fagan, for technical support.

Dr. Daniel Carey, Louise Newman, Dr. Hugh Nolan, Dr. Wilby Williamson and all of the TILDA research team for their direction and advice.

The staff in the Centre for Advanced Medical Imaging (CAMI), in particular Alison Toomey, for its professionalism and dedication in facilitating this research.

All of the TILDA participants for their continued commitment and co-operation.

The Health Research Board for funding this project, The Irish Government, Atlantic Philanthropies and Irish Life PLC for funding TILDA.

DEDICATION

I dedicate this thesis to my husband, Sumanth,

our daughter, Ciara,

my parents, Damhnait and Seán

and my siblings, Aisling, Barra and Muireann.

COMMUNICATIONS ARISING FROM THIS WORK

Peer-Reviewed Original Research Publication

Ní Leidhin C, McMorrow J, Carey D, Newman L, Williamson W, Fagan AJ, Chappell MA, Kenny RA, Meaney JF, Knight SP.
Age-related normative changes in cerebral perfusion: data from The Irish Longitudinal Study on Ageing (TILDA).
Neuroimage, 2021 Apr 1;229:117741. PMID: 33454406.

Maasakkers CM, Thissen DHJ, Knight SP, Newman L, O'Connor JD, Scarlett S, Carey D, Buckley A, McMorrow JP, Ní Leidhin C, Feeney J, Melis RJF, Kenny RA, Claassen JAHR, De Looze C.
Hemodynamic and structural brain measures in high and low sedentary older adults.
Journal of Cerebral Blood Flow and Metabolism, 2021 Apr 17;271678X21100938. PMID: 33866848.

Oral Presentations

International

Ní Leidhin C, McMorrow J, Murphy K, Fagan AJ, Nolan H, Toomey A, Byrne J, Kenny RA, Meaney JF.
Measuring cerebral blood flow and cerebrovascular reactivity using arterial spin labeling MRI in neurologically asymptomatic, community dwelling subjects, aged 50 years and older.
Radiological Society of North America's Annual Meeting, Chicago, 27-11-2016 to 02-12-2016.

Ní Leidhin C, McMorrow J, Murphy K, Fagan AJ, Nolan H, Toomey A, Byrne J, Kenny RA, Meaney JF.
The use of arterial spin labeling MRI to measure cerebral blood flow and cerebrovascular reactivity in neurologically asymptomatic subjects aged 50 years and older.
Vas-Cog Congress, Amsterdam, 13-10-2016 to 15-10-2016.

National

Ní Leidhin C, McMorrow J, Murphy K, Fagan AJ, Nolan H, Toomey A, Byrne J, Kenny RA, Meaney JF.

The use of arterial spin labeling MRI to measure cerebral blood flow and cerebrovascular reactivity in neurologically asymptomatic subjects aged 50 years and older.

Faculty of Radiologists' Annual Scientific Meeting, Dublin, 22-09-2016 to 24-09-2016.

Poster Presentation

International

Ní Leidhin C, McMorrow J, Chappell M, Fagan AJ, Nolan H, Carey D, Kenny RA, Meaney JF.

Quantifying cerebral blood flow using arterial spin labeling MRI and assessing the effects of age, gender and cardiovascular risk factors on cerebral blood flow. European Congress of Radiology, Vienna, 28-02-2018 to 04-03-2018.

ABBREVIATIONS

ACA	Anterior cerebral artery
AFNI	Analysis of functional neuroimages
AlzD	Alzheimer's disease
ARB	Angiotensin receptor blocker
ASL	Arterial spin labeling
ATT	Arterial transit time
BASIL	Bayesian inference for arterial spin labeling
BBB	Blood brain barrier
BMI	Body mass index
BOLD	Blood oxygen level dependent
BP	Blood pressure
CAMI	Centre for advanced medical imaging
CAPI	Computer-assisted personal interview
cASL	Continuous arterial spin labeling
CBF	Cerebral blood flow
CBF_{GM}	Grey matter cerebral blood flow
CBV	Cerebral blood volume
CESD	Center for epidemiologic studies depression scale
CI	Cognitive impairment
CI	Confidence interval
$CMRO_2$	Cerebral metabolic rate of oxygen
CO_2	Carbon dioxide
CSF	Cerebrospinal fluid
CT	Computed tomography
CVA	Cerebrovascular accident/stroke
CVR	Cerebrovascular reactivity
CVR_{GM}	Grey matter cerebrovascular reactivity
DBP	Diastolic blood pressure
DCE	Dynamic contrast-enhanced
DM	Diabetes mellitus
DPCT	Dynamic perfusion computed tomography
DSC	Dynamic susceptibility contrast
DTI	Diffusion tensor imaging
DWI	Diffusion weighted imaging
EPI	Echo-planar imaging

$EtCO_2$	End-tidal carbon dioxide
FA	Flip angle
FDG-PET	Fluorodeoxyglucose-positron emission tomography
FLAIR	Fluid attenuated inversion recovery
FMRIB	Functional magnetic resonance imaging of the brain
FOV	Field of view
FSL	FMRIB software library
GAMLSS	Generalized additive models for location shape and scale
GM	Grey matter
GUI	Graphical user interface
Hb	Haemoglobin
HTN	Hypertension
ICA	Internal carotid artery
IQR	Interquartile range
ISMRM	International society for magnetic resonance in medicine
IV	Intravenous
M0	Equilibrium magnetization
M0a	Equilibrium magnetization of arterial blood
MAP	Mean arterial blood pressure
MCA	Middle cerebral artery
MCI	Mild cognitive impairment
MMSE	Mini-mental state examination
MNI	Montreal neurological institute
MPRAGE	Magnetization-prepared rapid gradient echo
MRI	Magnetic resonance imaging
MTT	Mean transit time
NO	Nitric oxide
OEF	Oxygen extraction fraction
$PaCO_2$	Partial pressure of arterial carbon dioxide
pASL	Pulsed arterial spin labeling
PC	Phase contrast
PCA	Posterior cerebral artery
pcASL	Pseudocontinuous arterial spin labeling
PET	Positron emission tomography
PLD	Post labeling delay
PWV	Pulse wave velocity
RF	Radiofrequency

SBP	Systolic blood pressure
SENSE	Sensitivity encoding
SI	Signal intensity
SNR	Signal to noise ratio
SPECT	Single photon emission computed tomography
T	Tesla
T1W(I)	T1 weighted (image/imaging)
T2W(I)	T2 weighted (image/imaging)
T2DM	Type 2 diabetes mellitus
TCD	Transcranial Doppler
TE	Echo time
TIA	Transient ischaemic attack
TILDA	The Irish longitudinal study on ageing
TSE	Turbo spin echo
TR	Repetition time
US	Ultrasound
USA	United States of America
VaD	Vascular dementia
WM	White matter
WMH	White mater hyperintensities
Xe	Xenon

TABLE OF CONTENTS

LIST OF FIGURES

LIST OF TABLES

CHAPTER 1: INTRODUCTION

1.1 Neuroanatomy

1.1.1 Brain anatomy

The central nervous system - both the brain and spinal cord, are composed of grey and white matter. The main components of the grey matter (GM) are neuronal cell bodies, dendrites and glia. Dendrites are short processes extending from the cell body that collect information from adjacent neurons and transmit them to the nucleus. The cell body, which contains the nucleus and nucleolus, processes that information. Axons, some of which have a fatty/white conductive myelin sheath, are contained within the white matter (WM). Axons conduct nerve impulses from the cell body to other neurons, muscles and glands, via neurotransmitters at synapses. Glia are cells that provide support to neurons and aid in information processing.[1, 2] *See figure 1.*

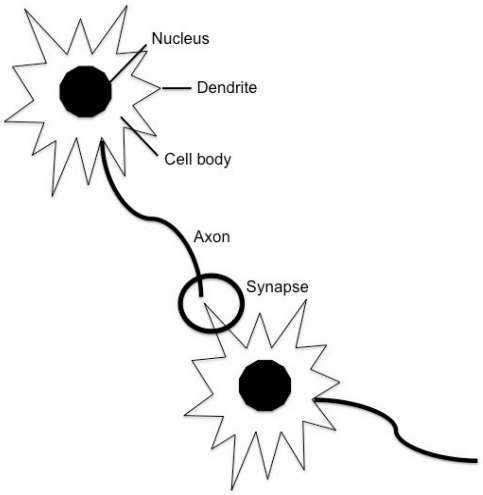

Figure 1 illustrates neuronal anatomy. Signals are transmitted within neurons from the dendrites and cell body to the axonal terminals. Electrochemical signals are transmitted between axonal terminals and receiving cells via synapses.

The cerebral and cerebellar hemispheres consist of an outer cortex of grey matter and an inner mass of white matter, in which other deep grey matter structures i.e. the basal ganglia and thalamus are embedded. Grey matter is rich in neuronal cell bodies. White matter consists of compact bundles of myelinated nerve fibres/axons, which form connections between different brain regions.

The cerebral cortex is the most highly evolved part of the brain, involved in the control of movement, sensation and higher mental functions i.e. language, memory and emotions.[3, 4] *See figures 2 & 3.*

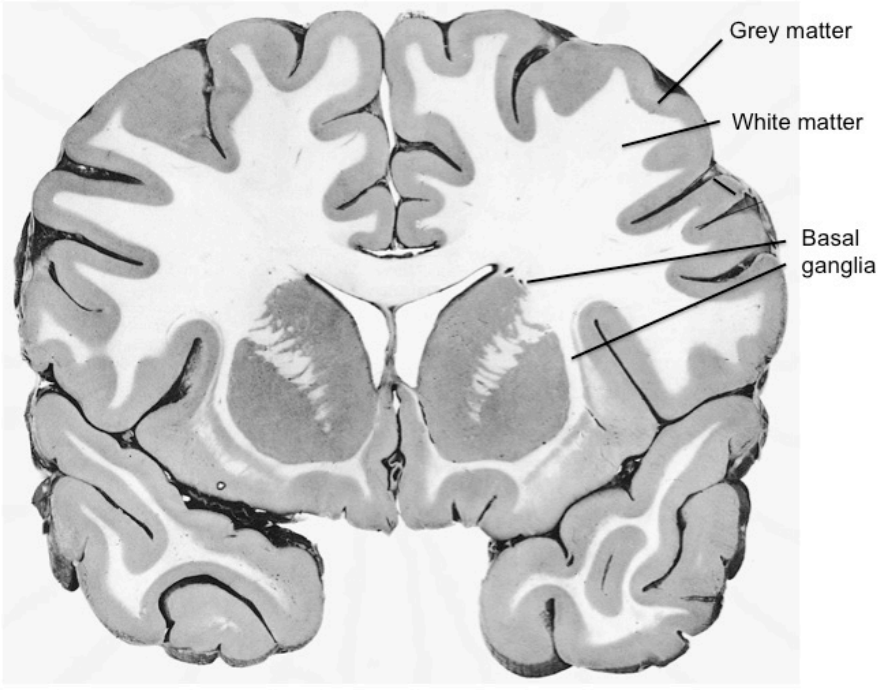

Figure 2: Cross-section image of the brain illustrates cerebral grey and white matter. (From: Roberts MP, Hanaway J, Morest DK. Atlas of the Human Brain in Section, 2nd ed.).

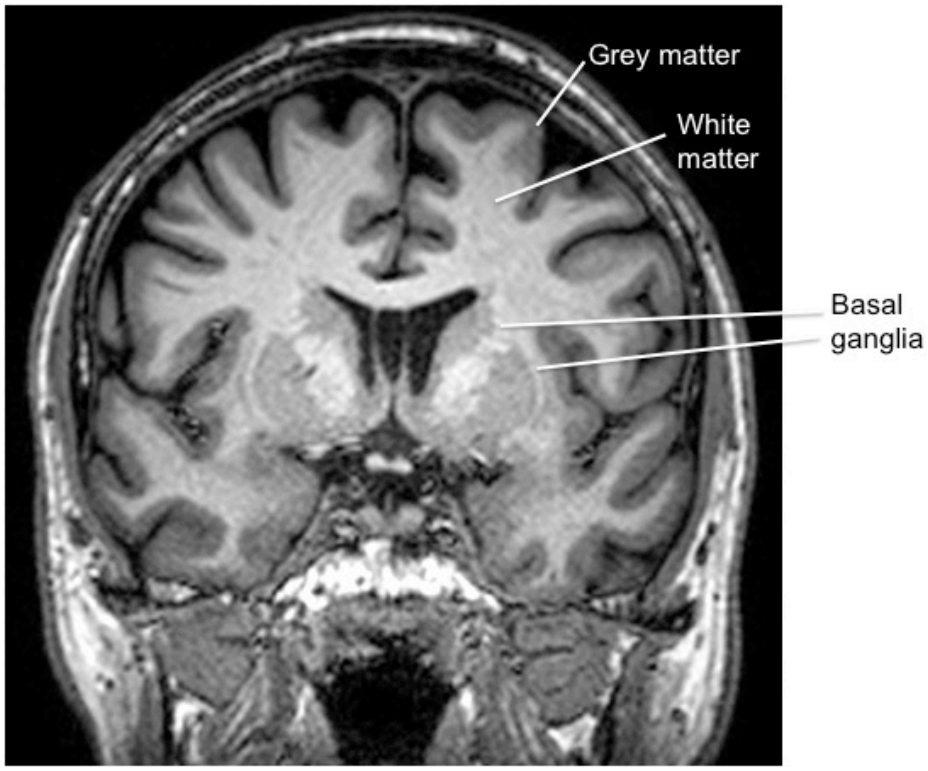

Figure 3: 3D T1 weighted Magnetic Resonance Image (MRI) of the brain illustrates cerebral grey and white matter.

1.1.2 Cerebrovascular anatomy

The cerebrovasculature is comprised of arteries and arterioles, which deliver blood to the brain, the capillary bed, which is involved in gas and nutrient exchange and venules and veins, which drain blood from the brain. *See figure 4.*

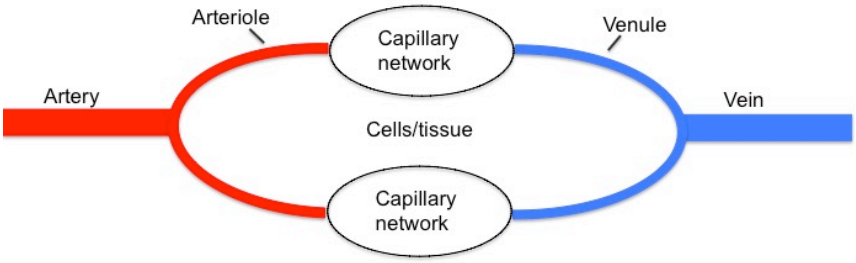

Figure 4 illustrates the anatomy of the cerebrovasculature.

The major arterial supply to the brain is from paired internal carotid and vertebral arteries, which contribute about 80% and 20% to cerebral blood flow (CBF) respectively.[5] The internal carotid arteries (ICA) supply bilateral anterior (ACA) and middle cerebral arteries (MCA), which perfuse the anterior cerebral hemispheres. The vertebral arteries anastomose to form a single basilar artery, which terminates in two posterior cerebral arteries (PCA). The PCAs perfuse the posterior cerebral hemispheres, the cerebellum, brainstem and spinal cord.

The circle of Willis is an arterial anastomotic ring, which allows for collateralization of blood flow between the anterior and posterior circulations and the right and left cerebral hemispheres. In theory, it is formed by the anterior communicating artery, bilateral proximal ACAs, distal ICAs, posterior communicating arteries, proximal PCAs and the basilar tip.[6] *See figure 5.* However, variations in circle of Willis anatomy are extremely common. Indeed, a complete/"textbook" circle of Willis is seen in only 11.9%, with a least one missing segment in the remaining 88.1%. The most common anatomic variant is absent bilateral posterior communicating arteries.[7]

As well as allowing collateralization of blood flow, the circle of Willis dampens pulsatile, high velocity blood flow from the cervical arteries to protect the sensitive neural tissue and blood brain barrier.[8]

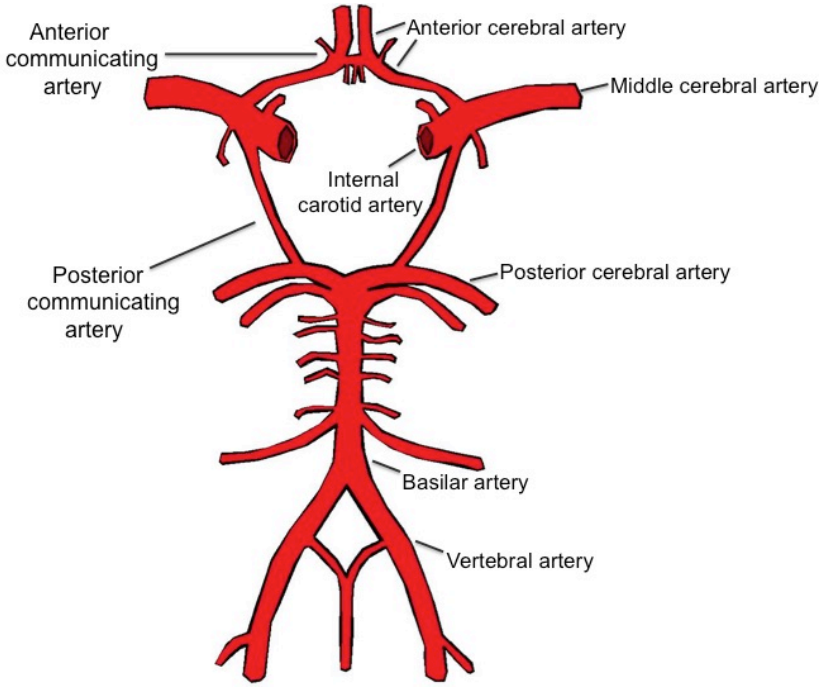

Figure 5 illustrates the anatomy of the circle of Willis.

The three paired major intracranial arteries (i.e. ACA/MCA/PCAs) divide into pial arteries and arterioles on the brain surface before penetrating the brain tissue and continuing as parenchymal arterioles. There is extensive collateralization between cortical vessels, however penetrating and parenchymal arterioles are long and non-branching, thus occlusion of one of these vessels can result in distal hypoperfusion/infarction.[9]

Structurally, the cerebral arteries and arterioles are comprised of three concentric layers – an inner tunica intima consisting of endothelial cells, an intermediate tunica media, comprising smooth muscle cells and an outer collagen layer known as the tunica adventitia.[9] *See figure 6.* The number of smooth muscle cell layers within the vessel wall decreases in accordance with vessel size.[9]

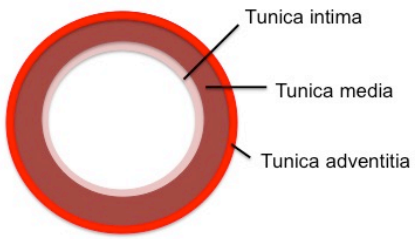

Figure 6 illustrates the anatomy of the cerebral arteries and arterioles.

The parenchymal arterioles give rise to capillaries. The capillary endothelial cells are separated from the end-feet of adjacent astrocytes by a basement membrane. It is the capillary endothelial cells and astrocytes, along with pericytes and adjacent neurons that make up the neurovascular unit, which plays a key role in coupling neuronal activity and blood flow.[9-11] *See figure 7.*

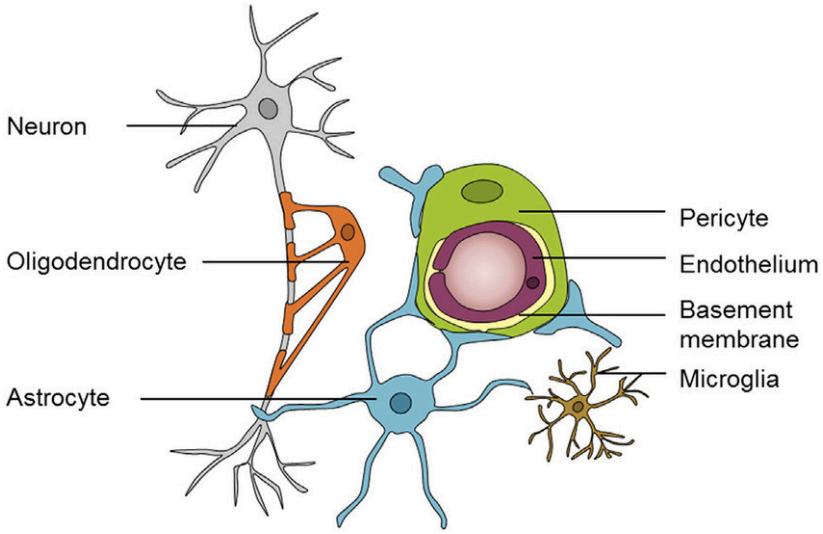

Figure 7 illustrates the anatomy of the neurovascular unit at the level of the brain capillary. (From: Nelson AR, Sweeney MD, Sagare AP, Zlokovic BV. Neurovascular dysfunction and neurodegeneration in dementia and Alzheimer's disease. Biochim Biophys Acta. 2016 May;1862(5):887-900).

Capillary endothelial cells are firmly bound to one another by highly specialized tight junctions, which help comprise the blood brain barrier (BBB) and ensure strict regulation of brain homeostasis.[9-11] Pericytes also play a role in maintaining and modulating the BBB.[12]

Post-capillary venules drain blood from the capillaries into the superficial and deep cerebral venous systems and ultimately into systemic veins.[13]

1.2 Cerebral blood flow

The brain comprises about 2% of total adult body weight yet cerebral blood flow (CBF) and cerebral oxygen consumption account for around 15% and 20% of resting cardiac output and total body oxygen consumption respectively.[14] The high metabolic rate of the brain, along with it's limited capacity for substrate storage and anaerobic metabolism,[15] mean that irreversible cellular injury can occur after as brief

as a 5 minute interruption in CBF.[16] CBF must therefore be tightly regulated to ensure both adequate delivery of oxygen and substrates to the brain and adequate removal of waste products. This occurs via several integrated regulatory mechanisms, as outlined below.

CBF is defined as the volume of blood per unit mass of brain tissue per unit time i.e. ml blood/100g brain tissue/minute. It is determined by the Hagen–Poiseuille equation:

$$Q = \frac{\pi R^4 \Delta P}{8 \eta L}$$

where Q is CBF, R is vessel radius, ΔP is cerebral perfusion pressure (the difference between systemic mean arterial blood pressure and intracranial pressure), η is blood viscosity and L is vessel length.

Vessel radius is very important in the regulation of CBF as evidenced by the fourth power in the equation. There are several factors, which affect the diameter and hence the resistance of cerebral arteries and arterioles - one of the most important is the partial pressure of arterial carbon dioxide ($PaCO_2$). Hypercapnia (i.e. elevated blood carbon dioxide (CO_2) levels) and hypoxia (i.e. decreased blood oxygen levels) result in vascular smooth muscle relaxation, vasodilatation and increased CBF, whereas hypocapnia (i.e. decreased blood CO_2 levels) has the opposite effect on the cerebrovasculature.[15]

Cerebral perfusion pressure (CPP) drives CBF according to the equation:
CPP = Mean arterial blood pressure – intracranial pressure,
where systemic mean arterial blood pressure (MAP) is the average of systolic (SBP) and diastolic blood pressures (DBP) and intracranial pressure is the pressure of the cerebrospinal fluid (CSF) in the subarachnoid space.[15, 17]

Cerebral autoregulation describes the process through which changes in blood pressure (BP) result in reflex adjustments in cerebrovascular resistance to ensure constant CBF.

Modulations in the radius and hence the resistance of small arteries/arterioles in response to BP occur via several integrated processes, including myogenic,

metabolic and neurogenic mechanisms. Of these, the myogenic mechanism, whereby vascular smooth muscle reacts to transmural pressure changes, is likely the most important.[17]

In the setting of low or falling BP, blood vessels dilate, cerebrovascular resistance decreases and there is resultant increase in CBF. The opposite happens with rising BP, thus maintaining constant CBF over a range of blood pressures.

Previously, it was believed that total CBF stability was ensured across a wide range of cerebral perfusion pressure (CPP) from ~60-150 mmHg,[18] however more recent literature suggests an imperfect autoregulatory capacity, which is dependent on both the severity and direction of perfusion pressure change.[15]

Blood viscosity is primarily determined by haematocrit i.e. the concentration of red cells in the blood. Lower haematocrit decreases blood viscosity, thus increasing CBF.[17]

Cerebral perfusion and neuronal activity are closely linked via neurovascular coupling. This is a process where modifications in CBF are dependent on interactions between the components of the neurovascular unit (*described in section 1.1.2*) i.e. the cerebral microvasculature, glia and neurons. Neuronal activation and/or increased metabolism result in transient increases in regional CBF through vasoactive mediators, including ions, metabolic by-products, neurotransmitters and nitric oxide (NO).[1, 17]

These rigorous regulatory mechanisms ensure, that in normal/physiological circumstances, CBF is sufficient to meet cerebral oxygen demand. If any of these regulatory mechanisms are comprised, there is the risk of cerebrovascular insufficiency, be that cerebral hypoperfusion, ischaemia or infarction.

1.3 Cerebrovascular reactivity

Cerebrovascular reserve describes the capacity of the cerebrovasculature to increase cerebral blood flow (CBF) in response to a challenge. Cerebrovascular reactivity (CVR) is a marker of cerebrovascular reserve. CVR refers to the ability of the small arteries and arterioles in the brain to alter their calibre and hence their

resistance in response to a vasoactive stimulus.[19] Carbon dioxide (CO_2) is often used as the vasoactive stimulus because it causes intracranial arterial dilatation.[20]

CVR is determined by the equation:

$$CVR = \frac{\%\Delta\ CBF}{mmHg\Delta\ EtCO2}$$

where %Δ CBF is the difference in CBF between normo- and hypercapnia and *mmHg*Δ $EtCO_2$ is the mmHg change in end-tidal CO_2.

CO_2 causes vascular smooth muscle relaxation, vasodilation and hence increased CBF, such that a 1 mmHg increase in $EtCO_2$ results in 5% increase in CBF.[19] The mechanisms by which hypercapnia affects vessel reactivity are incompletely understood but likely involve calcium-mediated vascular smooth muscle relaxation and nitric oxide-induced vasodilation.[19]

Like CBF, CVR can be considered an important measure of cerebrovascular health. CVR may detect abnormalities in the cerebral circulation earlier than CBF.[19] Healthy or "reactive" blood vessels dilate to augment CBF in response to a vasoactive stimulus. However, diseased vessels may not dilate in the face of increased CBF requirements, thereby increasing the risk of cerebrovascular insufficiency.

1.4 Magnetic resonance imaging

Magnetic resonance imaging (MRI) is the most sophisticated imaging modality. Simplistically, it employs a strong magnetic field and radiofrequency pulses to generate signal and, from that, images of the body.

Water and fat molecules in the body contain hydrogen atoms. Hydrogen nuclei are protons, which have a positive electrical charge. Normally, protons within the body are randomly oriented. *See figure 8.*

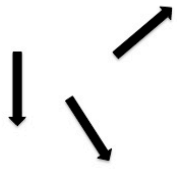

Figure 8 illustrates normal proton alignment within the body.

When the body is exposed to a strong external magnetic field, as in an MRI scanner, hydrogen protons align mostly in the direction of the magnetic field. *See figure 9*. This produces net magnetization parallel to the magnetic field i.e. longitudinal magnetization.

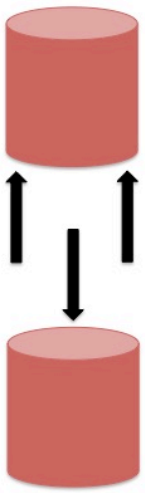

Figure 9 illustrates proton alignment in an external magnetic field.

Not only do protons in the body have a positive charge, they also possess rotational spin/precession. *See figure* 10.

Figure 10 illustrates proton precession.

When a radiofrequency (RF) pulse with the same frequency as the precessional frequency of the protons is applied, the protons absorb energy and are elevated to a higher energy state, antiparallel to the magnetic field. Thus, the net magnetization rotates away from the longitudinal direction, resulting in a decrease in longitudinal magnetization. Additionally, the protons, which were previously spinning

independently, begin to precess in sync. This establishes a new magnetic vector in the transverse plane i.e. transverse magnetization. *See figure 11.*

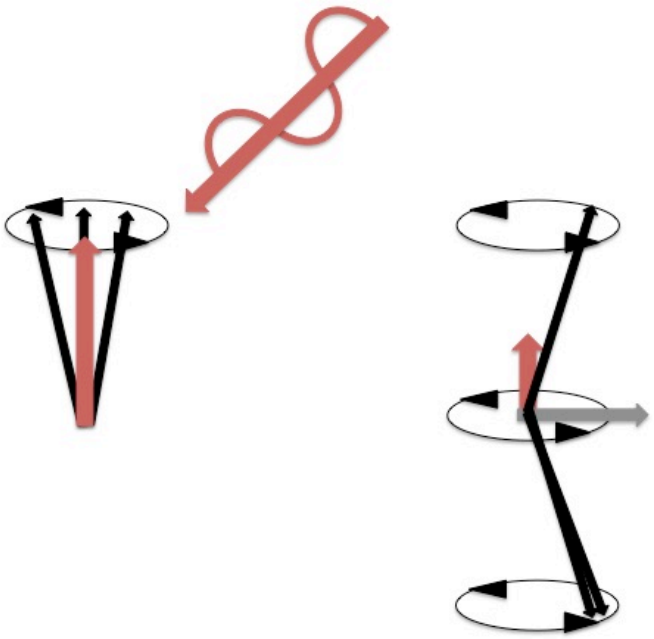

Figure 11 illustrates proton alignment and precession with application of a radiofrequency pulse.

Once the RF pulse is switched off, the protons return to their lower energy state, thus longitudinal magnetization begins to grow back (i.e. longitudinal/T1 relaxation). The protons also fall out of phase with one another, thus transverse magnetization disappears (i.e. transverse/T2 relaxation).

As the system returns to equilibrium, energy is emitted in the form of a RF signal, which is detected by a receiver coil and reconstructed as a magnetic resonance image.

The rates at which longitudinal and transverse relaxation occur vary according to tissue type, allowing us to distinguish between different tissues in the body based on inherent differences in signal characteristics. Tissues with short longitudinal/T1 relaxation recover their longitudinal magnetization quickly, resulting in strong signal on T1 weighted images. In tissues with short transverse/T2 relaxation, transverse magnetization decays rapidly, resulting in weak signal on T2 weighted images. T2*-effects are due to magnetic field inhomogeneities causing faster T2 signal decay.[21-23]

Most MRI scanners operate at a field strength of 1.5 Tesla. 3 Tesla MRI generates higher quality images, mainly due to increased signal to noise ratio (SNR). SNR is the ratio between the intensity of the signal and the background noise or "graininess" in an image. Increased SNR results in higher spatial resolution, which is the ability of an imaging modality to differentiate between two nearby objects. It also results in higher temporal resolution/faster scan times.[24]

1.5 Arterial spin labeling MRI

1.5.1 Basic principles of ASL

Arterial spin labeling (ASL) is a magnetic resonance imaging (MRI) technique, which can be used in the quantification of cerebral blood flow (CBF).

ASL was conceptualized in rats approximately 30 years ago,[25] however it has only recently began to evolve from a research to a clinical tool, both because of increased awareness of its capabilities amongst clinicians/radiologists and because of technical advancements, which have improved its reliability and availability.[26]

ASL uses magnetically labeled arterial blood water protons as an endogenous flow tracer to study cerebral haemodynamics. *See figure 12.*

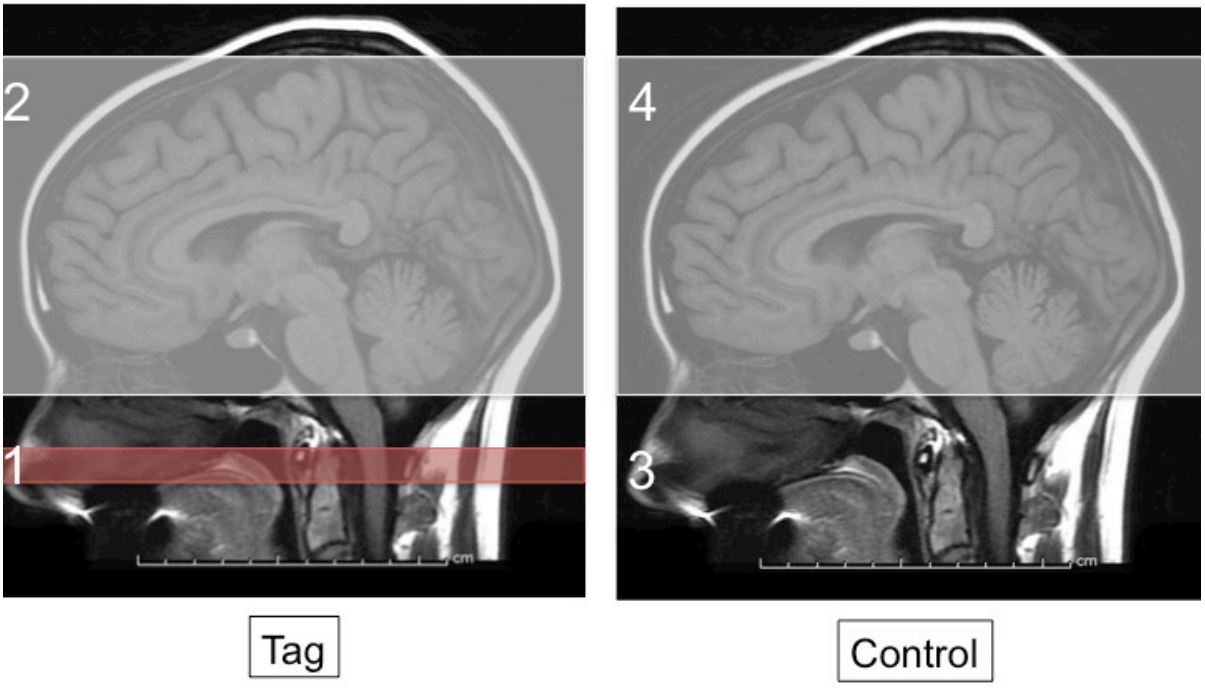

Figure 12 illustrates the principles of arterial spin labeling.

Radiofrequency (RF) pulses are used to invert water protons in inflowing arterial blood below the region of interest [1]. A delay between magnetic labeling [1] and image acquisition [2] allows tagged blood to reach the capillaries and exchange with brain tissue, altering tissue magnetization. The process is then repeated without arterial blood labeling [3] to generate a control image [4]. ASL has inherently low signal to noise ratio (SNR), therefore multiple pairs of tag and control images are required. Subtraction between averaged control and tag images yields flow-weighted maps.[27-29]

1.5.2 ASL kinetic models

The tag-control signal difference measured using arterial spin labeling (ASL) can be converted into absolute perfusion values (in ml/100g/min.) using kinetic models, which have three main components, relating to tracer delivery, washout and relaxation.

The delivery function *c(t)* describes the concentration of magnetically labeled arterial blood water protons arriving at a given voxel at time *t*.

The residue function, $r(t - t')$ describes the washout of labeled spins from a voxel between times t' and *t.*

The magnetization relaxation function $m(t - t')$ describes the longitudinal magnetization relaxation effects on the tracer between times t' and *t.*

The ASL signal at time *t* can therefore be expressed according to the equation:

$$\Delta M(t) = 2\alpha M_{0a} f \int_0^t c(t) r(t - t') m(t - t') dt'$$

where α is the labeling efficiency of pseudocontinuous (pc)ASL (which accounts for imperfect magnetic labeling), M0a is the equilibrium magnetization of arterial blood (*further described in Chapter 2*, *section 5.1)* and f is CBF.[30-32]

Because this general kinetic model didn't take into account transit delays between tagging and imaging regions, a standard kinetic model was devised and it is this model that is used in current ASL studies. This model makes three key assumptions about the delivery, residue and magnetization relaxation functions outlined above, namely that:

1. The arrival of labeled blood water is uniform, so that the *c* function can be expressed as:

$$c(t) = \begin{cases} 0, & 0 < t < \Delta t \\ \alpha e^{-\Delta t/T_{1b}} & \Delta t < t < \Delta t + \tau \\ 0, & \Delta t + \tau < t \end{cases}$$

where Δt is the arterial transit time (ATT) i.e. the time taken for blood to travel from the labeling slab to the region of interest, $T1_b$ the longitudinal relaxation time of blood and τ is the label duration.

2. The kinetics are subject to a single compartment model, with rapid exchange of labeled blood water between the blood vessels and the brain tissue. As a result, the ratio of tissue to venous concentration is constant and equal to the equilibrium blood/brain partition coefficient of water, λ. This can be expressed as:

$$r(t) = e^{-ft/\lambda}$$

3. Labeled spins initially decay with the relaxation time (T1) of blood. Once labeled spins reach the brain, however, magnetization decays with the T1 of brain tissue, according to the equation:

$$m(t) = e^{-t/T1}$$

Taking all of these assumptions into account, ASL signal can be described as follows:

$$\Delta M(t) = \begin{cases} 0, & 0 < t < \Delta t \\ 2M0_a f T1^{app} \alpha e^{-\Delta t/T1b}(1-e^{-(t-\Delta t)/T1app}) & \Delta t < t < \Delta t + \tau \\ 2M0_a f T1^{app} \alpha e^{-\Delta t/T1b} e^{-(t-\tau-\Delta t)/T1app})(1-e^{-\tau/T1app}) & \Delta t + \tau < t \end{cases}$$

where $T1^{app}$ is the apparent relaxation time of T1 and $1/T1^{app} = 1/T1 + f/\lambda$.[30-32]

1.5.3 ASL pulse sequences

Although there are several different arterial spin labeling (ASL) methods (pulsed, continuous, pseudocontinuous), they are all based on the same principles. Pulsed (p)ASL utilizes a single/small number of short radiofrequency (RF) pulse(s) to label blood within a slab of tissue adjacent to the region of interest. With continuous (c)ASL, blood flowing through a defined region is effectively continuously labeled using RF pulses.[33] Pseudocontinuous (pc)ASL replaces the continuous RF pulse of cASL with a train of short RF and gradient pulses, thus improving labeling efficiency

and signal to noise ratio (SNR). *See figure 13.* pcASL is the labeling scheme recommended by the International Society for Magnetic Resonance in Medicine (ISMRM) in its consensus paper[27] and it is this labeling technique, which we employed in this study.

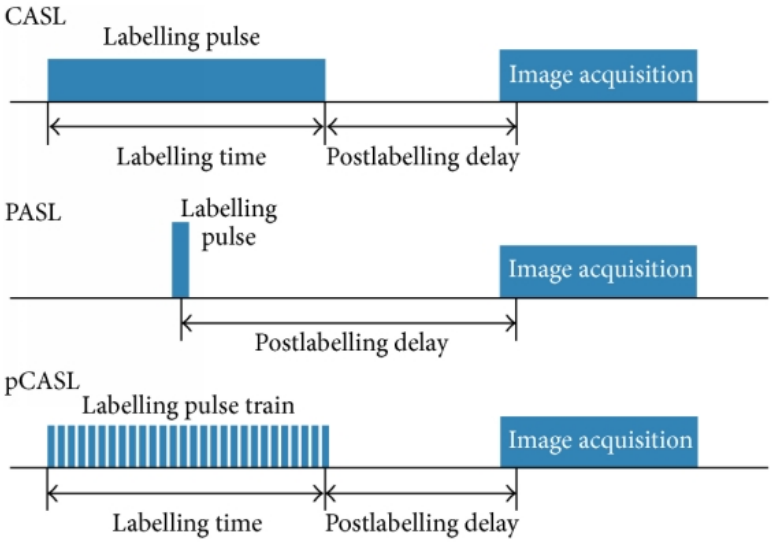

Figure 13 illustrates the implementation of the different ASL pulse sequences. (From: Vaghefi E, Pontré B. Application of Arterial Spin Labelling in the Assessment of Ocular Tissues. Biomed Res Int. 2016;2016:6240504).

Although ASL MRI can accurately measure grey matter (GM) CBF, reliable ASL estimates of white matter (WM) CBF have proven unobtainable to date because of both decreased perfusion/longer arterial arrival times in white matter and the inherently poor signal of ASL MRI.[34] Thus, grey matter perfusion is often assessed, as in this study, as a measure of global cerebral perfusion.

1.6 Imaging methods for measuring CBF

Various imaging methods, old and new, have been trialled to date in the measurement of cerebral perfusion. These include ultrasound (US) techniques like Doppler, nuclear medicine techniques i.e. positron emission tomography (PET) and single photon emission computed tomography (SPECT), computed tomography (CT) i.e. Xenon (XeCT) and dynamic perfusion (DPCT) and magnetic resonance imaging (MRI), including dynamic contrast-enhanced (DCE), dynamic susceptibility contrast (DSC), phase contrast (PC) and arterial spin labeling (ASL) MRI. *See table 1.*

CBF	CVR
US	US
PET*	PET
SPECT(*)	SPECT
XeCT*	XeCT
DPCT	DPCT
DCE/DSC MRI	-
PC MRI*	-
ASL MRI*	ASL MRI
-	BOLD MRI

Table 1 illustrates the various imaging techniques employed in the measurement of cerebral blood flow (CBF) and cerebrovascular reactivity (CVR). Only those marked with an asterisk (some SPECT techniques) provide quantitative CBF measurements; the others provide estimates of CBF.

Doppler ultrasound

Doppler ultrasound (US) is simple, fast, cheap, portable, non-invasive, has no known adverse effects, involves neither ionizing radiation nor exogenous contrast and is therefore suitable for repeatable measurements.[28] It can be used to measure blood-flow-volume in the internal carotid artery (ICA) as a correlate for ipsilateral hemispheric CBF or transcranially for calculation of middle cerebral artery (MCA) blood flow velocity.[35] Ultrasound does not provide a quantitative measure of CBF, rather it interrogates blood flow at the level of feeding arteries supplying the brain; these measurements can be used to estimate CBF. Another drawback with US is that it is operator dependent.[28] However, prior research demonstrates high reproducibility of extracranial arterial blood-flow-volume measurements[36] and good intra- and interrater agreement in MCA flow velocity measurements[37] using ultrasound.

Positron emission tomography

Positron emission tomography (PET) is currently considered the gold standard for CBF measurement.[38]

PET employs radiopharmaceuticals or "tracers" (typically [^{15}O]-H_2O, $^{15}O_2$ and $C^{15}O_2$), injected intravenously (IV) or inhaled. These tracers diffuse freely and rapidly into body tissues. Once equilibrium is achieved, regional tissue tracer concentrations can be measured using dedicated scintillation detectors external to the subject.

Tissue tracer concentrations can be converted into quantitative blood flow values - both total and/or region-specific. Not only does PET quantitatively measure cerebral perfusion, it can also be used to calculate cerebral blood volume (CBV), cerebral metabolic rate of oxygen ($CMRO_2$), oxygen extraction fraction (OEF) and glucose metabolism.[28] PET has several disadvantages, however. It is costly, technically complex, involves administration of radioactive pharmaceuticals, arterial blood sampling and ionizing radiation and is therefore poorly suited to repeated studies.[28] Furthermore, [^{15}O]-H_2O has a short half-life and requires an on-site cyclotron.[39]

Single photon emission computed tomography

Single photon emission computed tomography (SPECT) is another nuclear medicine imaging technique that uses a gamma camera in conjunction with a radiopharmaceutical (often ^{133}Xenon (^{133}Xe) inhaled, [^{99m}Tc]HMPAO or [^{99m}Tc]ECD injected), to generate maps of regional CBF. Like PET, these radiotracers are taken up by the brain parenchyma in proportion to CBF. While ^{133}Xe SPECT quantitatively assesses CBF, other radiotracers provide semi-quantitative CBF estimates. SPECT perfusion imaging involves radioactive pharmaceuticals and ionizing radiation. Additionally, the gamma rays emitted by ^{133}Xe are low in energy, meaning that they are prone to scatter and resultant images can be of low spatial resolution.[28]

Xenon-enhanced CT

Xenon-enhanced computed tomography (XeCT) involves dynamic CT scanning during inhalation of stable (non-radioactive) Xenon. The radiodensity of Xenon allows its concentration in the brain to be determined by the CT scanner. Like other perfusion techniques, cerebral Xe concentration is related to CBF. XeCT generates maps of quantitative CBF data superimposed on cerebral anatomy. XeCT is non-invasive but involves exposure to Xenon gas and ionizing radiation. It is also reliant on patient co-operation.[40, 41]

Dynamic perfusion CT

Dynamic perfusion computed tomography (DPCT) involves continuous cine CT scanning during IV infusion of an exogenous, non-diffusible iodinated contrast agent. With this technique, changes in the attenuation of the brain tissue during the first pass of an IV contrast bolus reflect cerebral perfusion. DPCT provides estimates of cerebral blood volume (CBV), mean transit time (MTT) and CBF. Comparison of these parameters between normal and abnormal regions permits identification of cerebral ischaemia/infarction and is particularly useful in detecting

"at risk" tissue in the setting of acute stroke. DPCT is quick to perform. The required equipment is readily available. However, DPCT involves exposure to ionizing radiation.[28] Additionally, the use of IV iodinated contrast media in patients with reduced renal function has been associated with acute kidney injury.[42]

Dynamic contrast-enhanced and dynamic susceptibility contrast MRI

Both dynamic contrast-enhanced (DCE) and dynamic susceptibility contrast (DSC) MRI are based on the same principles as DPCT, whereby dynamic images are acquired during IV injection of an exogenous contrast medium - in this case, gadolinium as opposed to iodinated-based contrast. The signal changes in the brain induced by IV contrast relate to cerebral perfusion.[43] DCE relies on gadolinium causing T1 shortening within the blood pool, thereby increasing signal intensity on T1 weighted imaging (T1WI). Signal loss on T2(*)-weighted imaging caused by gadolinium passing through the capillary bed forms the basis of DSC MRI.[43] Using time intensity curves, maps of various vascular biomarkers can be constructed, including bolus time-to-peak, apparent mean transit time (MTT) and cerebral blood volume (CBV). These techniques do not quantitatively assess CBF but effectively identify areas of haemodynamic disturbance and like DPCT, may be useful in the evaluation of acute stroke. MRI does not involve exposure to ionizing radiation, however it's use is limited by availability/accessibility, contraindications to MRI/gadolinium and claustrophobia.[28]

Phase contrast MRI

Phase contrast (PC) is a non-invasive MRI technique that uses flow-encoding magnetic gradients to visualize and quantify the velocity of moving fluid. It is a useful technique for measuring flow velocities in the main feeding arteries to the brain – the internal carotid and vertebral arteries. Flow velocities can be combined with brain volume (obtained from a structural sequence) to estimate whole-brain CBF. PC MRI has advantages over other perfusion techniques in that it is non-invasive and involves neither exogenous tracer nor exposure to ionizing radiation. It is more costly but less operator dependent than other flow velocity-based techniques such as transcranial Doppler ultrasound.[39, 44]

Arterial spin labeling MRI

Arterial spin labeling (ASL) MRI, like PC MRI, is non-invasive and involves neither exogenous tracer nor exposure to ionizing radiation.[28] This makes it suitable for repeated studies. It also demonstrates excellent intra- and interscanner reliability

and reproducibility.[45] There are a few limitations of ASL MRI. It has relatively low signal to noise ratio (SNR) per unit time and can underestimate CBF in cases where arterial transit time (ATT) is delayed[28] i.e. in cases of reduced cardiac output/proximal arterial stenosis.

Given its advantages over PET, the current gold standard for CBF assessment, ASL MRI offers a promising alternative for quantitative measurement of cerebral perfusion, particularly in large cohort studies such as ours. *See table 2.* Previous studies have demonstrated excellent correlation between PET and ASL measurement of CBF.[46]

	PET	ASL
Age range	Adults (+/- children)	Adults (+/- children)
Contrast material	Exogenous tracer [^{15}O]-H_2O, $^{15}O_2$ and $C^{15}O_2$	**No exogenous tracer**
Radiation per study	0.5-2mSv	**No ionizing radiation**
Data acquisition	5-9 minutes	5-10 minutes
Data processing	5-10 minutes	5 minutes
Parameters assessed	CBV, $CMRO_2$, OEF, glucose metabolism	CBF, can be combined with a vasoactive stimulus to measure CVR
Quantitative accuracy	Quantitative CBF measurement	Quantitative CBF measurement
Coverage	Whole brain	Whole brain
Spatial resolution	4-6mm	2mm
Repeatability	10 minute interval minimum required between scans	Can be repeated immediately
Reproducibility	Reproducible	Reproducible
Cost	Expensive	Expensive

Table 2 compares ASL MRI with PET, the current gold standard for CBF measurement.

1.7 Imaging methods for measuring CVR

Similar to cerebral blood flow (CBF), many techniques, in conjunction with a vasoactive stimulus, have been employed in the measurement of cerebrovascular reactivity (CVR). These include ultrasound (US), positron emission tomography (PET), single photon emission computed tomography (SPECT), Xenon (XeCT) and dynamic perfusion computed tomography (DPCT) and arterial spin labeling (ASL) and blood oxygen level dependent (BOLD) magnetic resonance imaging (MRI). *See*

table 1. Of these, the most relevant in terms of recent research are Doppler US, BOLD and ASL MRI.

Doppler ultrasound

Doppler ultrasound (US) can be used to non-invasively assess changes in blood flow velocity (as a proxy for CBF) and vessel reactivity in response to a vasoactive stimulus. A major disadvantage in this setting is that Doppler assumes that the insonated arterial diameter remains stable throughout hypercapnia,[20] when it is known that carbon dioxide (CO_2) causes vasodilation.[15] In addition, other factors i.e. blood pressure (BP) can influence the reliability of transcranial Doppler (TCD) CBF and hence CVR measurements.[20]

Blood oxygen level dependent MRI

Blood oxygen level dependent (BOLD) is a functional MRI technique, in which image contrast is determined by regional concentrations of oxygenated (oxy-Hb) and deoxygenated (deoxy-Hb) haemoglobin. Increased CBF i.e. in response to a vasoactive stimulus, results in increased oxy-Hb and decreased deoxy-Hb. Increased oxy-Hb produces increased signal on T2*-weighted images, because of decreased magnetic susceptibility of oxy-Hb compared with deoxy-Hb.[47]

Although BOLD is frequently used in CVR assessment, BOLD signal is not a direct reflection of CBF/CVR and is influenced by various other factors including cerebral blood volume (CBV), cerebral metabolic rate of oxygen ($CMRO_2$), oxygen extraction fraction (OEF) and haematocrit.[48] ASL, on the other hand, exclusively and quantitatively measures CBF and therefore provides a superior measure of CVR.

Vasoactive stimuli

As alluded to earlier, various vasoactive stimuli can be used to induce cerebral vasodilation.

Hypercapnia can be achieved by exogenous administration of a carbon dioxide (CO_2)-containing gas or by breath holding. These techniques increase the partial pressure of arterial CO_2 ($PaCO_2$), without changing the $CMRO_2$. CO_2 inhalation is a passive task. It does not require much co-operation from the subject. Additionally, administration of a fixed CO_2 concentration allows hypercapnia levels to be controlled.[47] Breath-holding, on the other hand, is hugely dependent on subject performance and $PaCO_2$ elevations vary between participants.[47]

Acetazolamide, a reversible, selective carbonic anhydrase inhibitor, is a pharmacological vasodilatory substance, which can be injected intravenously (IV). It induces carbonic acidosis, with resultant smooth muscle relaxation and vasodilation, thereby rapidly and considerably increasing CBF. This technique requires minimal co-operation from the subject but is invasive and adverse reactions to acetazolamide have been reported.[49]

Alternatively, functional tasks can be used to increase regional CBF.[20]

1.8 Clinical relevance of CBF/CVR

The world's population is rapidly ageing. The global population aged 60 years and older is predicted to more than double from 901 million to 2.1 billion between 2015 and 2050, with an anticipated more than threefold increase in the "oldest old" i.e. those aged 80 years and older.[50] Ageing is associated with increased morbidity and mortality from multiple causes, including dementia and stroke, for which it is among the most important risk factors.[51] Expected demographic changes will have profound healthcare, social and economic implications. Therefore, research into the mechanisms contributing to healthy brain ageing has never been more timely.

Cerebral blood flow (CBF) and cerebrovascular reactivity (CVR) are considered important measures of cerebrovascular integrity. They can be altered in various disease states. Prior research suggests that decreased CBF and CVR are associated with cognitive decline and dementia.[19, 52] A reduction in CBF in high-risk subjects for Alzheimer's disease (AlzD) has been observed *before* the onset of cognitive decline, brain atrophy or amyloid-β accumulation,[53] suggesting that cerebral hypoperfusion may act as an early biomarker of the disease and, more importantly, as a potential target for intervention. Impaired CVR has been associated with increased risk of ischaemic stroke.[54]

Many modifiable and non-modifiable factors are thought to influence CBF and CVR. Ageing affects the mechanisms regulating CBF. Prior studies using a variety of imaging modalities have revealed decreasing CBF with increasing age[52, 55-65] and higher CBF in females.[52, 56, 57, 62, 65] Unsurprisingly, given that CBF is considered a measure of cerebrovascular health, various cardiovascular risk factors including body mass index (BMI),[55, 59, 62, 66] hypertension (HTN),[59, 67-69]

hypercholesterolaemia,[52] type 2 Diabetes Mellitus (T2DM),[55, 70] metabolic syndrome[62, 71] and smoking[52, 59] have also been shown to negatively affect CBF. Similarly, significant differences in CVR between younger and older subjects have been observed[60, 61, 63, 72, 73] and various cardiovascular diseases, including HTN[35, 74, 75] and T2DM[70, 76, 77] have also been associated with impaired CVR.

However, measures like aerobic exercise, weight loss and improved blood pressure (BP) control have been associated with increased CBF[68, 78-80] and CVR,[81, 82] thereby offering targets for intervention.

To date, the lack of published reference values for CBF and CVR in large populations has hindered acceptance of these potentially useful biomarkers in assessing the integrity of the cerebrovasculature. As ageing itself is associated with altered cerebral haemodynamics, the lack of normative values for CBF/CVR in older adults has prevented researchers and clinicians from distinguishing expected age-related decline from pathological reduction.

Previous studies assessing CBF and CVR have varied significantly in methodology and sample size. Many researchers used non- or semi-quantitative techniques to assess CBF. Of those that employed arterial spin labeling (ASL) magnetic resonance imaging (MRI), not all studies followed the International Society for Magnetic Resonance in Medicine (ISMRM) consensus guidelines.[27] The vast majority of MRI CVR research used blood oxygen level dependent (BOLD) as opposed to ASL. As outlined in *section 7* of this chapter, BOLD does not provide a direct measure of CBF/CVR,[48] whereas ASL exclusively and quantitatively determines CBF, providing a superior measure of CVR. Most MRI studies had small sample sizes, likely due to the costs associated with performing and analysing MRI. Indeed, a prior systematic review and meta-analysis examining ASL and BOLD-assessed CVR in cerebrovascular disease reported a mean study sample size of only 19.[20]

As part of this research, grey matter CBF and CVR were quantitatively measured using ASL MRI in a large population-based cohort and the effects of age, sex and various cardiovascular risk factors, including BMI and BP on both CBF and CVR were assessed. My hypothesis was that both CBF and CVR, as measures of cerebrovascular health, would be negatively affected by age and select cardiovascular risk factors.

Additionally, by obtaining reference values for CBF/CVR in a large, population-based, ageing cohort, I hoped that we could identify subjects with compromised CBF/CVR, at increased risk of cognitive impairment/dementia and stroke, who may benefit from intervention.

1.9 Project aims

The aims of this study were to:

1. Obtain a reference set of normative values for grey matter cerebral blood flow (CBF_{GM}) using pseudocontinuous arterial spin labeling (pcASL) magnetic resonance imaging (MRI) in a group of nationally representative, neurologically asymptomatic, community dwelling adults aged 50 years and older, enrolled in The Irish Longitudinal Study on Ageing (TILDA).
2. Assess the effects of age, sex and various cardiovascular risk factors, including body mass index (BMI) and blood pressure (BP) on CBF.
3. Map grey matter (GM) cerebrovascular reactivity (CVR) using pcASL MRI and carbon dioxide (CO_2) in a subset of the above-outlined TILDA participants.
4. Assess the effects of age, sex, BMI and BP on CVR.

CHAPTER 2: MATERIALS AND METHODS

2.1 Study design, subject cohort

This research was carried out on a subset of participants enrolled in The Irish Longitudinal Study on Ageing (TILDA). TILDA is a prospective cohort study, which collects health, social and economic data from nationally representative, community dwelling Irish adults and investigates how these factors interact.[83, 84] 8,507 adults were enrolled in the first wave of TILDA between 2009 and 2010. The cohort used in the present study was comprised of a subset of TILDA wave 3 participants, recruited between May 2014 and 2015. Of 4,309 participants attending for health assessment in one of two dedicated centres, a random subset was invited to return for multi-parametric magnetic resonance imaging (MRI) brain at the Thomas Mitchell Centre for Advanced Medical Imaging (CAMI), St. James's Hospital, Dublin. Inclusion and exclusion criteria were as follows:

Inclusion criteria:

- TILDA participant
- Age ≥50 years, participants aged ≥65 years were prioritized initially

Exclusion criteria:

- Contraindication to MRI i.e. MRI-incompatible device - cardiac pacemaker/defibrillator, intracranial aneurysm clip/neurostimulator, cochlear implant, drug delivery device, recent surgery
- Prior stroke or head injury
- Respiratory disease i.e. chronic obstructive pulmonary disease/severe asthma and clinical concern regarding ability to tolerate abnormal gas concentrations (in hypercapnic challenge participants only)

A total of 546 baseline/normocapnic arterial spin labeling (ASL) datasets were obtained from 578 subjects attending for MRI. There was attrition due to claustrophobia, MRI contraindication(s) and inability to complete study (ASL was performed as the last sequence in the examination).

Following data acquisition, prior to and during data analysis, further subjects (n = 78) were excluded on the basis of clinical and radiological abnormalities.

Additional exclusion criteria:

- Structural abnormalities on T1 weighted imaging (T1WI) (*see section 2.5.4*) (n = 22)
- Abnormalities on perfusion imaging (*see section 2.5.4*) (n = 32)
- Neurological disease (n = 9) - Parkinson's disease (n = 1), history of stroke (n = 4), cognitive impairment (Mini–Mental State Examination [MMSE] score <24) (n = 4)

Additionally, 15 subjects were excluded due to extremes of age. The small numbers of participants aged younger than 54 and older than 84 years would render normative value estimates in these ages unreliable and as such, data from these participants was excluded from the analysis. *See figure 14.*

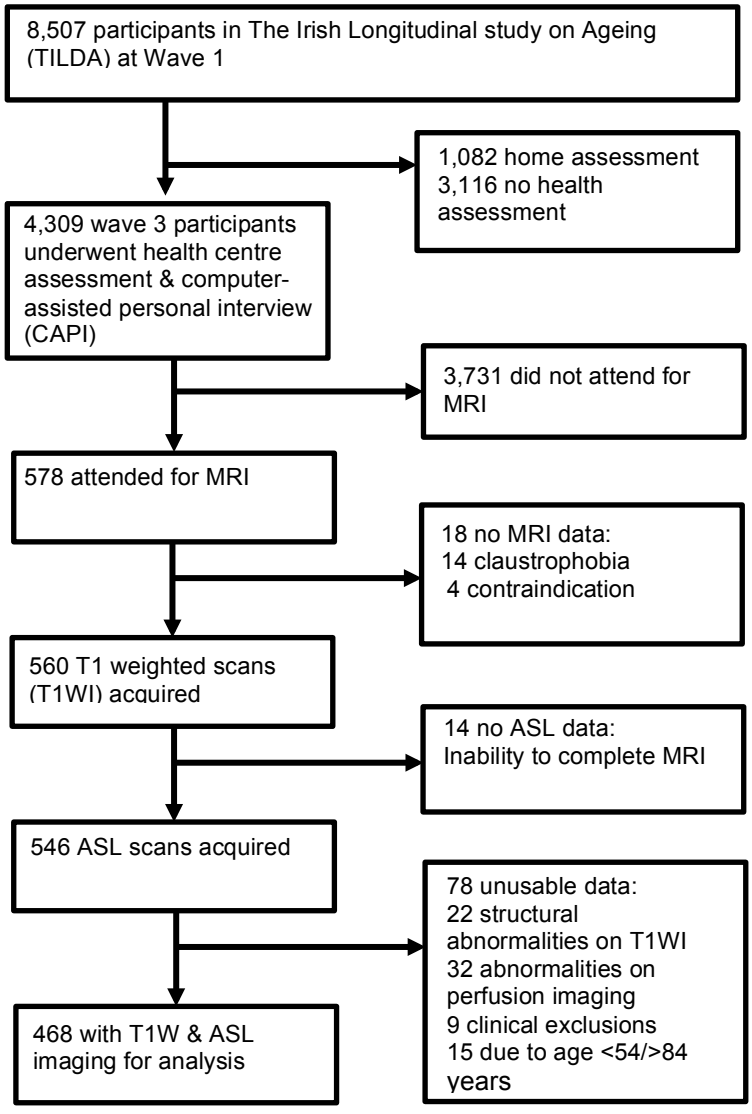

Figure 14: Flow chart outlining sample selection and exclusions for the baseline/normocapnic cohort.

A subset of 147 participants was also invited to undergo a hypercapnic challenge, as illustrated in *section 4* of this chapter. Data from 43 hypercapnic challenge participants were excluded from final analyses. Of those, four participants had incomplete datasets (scan stopped prematurely by subject/technical problems), three had structural abnormalities on T1 weighted imaging (T1WI) (*see section 2.5.4*), 35 had abnormalities on perfusion imaging (*see section 2.5.4*) and there was one clinical exclusion (prior stroke). *See figure 15.*

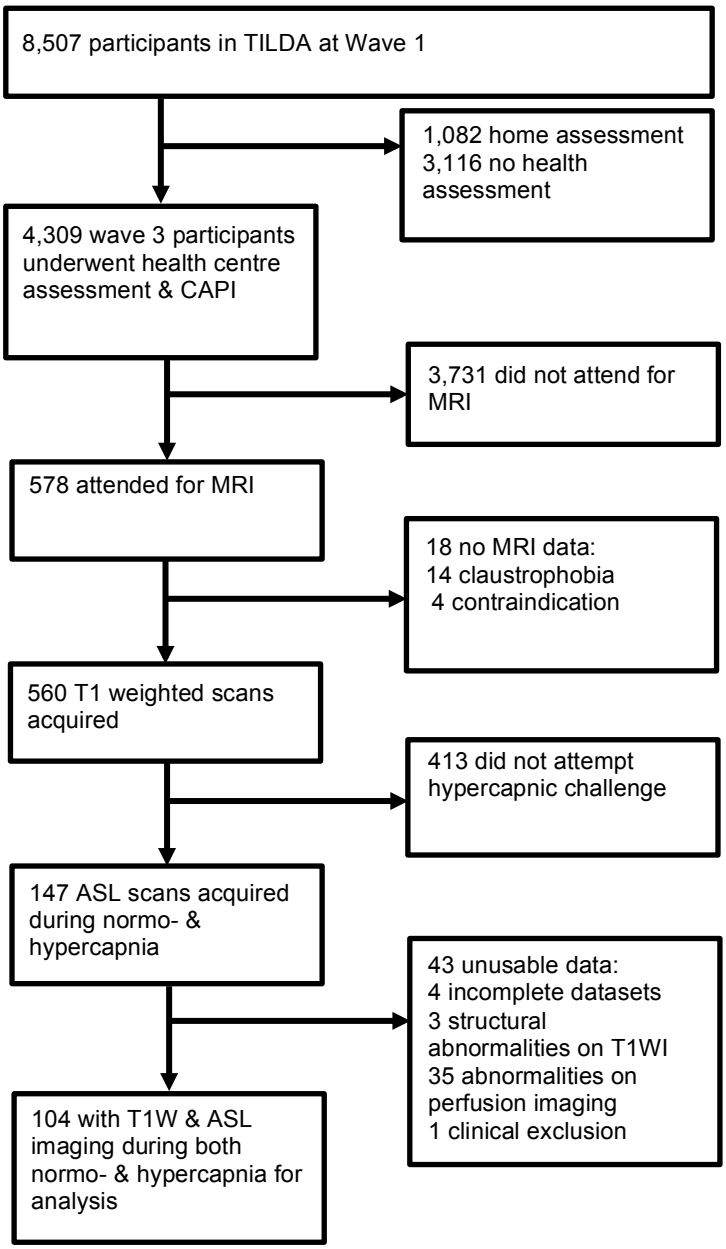

Figure 15: Flow chart outlining sample selection and exclusions for the hypercapnic challenge cohort.

All research was performed in accordance with the Declaration of Helsinki. Ethical approval was obtained for each wave of TILDA from the Health Sciences Research Ethics Committee at Trinity College Dublin. All TILDA participants provided written informed consent prior to their participation in the study. Additional ethics approval was obtained from St James's Hospital Research Ethics Committee, Dublin. Those attending for MRI were required to complete an additional MRI-specific consent form and an MRI safety questionnaire on arrival at CAMI on the day of MRI.

2.2 TILDA assessment

As part of the third wave of The Irish Longitudinal Study on Ageing (TILDA), participants completed a comprehensive health assessment in a dedicated centre and a computer-assisted personal interview (CAPI) in their own home. A wealth of socio-demographic, behavioural and physical health information was gathered from participants. Age, sex, physical activity level, smoking status and alcohol consumption were documented. Participants were asked to self-report a doctor's diagnosis of any of the following cardiovascular conditions: high cholesterol, high blood pressure (BP), angina, heart attack, heart failure, murmur, cardiac arrhythmia, type 2 Diabetes Mellitus (T2DM), cerebrovascular accident (CVA)/stroke, transient ischaemic attack (TIA). Use of antihypertensive medication(s) was documented. Multiple physical measures were also recorded, including height and weight (thereby allowing calculation of body mass index (BMI)), waist and hip size and BP - static seated and standing. Participants were screened for depression and cognitive impairment (CI)/dementia using the Center for Epidemiologic Studies Depression scale (CESD) and Mini-Mental State Examination (MMSE) respectively.[85, 86]

2.3 MRI data acquisition

All MRIs were acquired in the Centre for Advanced Medical Imaging (CAMI) on a 3 Tesla (T) Philips Achieva magnetic resonance imaging (MRI) scanner (Philips Medical Systems, The Netherlands), using a 32-channel head coil. The receiver coil was tight-fitting to optimize detected signal and limit subject movement. *See figures 16 & 17.*

Figure 16 depicts the Philips 3T Achieva MRI scanner.

Figure 17 depicts the Philips 32-channel head coil.

The MRI protocol comprised the following sequences: fluid-attenuated inversion recovery (FLAIR) – duration 2 minutes 34 seconds, T2 turbo spin echo (TSE) – duration 1 minute 6 seconds, T1 3D magnetization-prepared rapid gradient echo (MPRAGE) – duration 5 minutes 24 seconds, pseudocontinuous arterial spin labeling (pcASL) (performed either once or twice depending on whether or not the subject participated in the hypercapnic challenge) – duration 4 minutes 16 seconds, diffusion weighted imaging (DWI) – duration 1 minute, diffusion tensor imaging (DTI)

– duration 16 minutes 37 seconds, MR spectroscopy – duration 7 minutes and a resting state functional MRI sequence of 6 minutes 51 seconds duration.

Of these, the sequences outlined below, are relevant for this research.

T1W imaging

T1W 3D MPRAGE anatomical images were acquired over 5 minutes 24 seconds with the following scan parameters: field of view (FOV) = 240 x 240 x 162 mm^3, matrix = 288 x 288 x 180, repetition time (TR) = 6.7 ms, echo time (TE) = 3.1 ms, flip angle (FA) = 8°, sensitivity encoding (SENSE) = 2.

ASL imaging

The specific ASL implementation used in this study was pseudocontinuous (pc)ASL. As illustrated in *Chapter 1, section 5.3,* this technique involves the application of a closely-spaced train of inversion pulses to label upstreaming arterial blood in the neck, followed by a delay to allow the labeled blood to perfuse the brain tissue. Then, imaging of the perfused brain was performed with 2D multislice single shot echo-planar imaging (EPI).

The distance between the centre of the imaged volume and the centre of the labeling slice was 90 mm. Positioning the labeling plane 32 mm below the base of the imaging volume ensured that the feeding/carotid arteries were consistently perpendicular to the labeling plane and below the inferior border of the cerebellum. This prescription further ensured the labeling plane was remote from regions of strong susceptibility artefact such as air/tissue interfaces.

Background tissue suppression was performed twice during the pcASL sequence. Firstly, prior to the labeling block, pre-saturation of the tissue within the imaged volume was performed using water suppression enhanced through T1 effects.[87] Secondly, two 180° inversion pulses were applied between the labeling and image acquisition blocks. The first inversion pulse was selective to the imaged volume and was applied 60 ms after the end of the labeling pulse, while the second inversion pulse was non-selective and was applied 1,080 ms after the end of the labeling pulse. Two inversion pulses were found to represent a good trade-off between background tissue suppression and ASL signal.

pcASL images were acquired over 4 minutes 16 seconds with the following scan

parameters: FOV = 240 x 240 mm^2, matrix = 80 x 80, TR = 4,000 ms, TE = 9 ms, FA = 90°, SENSE = 2.5. 13 slices (8 mm slice thickness, 1 mm slice gap) were acquired sequentially in a caudocranial direction, yielding 30 dynamic scans and 780 images in total (390 labeled, 390 unlabeled). Given that 30 dynamic scans were acquired, an imaging volume of 116 mm was considered a compromise between covering as much of the brain as possible and limiting MRI scan time, in this ageing cohort.

A labeling duration of 1,800 ms and a delay time of 1,800 ms were used, as recommended in the ASL International Society for Magnetic Resonance in Medicine (ISMRM) consensus paper.[27] A labeling duration of 1,800 ms was selected because although ASL signal increases with label duration, there is decreased signal for label durations much longer than the longitudinal/T1 relaxation time of blood (approx. 1.6 s at 3T under physiologic conditions).[88] Given the broad age range among the study cohort (53 – 84, mean 68.2 years) and the desire to use a consistent acquisition protocol, a post labeling delay (PLD) of 1,800 ms was employed, as recommended for healthy adults aged less than 70.[27] *See table 3.* This took into account the 2D multislice readout and consequent prolonged PLDs in more superior slices. This PLD was chosen to minimize large vessel arterial inflow signal, while maximizing signal to noise ratio (SNR) in this ageing cohort with presumed longer arterial transit times.[26]

Parameter	Value
PCASL labeling duration	1800 ms
PCASL PLD: neonates	2000 ms
PCASL PLD: children	1500 ms
PCASL PLD: healthy subjects <70 y	1800 ms
PCASL PLD: healthy subjects >70 y	2000 ms
PCASL PLD: adult clinical patients	2000 ms
PCASL: average labeling gradient	1 mT/m
PCASL: slice-selective labeling gradient	10 mT/m
PCASL: average B_1	1.5 μT
PASL TI_1	800 ms
PASL TI	Use PCASL PLD (from above)
PASL labeling slab thickness	15–20 cm

Table 3 illustrates recommended ASL parameters. (From: Alsop DC, Detre JA, Golay X, Günther M, Hendrikse J, Hernandez-Garcia L, Lu H, MacIntosh BJ, Parkes LM, Smits M, van Osch MJ, Wang DJ, Wong EC, Zaharchuk G. Recommended implementation of arterial spin-labeled perfusion MRI for clinical applications: A consensus of the ISMRM perfusion study group and the European consortium for ASL in dementia. Magn Reson Med. 2015 Jan;73(1):102-16).

Calibration/M0 imaging

A calibration scan estimating the equilibrium magnetization (M0) was acquired over 20 seconds using the same geometry as the pcASL sequence with TR = 10,000 ms and TE = 9 ms.

B0 mapping

B0 field maps were acquired over 39 seconds using a two-echo 2D gradient echo sequence with the same in-plane resolution as the pcASL sequences and the following acquisition parameters: TR = 455 ms, TE_1 / TE_2 = 1.69 / 7.0 ms, FA = 90°. 38 slices (3.2 mm slice thickness, 0.3 mm slice gap) were acquired.

2.4 CO_2 data acquisition

In subjects undergoing the hypercapnic challenge, a non-rebreather mask was fitted to the patient's face beneath the magnetic resonance imaging (MRI) head coil before the initial arterial spin labeling (ASL) sequence. *See figure 18.*

Figure 18 illustrates the non-rebreather facemask used in the hypercapnic challenge.

During the first (normocapnic) pcASL sequence, subjects inhaled normal/atmospheric air through the facemask. During the second (hypercapnic) pcASL sequence, a mixture of 95% medical air/5% carbon dioxide (CO_2) was delivered to subjects via MRI-compatible tubing connected to a pre-mixed gas cylinder in the MRI control room.

Biopac Systems, Inc. MP150 system[89] combined with *AcqKnowledge* software was used in the acquisition and display of CO_2 data. A sampling line connected the facemask to a CO_2 sensor. CO_2 levels were displayed in real-time as a capnograph trace on the computer screen in the control room. This allowed us to evaluate the integrity of the circuit (i.e. ensure a tight seal with the non-rebreather facemask) and identify CO_2 leak/build-up. *See figure 19.*

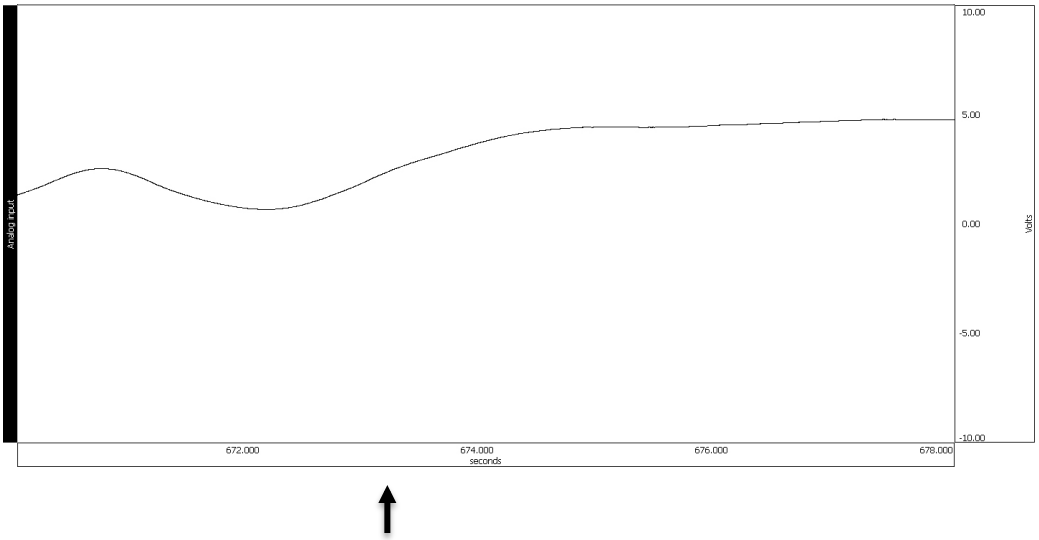

Figure 19 illustrates a sample capnograph trace from a TILDA participant. In this graph, the black arrow at approx. 673 seconds on the x-axis marks the onset of hypercapnia.

Vital observations, including heart rate and oxygen saturation of arterial blood were monitored during both normo- and hypercapnia using a pulseoximeter. Participants were encouraged to press the emergency call ball if experiencing discomfort.

2.5 MRI data analysis

2.5.1 Principles of ASL analysis

The principles of arterial spin labeling (ASL) analysis are complex but involve three key processes:

1. **Subtraction** i.e. subtraction of tag-control pairs to generate a perfusion-weighted map, as outlined in *Chapter 1, section 5.1.*
2. **Kinetic modelling,** which accounts for factors like label duration, arterial transit time (ATT) and label decay, which affect the amount of labeled blood water accumulating in the brain tissue between magnetic labeling and image acquisition and hence voxel intensity in the perfusion-weighted map *(see Chapter 1, section 5.2.).*
3. **Calibration**, which is necessary to convert the arbitrary signal intensities in the perfusion-weighted map into quantitative cerebral blood flow (CBF) values. This requires scaling of the perfusion-weighted map to the equilibrium magnetization of arterial blood (M0a), which varies between individuals and according to magnetic field strengths. The M0 of blood cannot be calculated directly because of the small size of the arteries, thus the M0 of brain tissue/cerebrospinal fluid (CSF) is often used to indirectly estimate M0a.

These three processes can be combined into a single equation, which is used to generate a quantitative value for CBF:

$$CBF = \frac{6000.\lambda.(SI_{control} - SI_{tag})e^{PLD/T1b}}{2.\alpha.T_{1b}SI_{calibration}(1 - e^{-\tau/T1b})}$$

In this equation:

6000 converts the final value into standard units i.e. ml/100g tissue/min.

λ is the blood-tissue partition coefficient i.e. the difference in proton density between a given tissue and blood, assumed to be 0.9 for brain

$SI_{control} - SI_{tag}$ is the signal intensity of the tag-control subtraction

PLD is the post labeling delay i.e. the time between the end of magnetic labeling and the start of image acquisition

T1 is the T1/longitudinal relaxation time of arterial blood, approx. 1.6 s at 3T

α is the labeling efficiency of pseudocontinuous (pc)ASL - this accounts for imperfect magnetic labeling - assumed to be 0.85

$SI_{calibration}$ is the signal intensity of the calibration image and

τ is the labeling duration i.e. the duration of magnetic inversion.[31]

2.5.2 AFNI

Initially, a software programme called Analysis of Functional NeuroImages (AFNI) was used to analyse magnetic resonance imaging (MRI) perfusion data.[90] AFNI is a software package for processing, analysing and displaying functional MRI data.

Data analysis with AFNI involved:

1. Segmentation of T1W (anatomical) images into grey matter (GM), white matter (WM) and cerebrospinal fluid (CSF) probability masks. *See figure 20.*
2. Generation of ΔM map (average of ASL tags – controls).
3. Calculation of M0 of CSF and, from that, M0 of blood.
4. Calibration of ΔM map to M0 of blood.
5. Co-registration of perfusion data to the GM probability mask derived from T1WI for calculation of grey matter (GM) CBF specifically. See *figure 21.*

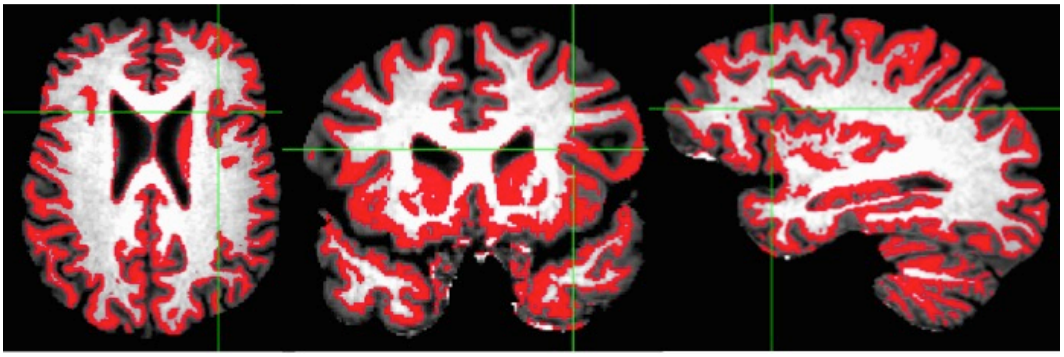

Figure 20 illustrates a grey matter probability mask (red) overlaid on a standard T1W/structural mask in AFNI in axial, coronal and sagittal imaging planes.

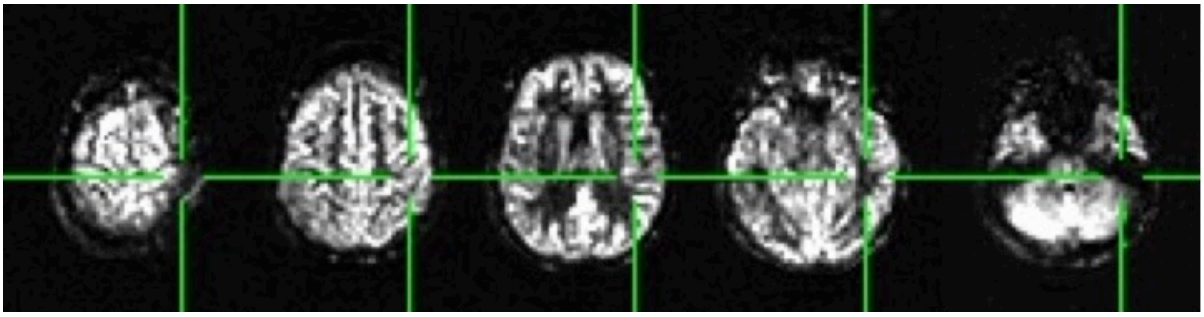

Figure 21 illustrates a perfusion map co-registered to a grey matter probability mask in AFNI.

Unfortunately, the CBF_{GM} values obtained using this method were not within the expected range. On reviewing the data, we identified a problem with the co-

registration between perfusion and anatomical data, whereby the perfusion and GM masks weren't overlapping fully.

To counteract this problem, another strategy was employed, whereby instead of co-registering the perfusion data to an anatomical mask as in step 5 above, the perfusion data was co-registered to a GM mask derived from the perfusion data itself. For each subject, a mask was generated from the perfusion data using an intensity threshold of 30. By thresholding the CBF data, we excluded from the analysis any GM voxels that did not demonstrate expected signal. The median value within this mask was calculated. In calculating the median value, we reduced the influence of outliers and avoided circularities by basing the mask on the perfusion data itself.

Regrettably, the results obtained with this technique were still unsatisfactory. Many patients had low cerebrovascular reactivity (CVR) values, inconsistent with the literature. Thus, it was decided to trial another software programme for MRI perfusion data analysis.

2.5.3 Oxford_ASL

Ultimately, perfusion data analysis was performed using *Oxford_ASLv4.0* in Functional Magnetic Resonance Imaging of the Brain (FMRIB) Software Library (FSL).[91-94]

Quantification in Bayesian inference for arterial spin labeling (BASIL) assumes a standard well-mixed, single-compartment kinetic model with no dispersion of the labeled blood water bolus.[95]

As outlined in *Section 2.3,* background suppression was used in the acquisition of tag-control data to limit the influences of motion/physiological noise sources.

Subtraction of tag-control pairs generated a perfusion-weighted image.

Acquisition parameters i.e. labeling duration, post labeling delay (PLD), ASL sequence were inputted. A tissue T1 value of 1,300 ms and an arterial blood T1 of 1,650 ms were assumed, along with a blood-brain partition coefficient of 0.9. The labeling efficiency was set at 0.85. Slice timing correction, which increases the PLD

for more superior slices, was applied to correct for a slice delay of 30 ms.

A voxelwise-approach was used for calibration. Because the equilibrium magnetization of arterial blood (M0a) cannot be measured directly, it was estimated indirectly using cerebrospinal fluid (CSF) as a 'reference-tissue'. CSF was measured in the ventricles using an automatically generated mask in BASIL that is based on a combination of the CSF segmentation from *fsl_anat* and the ventricular regions of interest in the Harvard-Oxford Atlas. A correction was made for incomplete recovery of the signal based on the repetition time (TR) and an assumed T1 value for CSF (4,300 ms), as well as the differences in T2 values between tissue (150 ms) and CSF (750 ms).

B0 maps were used to apply distortion corrections to ASL images to compensate for any spatially non-linear image distortion effects that B0 inhomogeneities may have had on echo-planar imaging data.

Motion correction was performed on the raw ASL data within BASIL using FSL MCFLIRT. Adaptive spatial regularization (spatial smoothing) was used to decrease the appearance of noise in the final perfusion image.[92]

T1W/anatomical image processing was performed using the *fsl_anat* function, including segmentation and registration to Montreal Neurosciences Institute (MNI) 152 standard space.

Mean whole brain grey matter cerebral blood flow (CBF_{GM}) was calculated in the native space of the perfusion image. In order to create a grey matter (GM) mask, the GM partial volume estimates from the structural segmentation were transformed into ASL space and a threshold of 70% GM applied.[31] A reasonably conservative threshold of 70% GM was chosen to reduce the partial volume effect on mean GM values.

See figures 22-26, illustrating the graphical user interface (GUI) of the BASIL tools. Each tab represents one step in the (notional) workflow of ASL analysis.

See figure 27 for an example of an Oxford_ASL processed perfusion map.

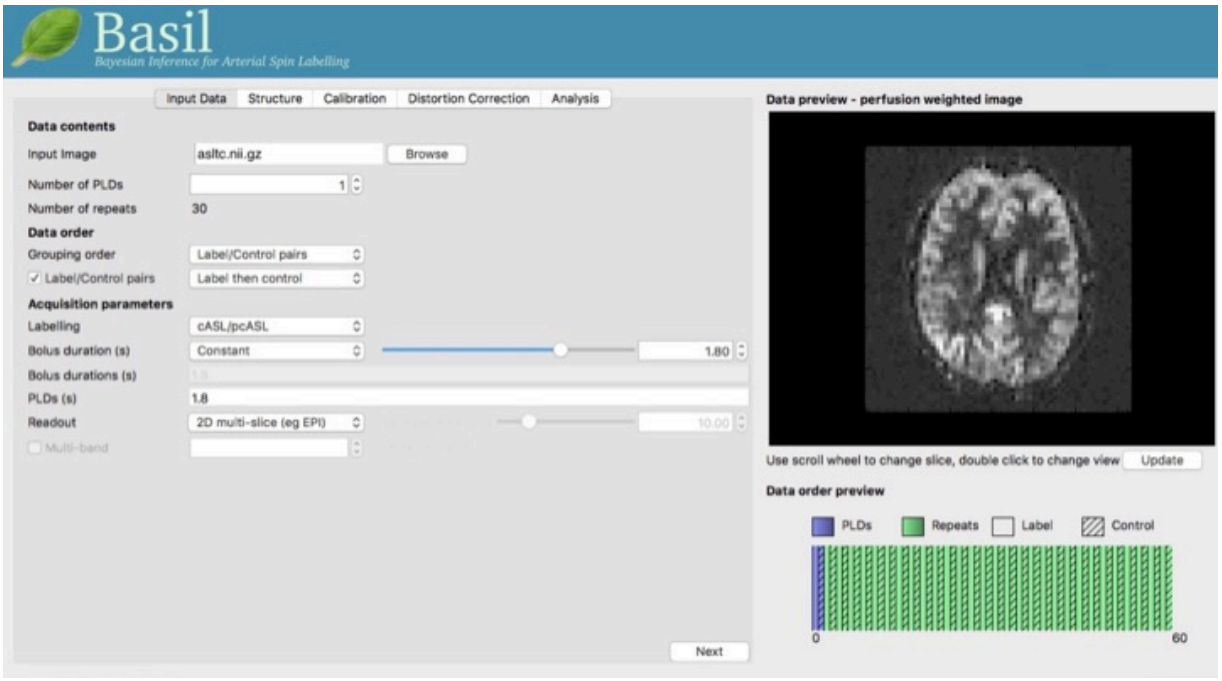

Figure 22 illustrates the "Input Data" tab of the BASIL GUI.

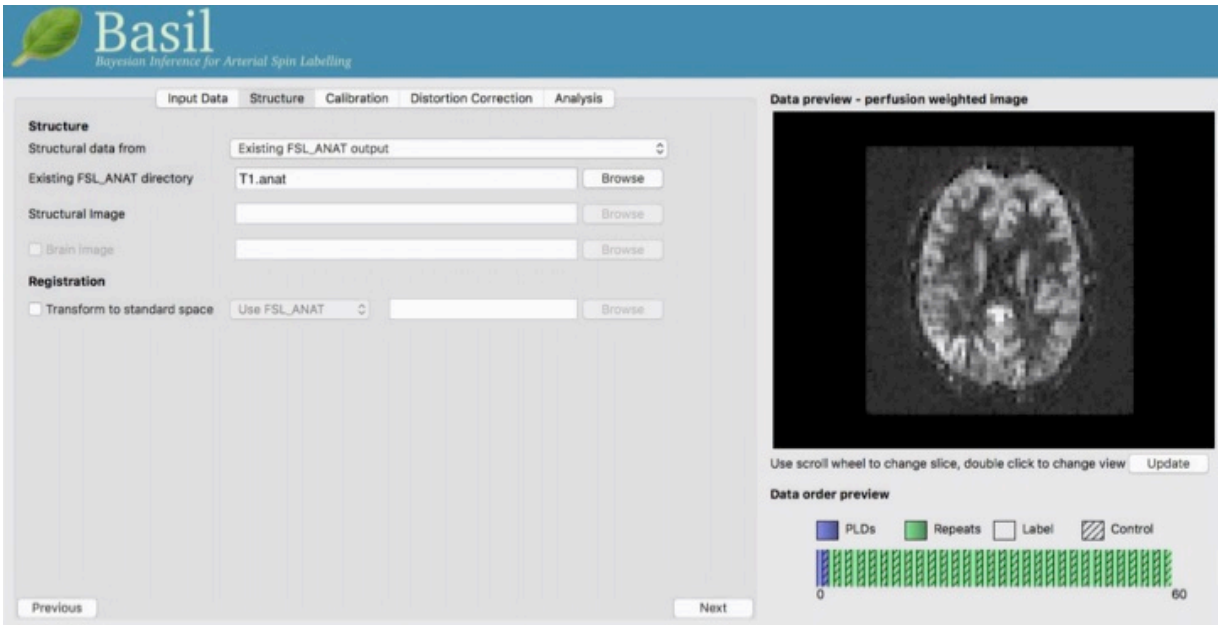

Figure 23 illustrates the "Structure" tab of the BASIL GUI.

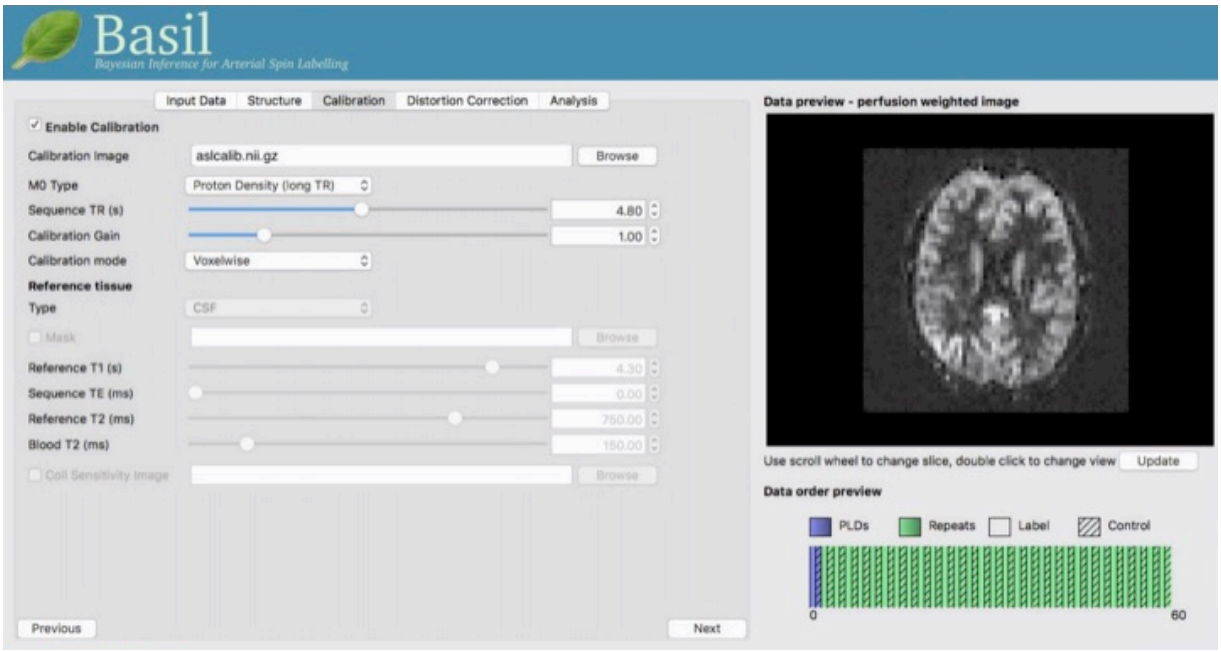

Figure 24 illustrates the "Calibration" tab of the BASIL GUI.

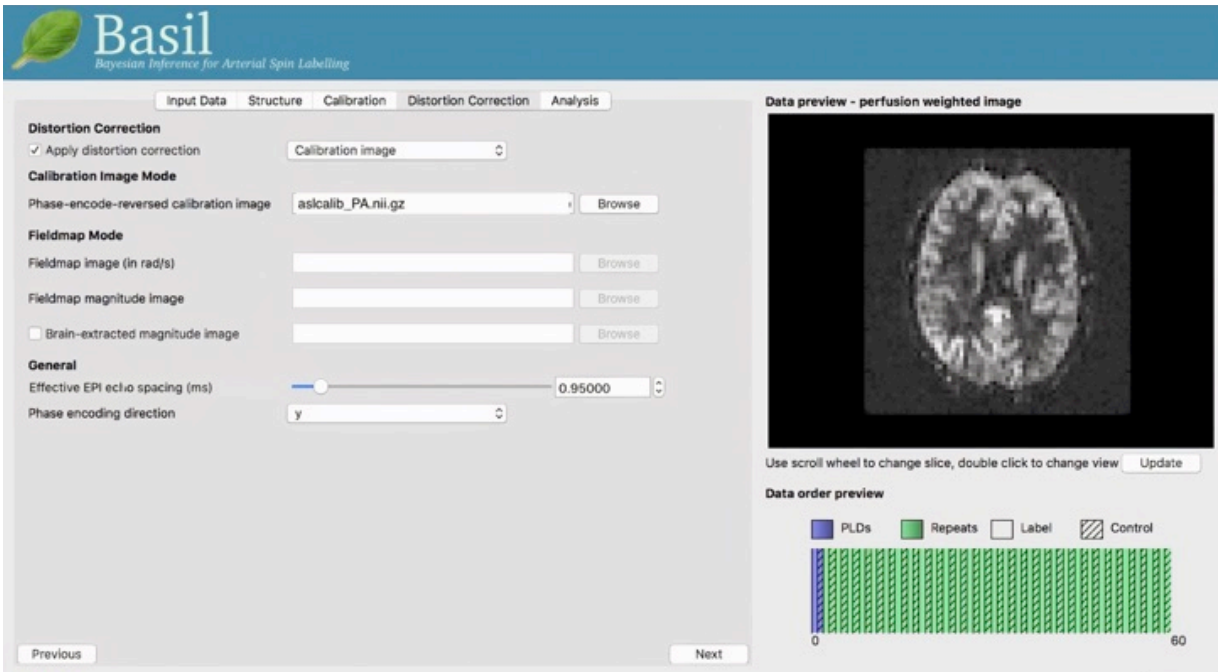

Figure 25 illustrates the "Distortion Correction" tab of the BASIL GUI.

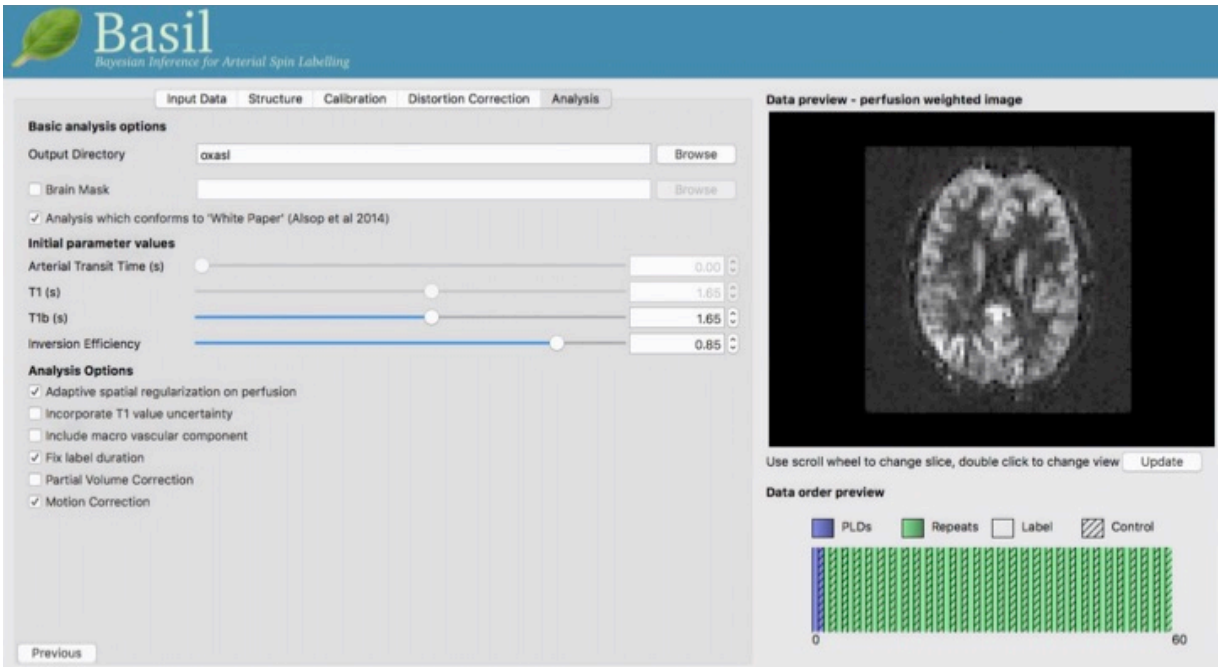

Figure 26 illustrates the "Analysis" tab of the BASIL GUI.

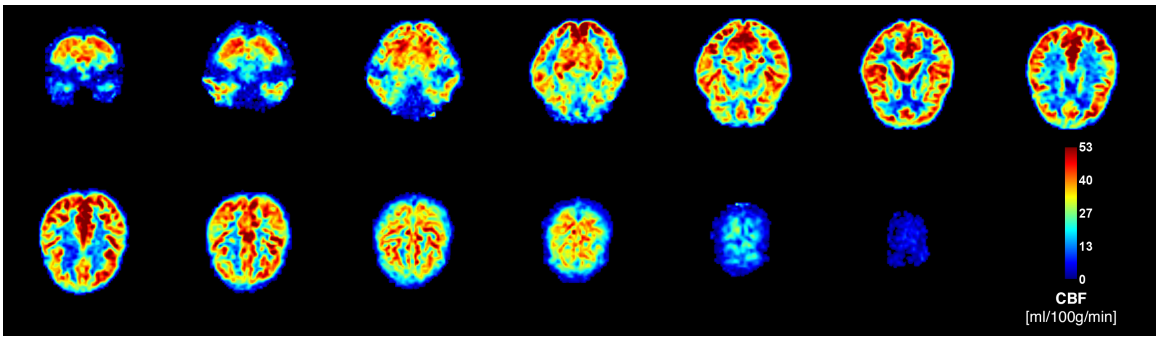

Figure 27 illustrates a typical Oxford_ASL processed perfusion map in a 65-year-old female TILDA participant.

2.5.4 Screening

T1WI screening

All T1 weighted imaging (T1WI) was inspected for image artefacts and/or gross cerebral pathology.

Of the baseline/normocapnic cohort, 22 subjects were excluded due to abnormalities on T1WI. Of those, 16 had gross abnormalities corresponding to confluent white matter hyperintensities (WMH) on T2 and fluid-attenuated inversion recovery (FLAIR) imaging, four had established large vessel infarcts and two had MRI evidence of prior brain contusion/haemorrhage.

Of the hypercapnic challenge cohort, three subjects were excluded due to abnormalities on T1WI, two of whom had confluent WMHs on T2/FLAIR imaging and one of whom had an established large vessel infarct. *See figures 29 & 30 for examples of image artefacts on T1WI.*

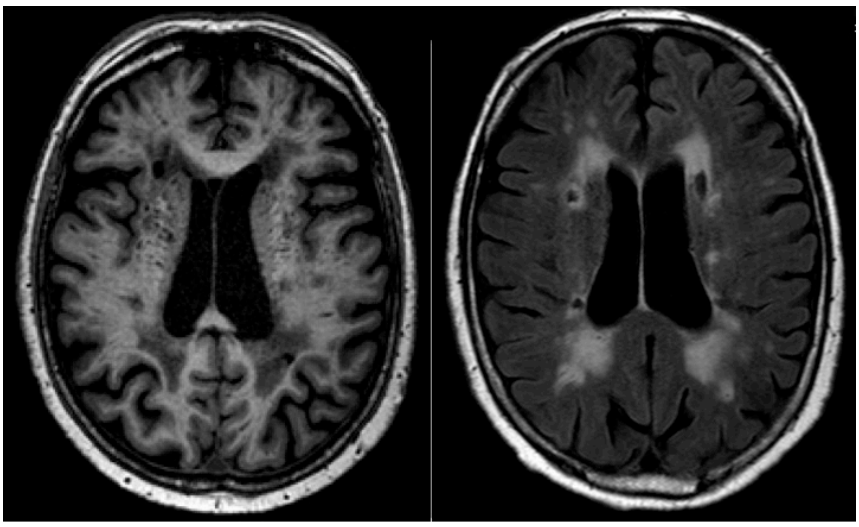

Figure 28 in a TILDA participant illustrates confluent periventricular T1 low signal (left) with corresponding high signal on FLAIR (right), consistent with significant chronic small vessel ischaemic change.

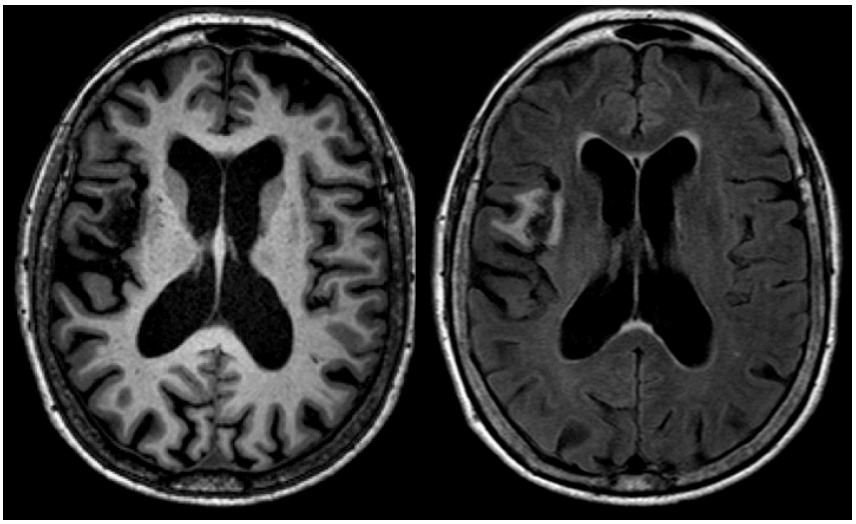

Figure 29 in a TILDA participant illustrates an established right middle cerebral artery infarct with focal T1 low signal in the right frontotemporal region on T1WI (left) and corresponding encephalomalacia and gliosis on FLAIR (right).

Perfusion imaging screening

All perfusion maps were screened for evidence of arterial artefact, poor labeling of a feeding artery, severe motion and/or other gross failure to produce a perfusion image.

By consensus between myself and Dr Michael Chappell, abnormal perfusion maps were categorized as follows:

- Failed labeling i.e. reduced labeling efficiency in an artery leading to globally decreased values in an arterial territory (visible as asymmetric left-right perfusion contrast)
- Delayed arrival i.e. evidence of arterial artefact, visible Circle of Willis
- Delayed arrival in the posterior territories only
- Severe motion corruption i.e. loss of grey-white matter contrast and abnormal intensities at the periphery of the brain
- Severe distortion i.e. failed distortion correction

Of the baseline/normocapnic cohort, 29 subjects with abnormal perfusion maps were removed from the final cohort. Of those, 18 were excluded due to labeling failure, four due to delayed arrival and seven due to severe motion artefact. An additional three subjects were removed as outliers due to extreme whole brain grey matter cerebral blood flow (CBF_{GM}) values (< 10 [n = 1] or >100 ml/100g/min. [n = 2]).

Of the hypercapnic challenge cohort, 32 subjects with abnormal perfusion maps were removed from the final cohort. Of those, eight were excluded due to labeling failure, three due to delayed arrival, 19 due to severe motion and one each due to a combination of delayed arrival/motion and failed labeling/motion. An additional three subjects were removed as outliers due to extreme whole brain percentage (%) change CBF (>85% [n = 1]) and grey matter cerebrovascular reactivity (CVR) values (>6 [n = 2]). *See figure 30 for examples of image artefacts on perfusion imaging.*

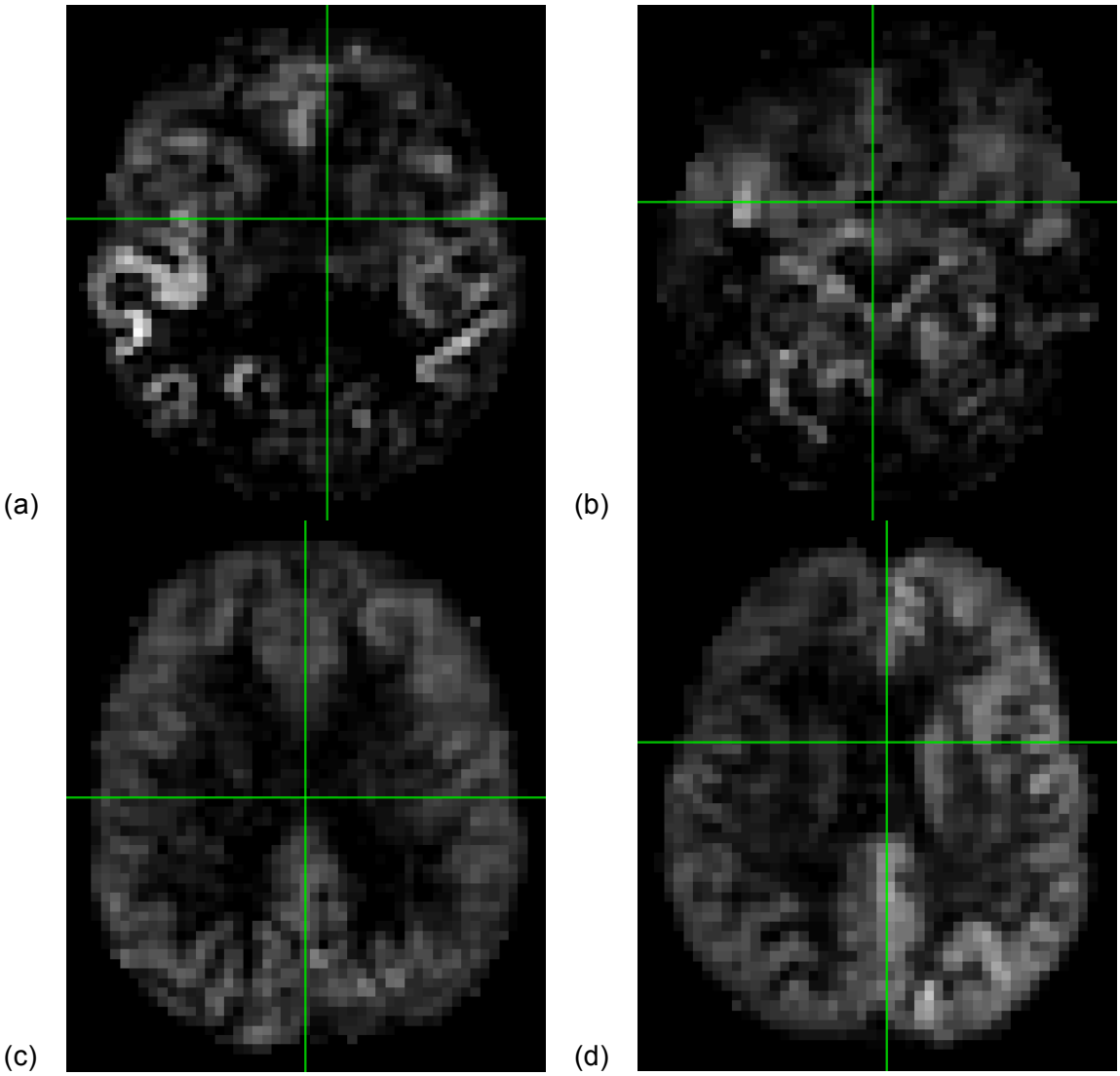

Figure 30 illustrates abnormal perfusion maps with:

(a) delayed arrival and arterial artefact in the temporal lobes bilaterally, more marked on the right

(b) delayed arrival and arterial artefact in the circle of Willis

(c) motion artefact, with loss of grey-white matter contrast and

(d) failed labeling, with globally decreased perfusion in the right cerebral hemisphere.

2.6 CO_2 data analysis

A *Matlab* script was created to calculate median end-tidal carbon dioxide ($EtCO_2$) during normo- and hypercapnia.[96] $EtCO_2$ describes the carbon dioxide (CO_2) peak at the end of expiration and is a marker for the partial pressure of arterial CO_2

($PaCO_2$).[97] The *Matlab* script identified CO_2 peaks in the capnograph trace and displayed the data in graphical format, as illustrated below:

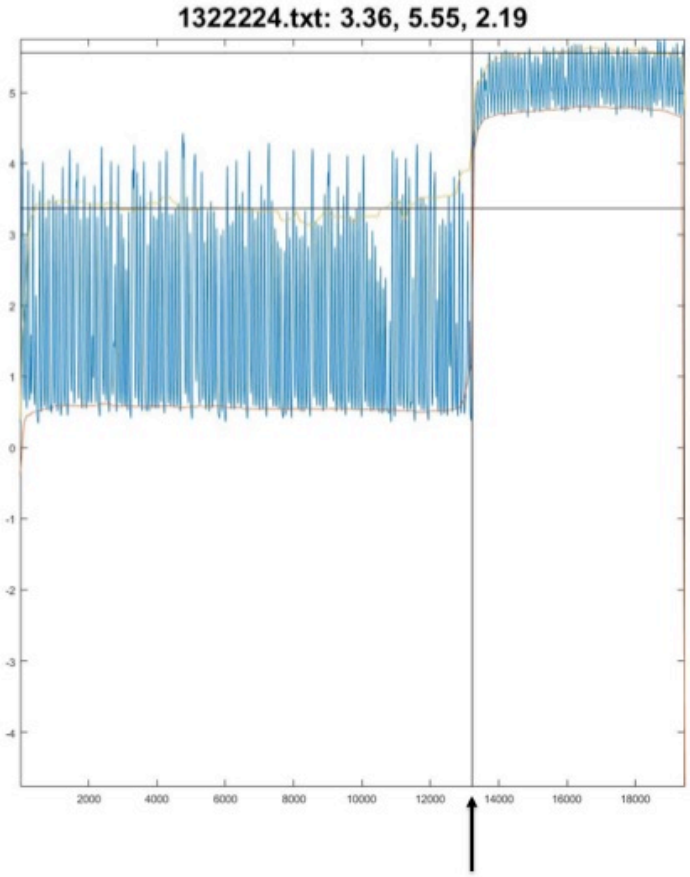

Figure 31 illustrates a sample $EtCO_2$ trace in a TILDA participant.

In this graph, time is displayed on the x-axis (not seconds, arbitrary time units) and $EtCO_2$ on the y-axis. The black vertical line at approx. 13000 on the x-axis (arrowed) marks the onset of hypercapnia. The values above the graph indicate average percentage (%) $EtCO_2$ during normo- (3.36) and hypercapnia (5.55), as well as % change in $EtCO_2$ between the two states (2.19). % change in $EtCO_2$ between normo- and hypercapnia was converted into mmHg by multiplying by 7.6, the conversion factor between kPa (the unit by which $PaCO_2$ is measured) and mmHg.[97] This was used in the calculation of cerebrovascular reactivity (CVR) according to the equation:

$$CVR = \frac{\%\Delta\ CBF}{mmHg\Delta\ EtCO2}$$

as illustrated in *Chapter 1, section 3.*

2.7 Statistical analysis

Generalized additive models for location, shape and scale (GAMLSS), calculated in statistical software *R* (version 3.4.3) were used to estimate normative reference values for grey matter cerebral blood flow (CBF_{GM}). CBF_{GM} was modelled using the Box-Cox Power Exponential (BCPE) distribution, which has four parameters corresponding to the location, scale, skew and kurtosis of the distribution.[98, 99] Age was included as a continuous variable in the models, with sex as a covariate. Interactions between age and sex were also considered. Restricted cubic splines were used in the models to account for the non-linear relationship between CBF and age. Model selection utilised a forward and backward stepwise selection criteria based on the Akaike Information Criterion. Among the baseline/normocapnic cohort, CBF_{GM} was estimated for the 5^{th}, 10^{th}, 25^{th}, 50^{th}, 75^{th}, 90^{th} and 95^{th} percentiles for every fifth year of age between 54 and 84, for both men and women.

Statistical analysis also included linear regressions performed in *STATA.*[100]

Statistical significance was set at $p < 0.05$.

CHAPTER 3: RESULTS

3.1 Study population

Flowcharts outlining the selection of The Irish Longitudinal Study on Ageing (TILDA) participants for inclusion in this magnetic resonance imaging (MRI) study are presented in figures 14 and 15 (*Chapter 2, section 1*). Of 578 participants attending for MRI, data from a total of 468 participants were included in the final baseline/normocapnic analyses. Of 147 participants that attempted the hypercapnic challenge, data from 104 subjects were included in the final hypercapnic analyses.

Demographics and clinical parameters of the baseline/normocapnic and hypercapnic challenge groups are as follows:

Mean age of the baseline/normocapnic and hypercapnic challenge groups at the time of scanning was 68.2 ± 6.9 years and 67.3 ± 6.4 years respectively. 51.7% of the baseline/normocapnic group and 49.0% of the hypercapnic challenge group were female. Mean body mass index (BMI) was 27.8 ± 4.3 in the normocapnic group and 27.3 ± 4.4 in the hypercapnic challenge group. 7.9% and 8.7% of the normocapnic and hypercapnic challenge groups respectively self-reported type 2 Diabetes Mellitus (T2DM), 36.1% and 41.4% respectively reported high cholesterol and 2.4% and 1.9% respectively reported a previous transient ischaemic attack (TIA). 38.5% and 59.6% respectively reported no cardiovascular conditions, 61.5% and 40.4% reported one or more. Mean systolic (MSBP), diastolic (MDBP) and mean arterial (MAP) blood pressures were 134.4 ± 19.3 mmHg/133.1 ± 16.9 mmHg, 80.1 ± 10.5 mmHg/80.5 ± 10.3 mmHg and 98.2 ± 12.5 mmHg/98.1 ± 11.5 mmHg in the normocapnic/hypercapnic challenge groups respectively. 60.5%/64.4% of the normocapnic/hypercapnic challenge groups were not taking antihypertensive medications, 39.5%/35.6% were on one or more. 9.0%/6.7% had a history of excess alcohol consumption, defined by CAGE (alcohol screening) questionnaire score ≥2. 50.9%/55.8% were “never”, 42.5%/41.3% prior and 6.6%/2.9% current smokers. 9.4%/8.7% had depression, as indicated by a Center for Epidemiologic Studies Depression scale (CESD) score ≥9. Mean Mini-Mental State Examination (MMSE) score was 28.9 ± 1.3/1.4 in the normocapnic/hypercapnic challenge cohorts respectively. *See table 4.*

	Normocapnic cohort (n = 468)	Hypercapnic challenge cohort (n = 104)
Age [years]		
Male	68.4 (SD: 7.2, range: 53 - 84)	67.4 (SD: 7.0, range: 54 - 83)
Female	68.0 (SD: 6.7, range: 53 - 84)	67.2 (SD: 5.7, range: 55 - 81)
Sex [% (n)]	Female: 51.7% (242)	Female: 49.0% (51)
Education [% (n)]		
Primary/none	19.7% (92)	22.1% (23)
Secondary	36.3% (170)	39.4% (41)
Third/higher	44.0% (206)	38.5% (40)
BMI[a] [kg/m^2]	27.8 (SD: 4.3, range: 17.9 - 45.8)	27.3 (SD: 4.4, range: 18.1 - 39.8)
T2DM[a] [% (n)]		
Yes	7.9% (37)	8.7% (9)
High Cholesterol[a] [% (n)]		
Yes	36.1% (169)	41.4% (43)
TIA[a] [% (n)]		
Yes	2.4% (11)	1.9% (2)
Number of Cardiovascular Conditions[a, b] [% (n)]		
0	38.5% (180)	59.6% (62)
1	35.9% (168)	32.7% (34)
2+	25.6% (120)	7.7% (8)
MSBP [mmHg]	134.4 (SD: 19.3, range: 87.0 - 211.5)	133.1 (SD: 16.9, range: 92.5 - 179.0)
MDBP [mmHg]	80.1 (SD: 10.5, range: 51.5 - 118.0)	80.5 (SD: 10.3, range: 60.0 - 118.0)
MAP [mmHg]	98.2 (SD: 12.5, range: 64.5 - 143.8)	98.1 (SD: 11.5, range: 70.8 - 138.3)
Antihypertensive Medication(s) [% (n)]		
Yes	39.5% (185)	35.6% (37)
CAGE (alcohol screening) questionnaire[a] [% (n)]		
CAGE < 2	80.1% (375)	83.7% (87)
CAGE ≥ 2	9.0% (42)	6.7% (7)
No response	10.9% (51)	9.6% (10)
Smoker[a] [% (n)]		
Never	50.9% (238)	55.8% (58)
Past	42.5% (199)	41.3% (43)
Current	6.6% (31)	2.9% (3)
CESD [% (n)]		
Non-depressed (CESD <9)	90.6% (424)	91.3% (95)
Depressed (CESD ≥9)	9.4% (44)	8.7% (9)
Mean MMSE	28.9 (SD: 1.3, range: 24 - 30)	28.9 (SD: 1.4, range: 24 - 30)

[a]Self-reported; [b]Cardiovascular conditions: high cholesterol, high blood pressure, angina, heart attack, heart failure, murmur, cardiac arrhythmia, DM, stroke, TIA.
Abbreviations: BMI, body mass index; T2DM, type 2 Diabetes Mellitus; TIA, transient ischaemic attack; MSBP, mean systolic blood pressure; MDBP, mean diastolic blood pressure; MAP, mean arterial (blood) pressure; CESD, Center for Epidemiologic Studies Depression scale; MMSE, Mini-Mental State Examination.

Table 4: Characteristics of the baseline/normocapnic and hypercapnic challenge study samples.

3.2 CBF_{GM} values

Mean grey matter cerebral blood flow (CBF_{GM}) was 36.5 ± 8.2 ml/100g/min.; range 12.9 to 66.4 ml/100g/min.

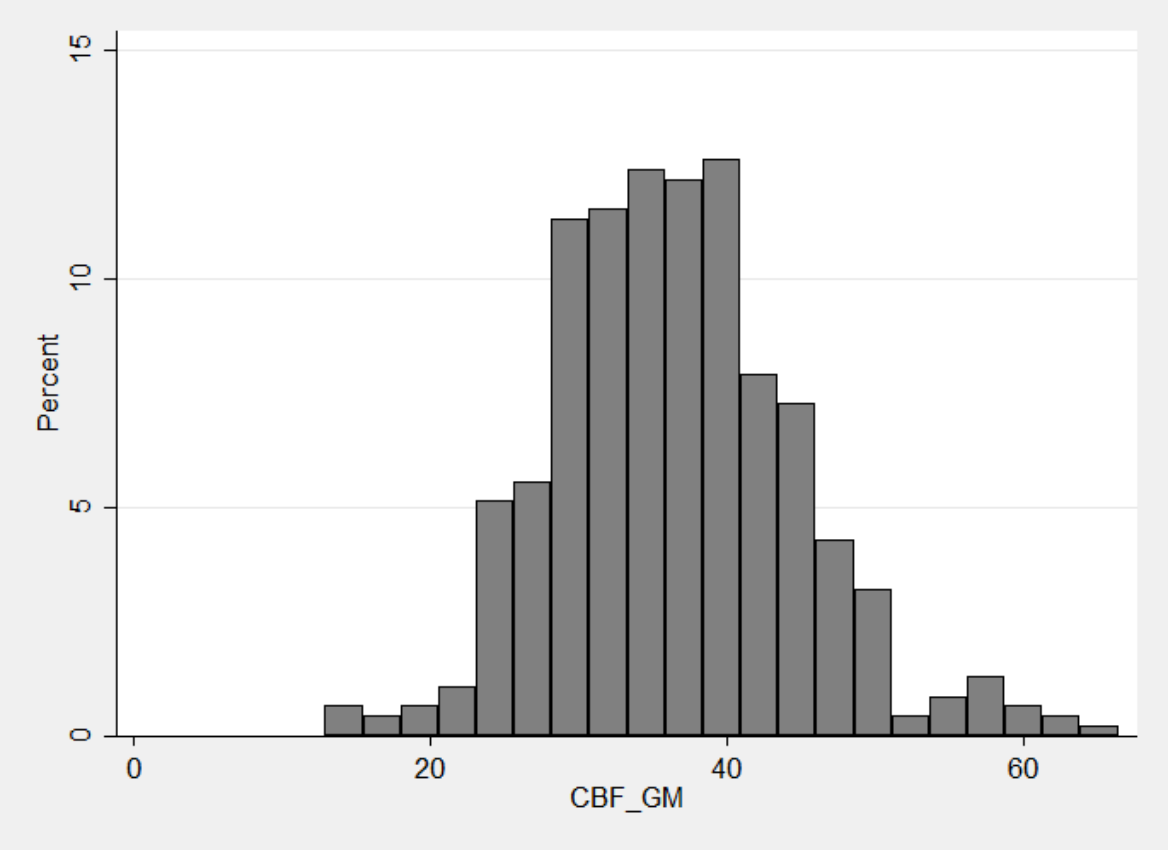

Figure 32: Histogram outlining the distribution of CBF_{GM} in the baseline/normocapnic cohort.

Normative reference values for CBF_{GM} are presented in *table 5* and illustrated in *figure 33,* stratified by age and sex according to percentiles.

In men, mean CBF_{GM} decreased by 15.2% across the age range tested from 37.6 ml/100g/min. (interquartile range [IQR]: 32.1 to 42.1 ml/100g/min.) in the youngest (54 years) to 31.9 ml/100g/min. (IQR: 27.3 to 35.8 ml/100g/min.) in the oldest (84 years). A similar trend was observed in women, with mean CBF_{GM} decreasing by 13.7% from 41.0 ml/100g/min. (IQR: 35.1 to 46.0 ml/100g/min.) to 35.4 ml/100g/min. (IQR: 30.3 to 39.7 ml/100g/min.) across the same age range.

Reference curves demonstrate linear CBF_{GM} decline with age, with comparable overall CBF decrease with time between men and women.

Percentile	Age [years] 54	59	64	69	74	79	84
Male CBF_{GM}							
P95	51.6	50.3	49.1	47.8	46.5	45.2	43.9
P90	47.8	46.6	45.4	44.2	43.0	41.8	40.6
P75	42.1	41.1	40.0	39.0	37.9	36.9	35.8
P50	37.0	36.0	35.1	34.2	33.3	32.36	31.4
P25	32.1	31.3	30.5	29.7	28.9	28.11	27.3
P10	27.5	26.9	26.2	25.5	24.8	24.1	23.4
P05	24.8	24.2	23.5	22.9	22.3	21.7	21.1
Mean ± SD	37.6 ± 10.1	36.6 ± 9.9	35.7 ± 9.6	34.8 ± 9.4	33.8 ± 9.1	32.9 ± 8.9	31.9 ± 8.6
Female CBF_{GM}							
P95	56.3	55.1	53.8	52.5	51.2	49.9	48.6
P90	52.1	50.9	49.8	48.6	47.4	46.2	45.0
P75	46.0	44.9	43.9	42.8	41.8	40.7	39.7
P50	40.3	39.4	38.5	37.6	36.7	35.7	34.8
P25	35.1	34.3	33.5	32.7	31.9	31.1	30.3
P10	30.1	29.4	28.7	28.0	27.3	26.6	26.0
P05	27.0	26.4	25.8	25.2	24.6	24.0	23.3
Mean ± SD	41.0 ± 11.1	40.1 ± 10.8	39.1 ± 10.6	38.2 ± 10.3	37.3 ± 10.1	36.3 ± 9.8	35.4 ± 9.6

Abbreviations: CBF_{GM}, whole grey matter cerebral blood flow [ml/100g/min.], SD = standard deviation.

Table 5: Normative values of cerebral perfusion measured using pcASL MRI, stratified by age in male and female participants (n = 468). Age corresponds to the exact year of age; values for intermediate ages should be estimated by interpolation between supplied values.

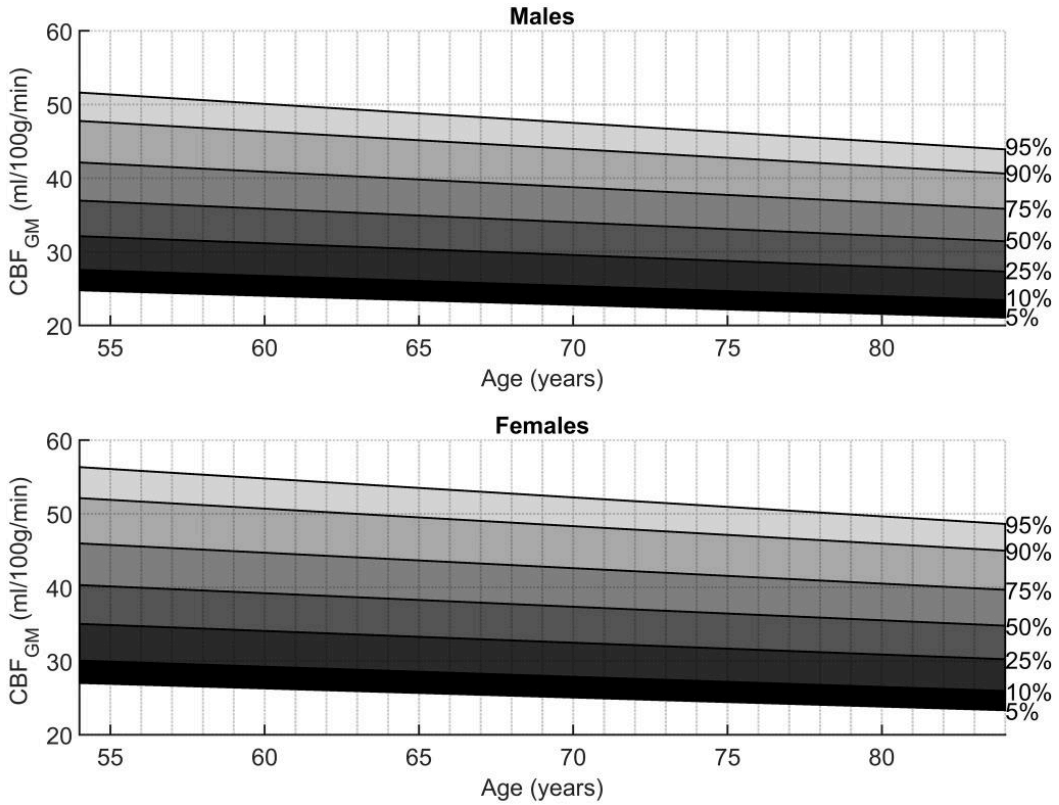

Figure 33: Age-dependence of total CBF_{GM} stratified by sex. Graph displays normative values for CBF_{GM} according to percentiles in male and female participants (n = 468).

3.3 Effect of age on CBF_{GM}

Grey matter cerebral blood flow (CBF_{GM}) decreased by 0.2 ml/100g/min. for every one-year increase in age (95% confidence interval (CI) = -0.28, -0.08, $p \leq 0.001$; linear regression, model adjusted for sex). *See figure 34.*

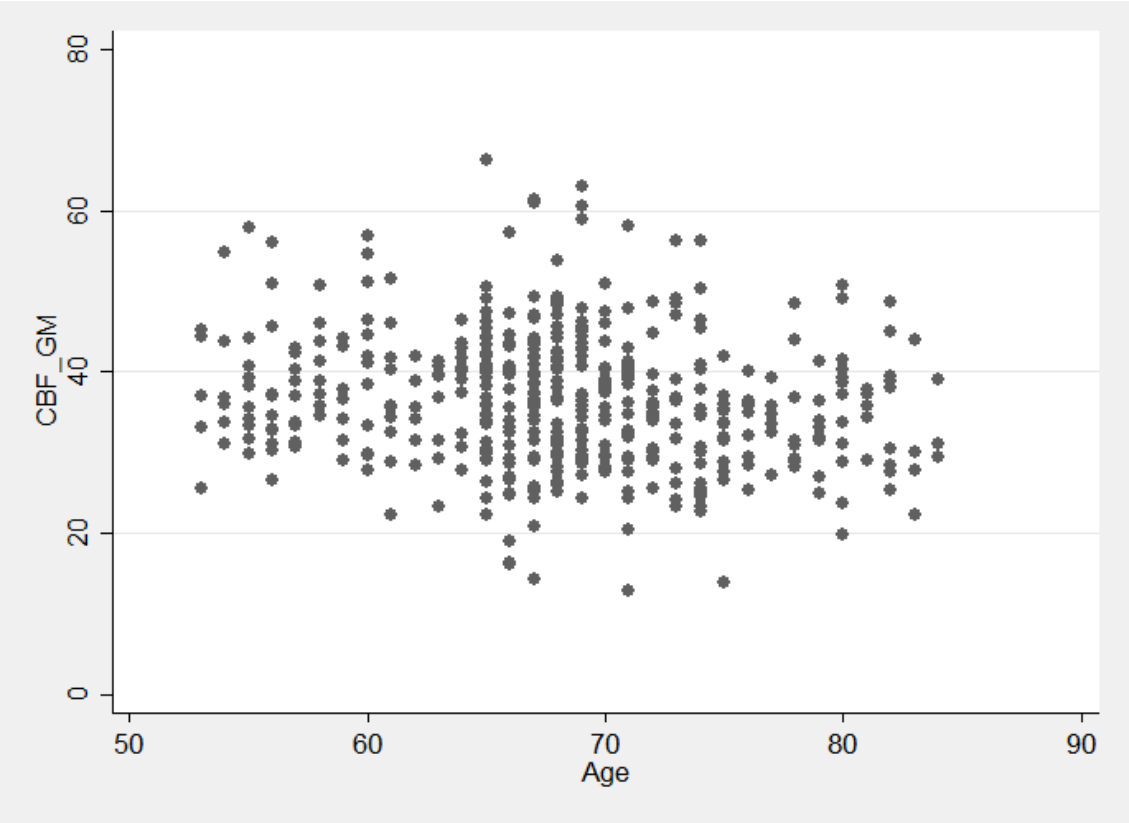

Figure 34: Scatterplot illustrating the negative correlation between CBF_{GM} and age.

3.4 Effect of sex on CBF_{GM}

Grey matter cerebral blood flow (CBF_{GM}) was 3.1 ml/100g/min. higher in females (95% CI = 1.64, 4.54, $p \leq 0.001$; linear regression, model adjusted for age). *See figure 35.*

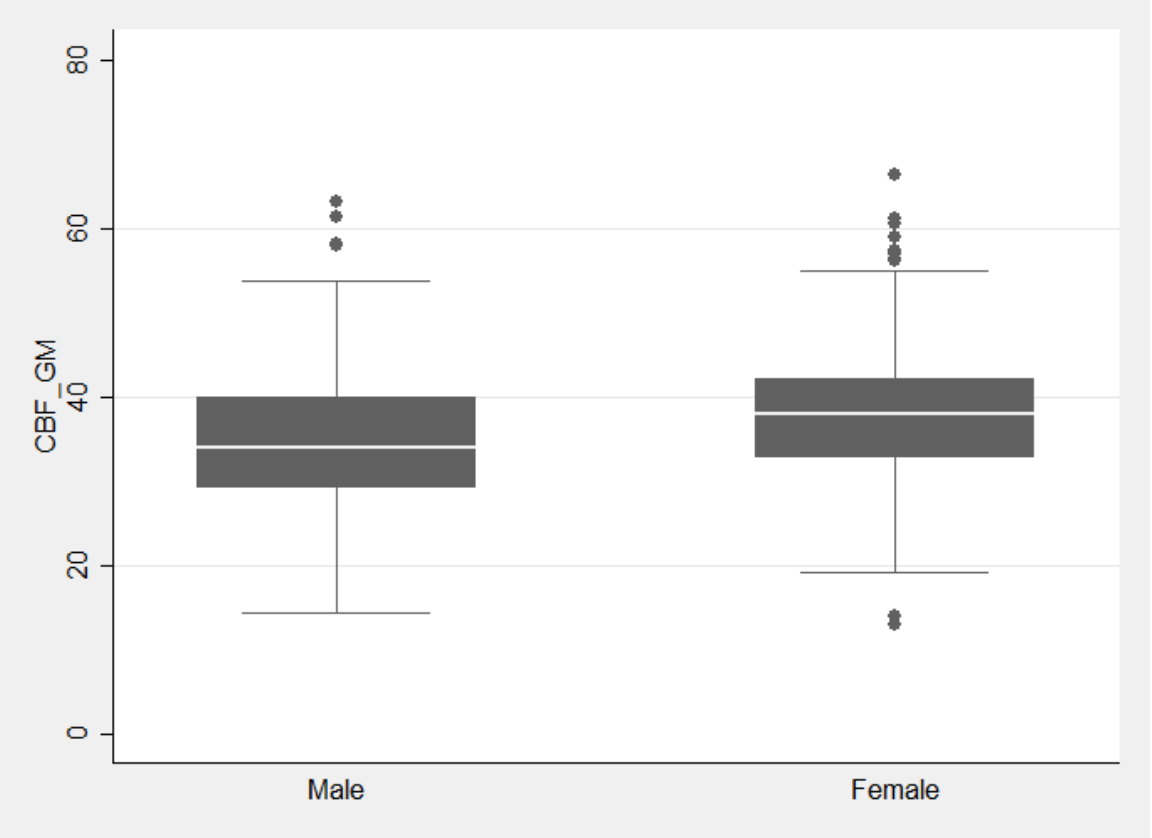

Figure 35: Boxplot illustrating the difference in CBF_{GM} between the sexes.

3.5 Effect of cardiovascular risk factors on CBF_{GM}

Grey matter cerebral blood flow (CBF_{GM}) decreased by 0.3 ml/100g/min. per 1 unit increase in body mass index (BMI) (95% CI = -0.51, -0.18, $p \leq 0.001$; linear regression, model adjusted for age and sex). *See figure 36.*

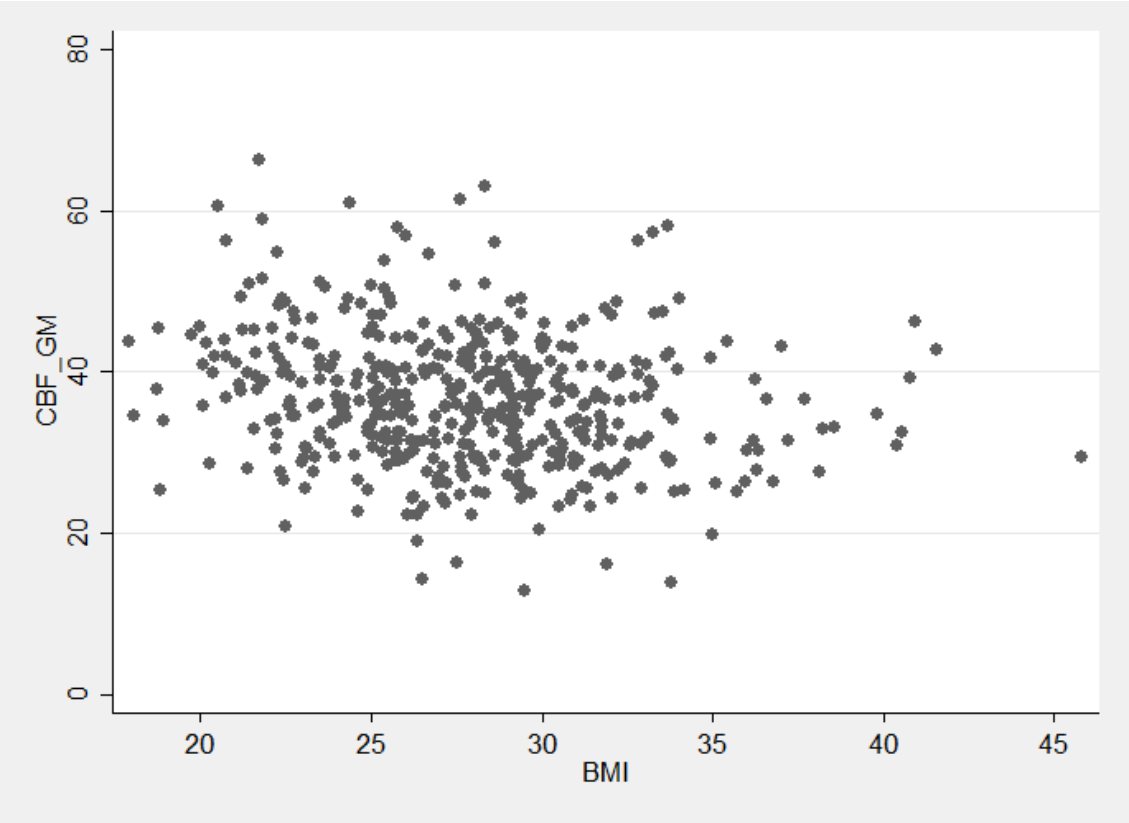

Figure 36: Scatterplot illustrating the negative correlation between CBF_{GM} and BMI.

Grey matter cerebral blood flow (CBF_{GM}) decreased by 0.1ml/100g/min. per 1 mmHg increase in mean systolic blood pressure (MSBP) (95% CI = -0.10, -0.03, $p \leq 0.001$), mean diastolic blood pressure (MDBP) (95% CI = -0.20, -0.07, $p \leq 0.001$) and mean arterial blood pressure (MAP) (95% CI = -0.17, -0.06, $p \leq 0.001$) respectively (all linear regressions, all models adjusted for age and sex). *See figures 37-39.*

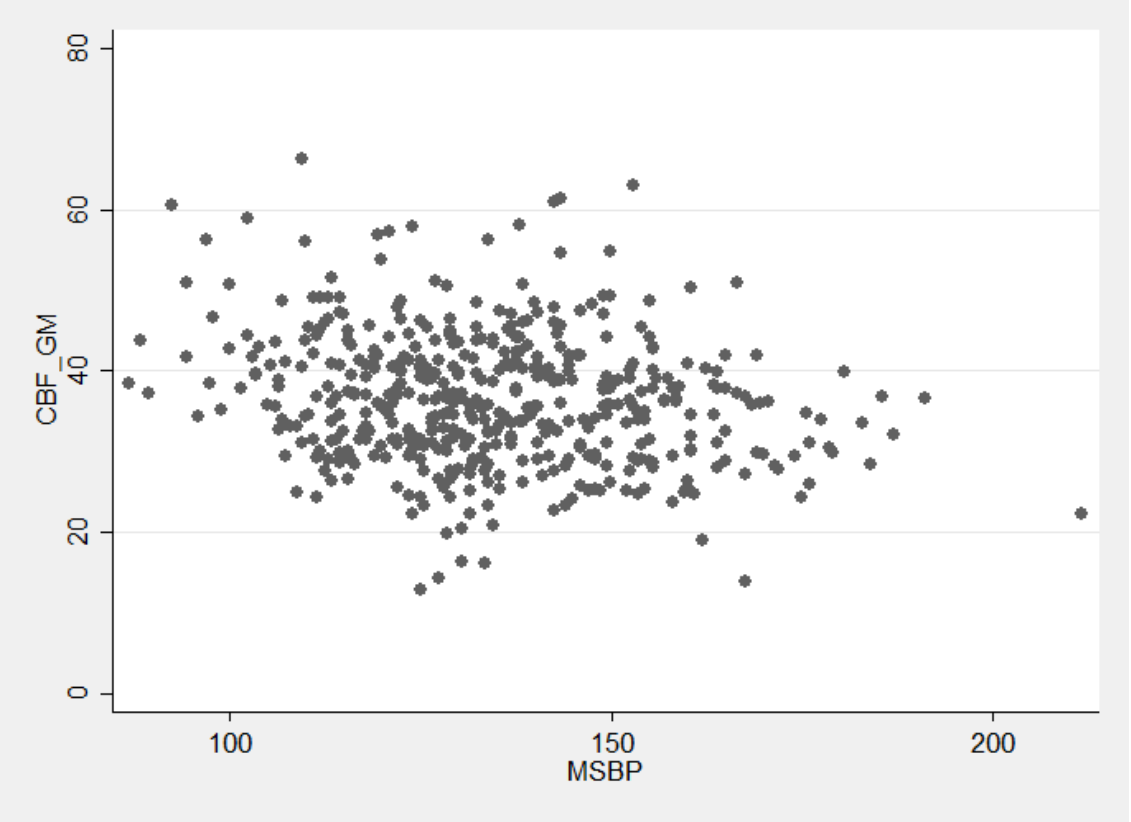

Figure 37: Scatterplot illustrating the negative correlation between CBF_{GM} and MSBP.

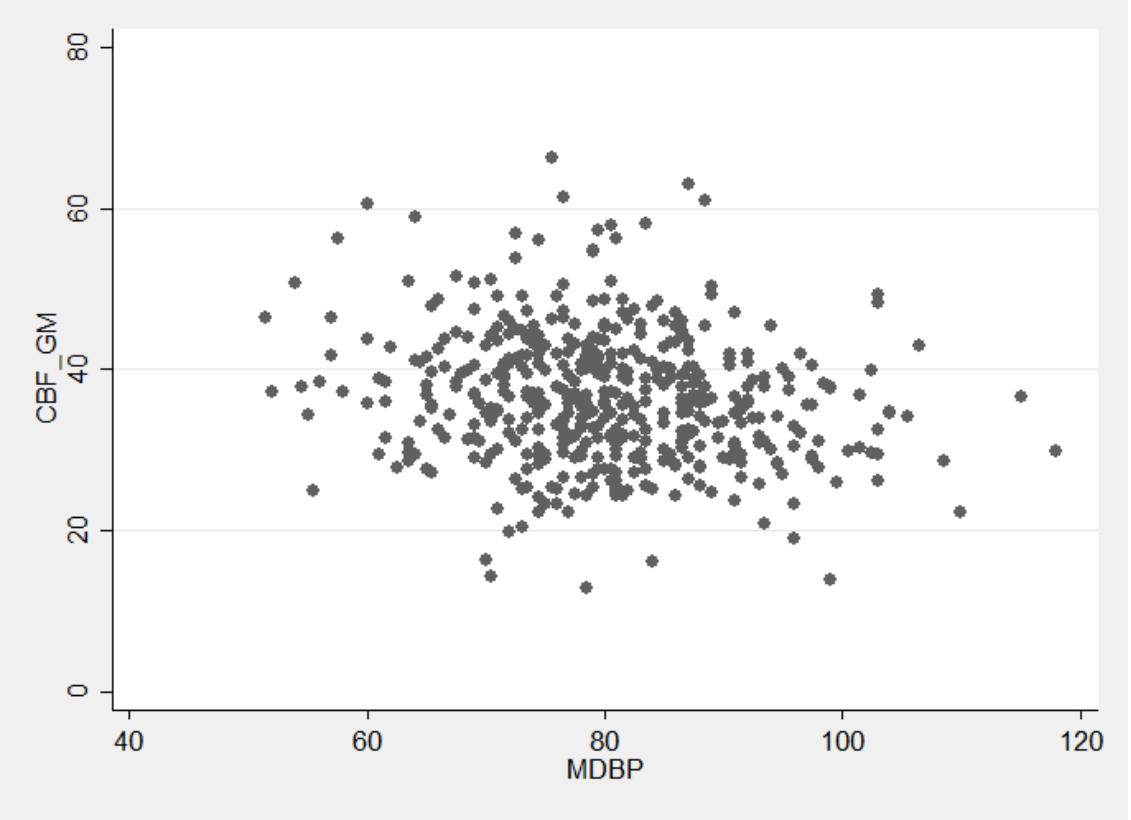

Figure 38: Scatterplot illustrating the negative correlation between CBF_{GM} and MDBP.

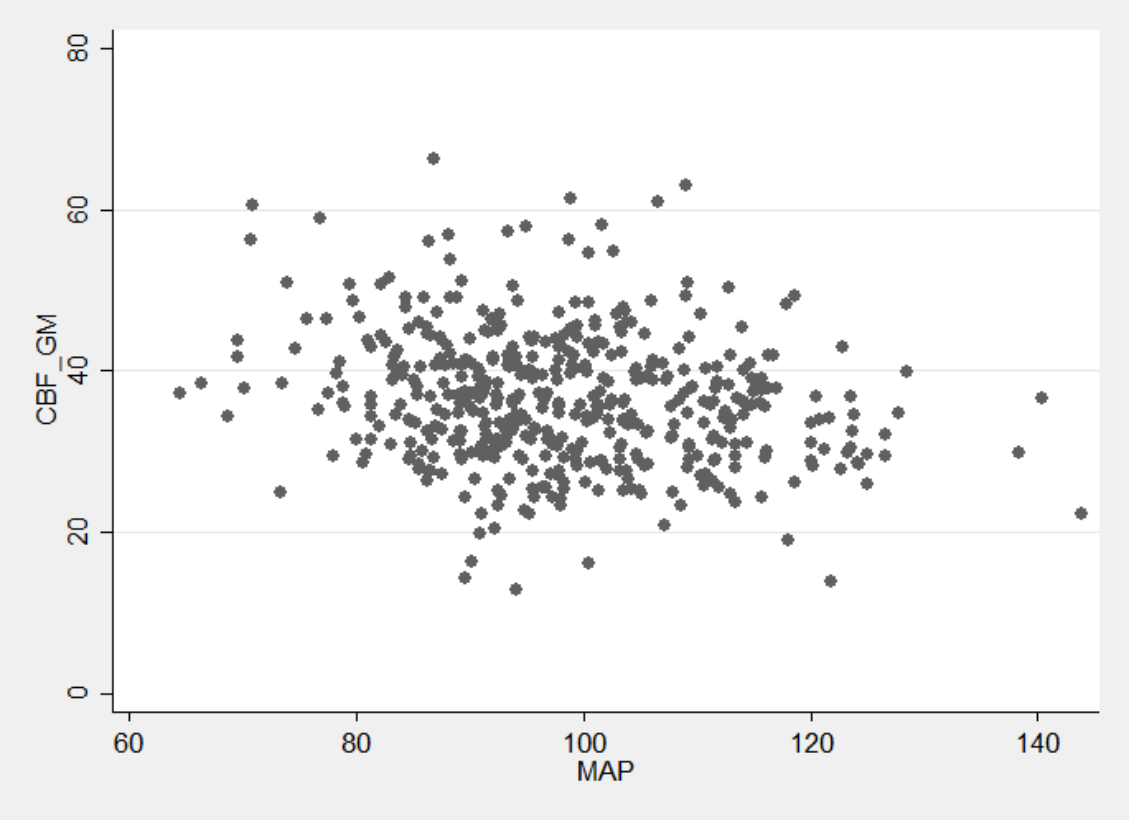

Figure 39: Scatterplot illustrating the negative correlation between CBF_{GM} and MAP.

There was no significant relationship between grey matter cerebral blood flow (CBF_{GM}) and self-reported type 2 Diabetes Mellitus (T2DM) (p = 0.408), high cholesterol (p = 0.328), transient ischaemic attack (TIA) (p = 0.864) or number of cardiovascular conditions (p = 0.919 [CVD=1]/0.657 [CVD≥2]) (all linear regressions, all models adjusted for age and sex).

Grey matter cerebral blood flow (CBF_{GM}) was not significantly lower in subjects on antihypertensive medication(s) (p = 0.244; linear regression, model adjusted for age and sex).

Neither excess alcohol consumption (p = 0.135) nor prior/current smoking was significantly associated with grey matter cerebral blood flow (CBF_{GM}) (p = 0.202 [prior smoking]/0.885 [current smoking]) (both linear regressions, models adjusted for age and sex).

There was no association between grey matter cerebral blood flow (CBF_{GM}) and depressive (p = 0.399; linear regression, model adjusted for age and sex) or

cognitive status (p = 0.512; linear regression, model adjusted for age, sex and educational level). *See table 6.*

	β (95% CI)	P Value
CBF_{GM} (n = 468)		
BMI[a] [per 1 kg/m^2]	-0.3 (-0.51 to -0.18)	**0.001**
T2DM[a] [Ref: No]		
Yes	-1.1 (-3.56 to 1.45)	0.408
High Cholesterol[a] [Ref: No]		
Yes	0.8 (-0.78 to 2.32)	0.328
TIA[a] [Ref: No]		
Yes	0.5 (-5.61 to 6.68)	0.864
Number of Cardiovascular Conditions [a, b] [Ref: 0]		
1	-0.1 (-1.70 to 1.53)	0.919
2+	-0.5 (-2.45 to 1.55)	0.657
MSBP [per 1 mmHg]	-0.1 (-0.10 to -0.03)	**0.001**
MDBP [per 1 mmHg]	-0.1 (-0.20 to -0.07)	**0.001**
MAP [per 1 mmHg]	-0.1 (-0.17 to -0.06)	**0.001**
Antihypertensive Medication(s) [Ref: No]		
Yes	-0.9 (-2.38 to 0.61)	0.244
CAGE (alcohol screening) questionnaire [a] [Ref: CAGE < 2]		
CAGE ≥ 2	-1.3 (-3.03 to 0.41)	0.135
Smoker [a] [Ref: Never]		
Past	-1.0 (-2.45 to 0.52)	0.202
Current	-0.2 (-3.42 to 2.95)	0.885
CESD [Ref: CESD <9]		
Depressed (CESD ≥9)	1.0 (-1.31 to 3.30)	0.399
Mean MMSE[c]	0.2 (-0.38 to 0.75)	0.512

[a]Self-reported; [b]Cardiovascular conditions: high cholesterol, high blood pressure, angina, heart attack, heart failure, murmur, cardiac arrhythmia, DM, stroke, TIA. [c]Adjusted for educational attainment.
Abbreviations: BMI, body mass index; T2DM, type 2 Diabetes Mellitus; TIA, transient ischaemic attack; MSBP, mean systolic blood pressure; MDBP, mean diastolic blood pressure; MAP, mean arterial (blood) pressure; CESD, Center for Epidemiologic Studies Depression scale; MMSE, Mini-Mental State Examination.

Table 6: Age and sex (and education for MMSE) adjusted associations of cardiovascular risk factors/measures, antihypertensive medication(s) and depressive/cognitive status with CBF_{GM}.

3.6 CO_2CBF_{GM}, % change CBF_{GM} and CVR_{GM} values

In the subset of participants who underwent pseudocontinuous arterial spin labeling (pcASL) during both normocapnia and hypercapnia (n = 104), normocapnic grey matter cerebral blood flow (CBF_{GM}) values were similar to those of the baseline ASL cohort, measuring 37.2 ± 7.8 ml/100g/min.; range 24.3 to 61.1 ml/100g/min.

Grey matter cerebral blood flow (CBF_{GM}) increased following the administration of CO_2. Mean hypercapnic grey matter cerebral blood flow (CO_2CBF_{GM}) was 49.9 ± 10.8 ml/100g/min.; range 30.5 to 81.5 ml/100g/min.

Mean percentage (%) change in grey matter cerebral blood flow (CBF_{GM}) between normo- and hypercapnia was 35.2 ± 16.2%; range -10.2 to 64.2%.

Mean cerebrovascular reactivity of the grey matter (CVR_{GM}) was 2.4 ± 1.2; range -0.5 to 4.9. *See figures 40-43.*

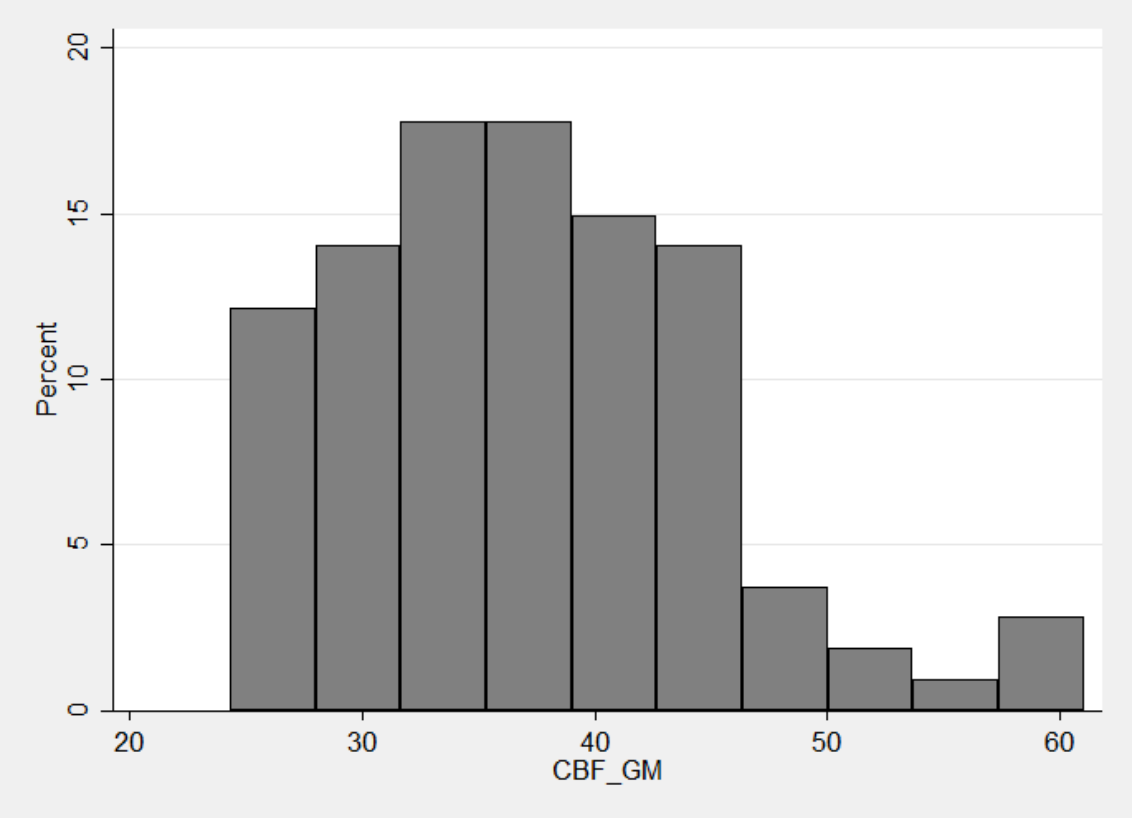

Figure 40: Histogram outlining the distribution of CBF_{GM} in the hypercapnic challenge cohort.

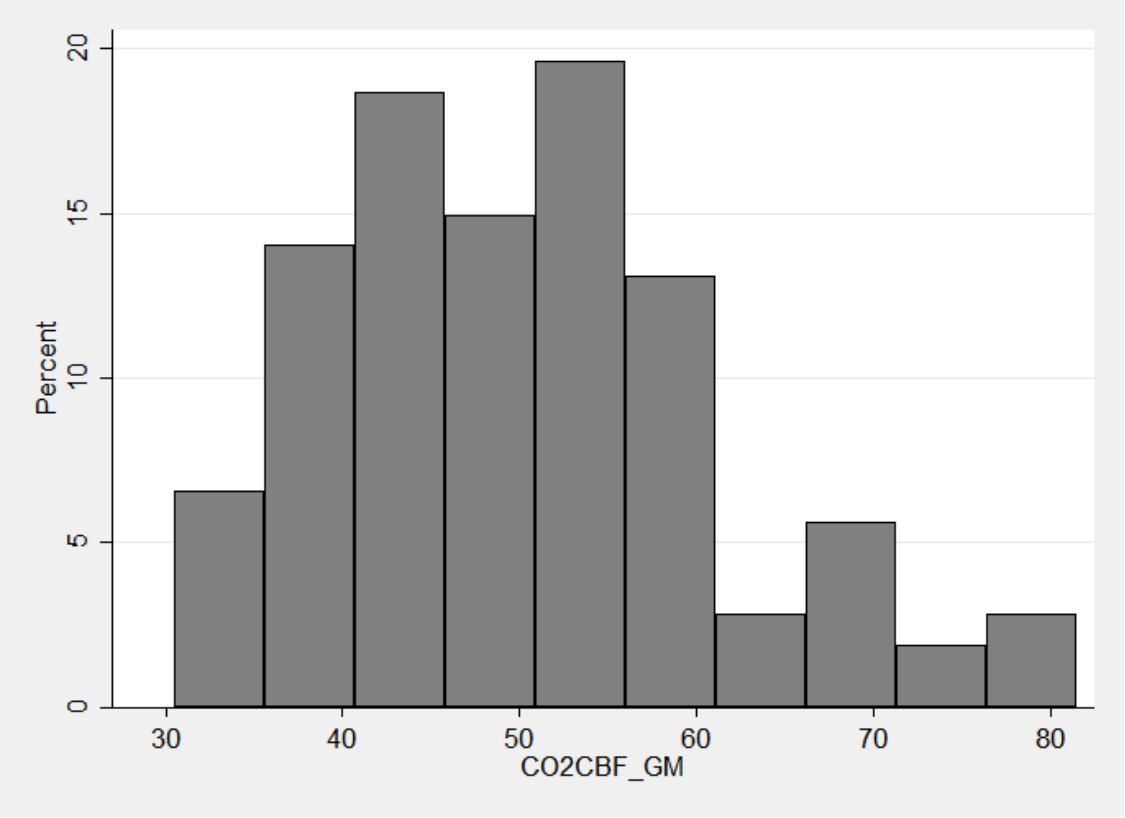

Figure 41: Histogram outlining the distribution of CO_2CBF_{GM} in the hypercapnic challenge cohort.

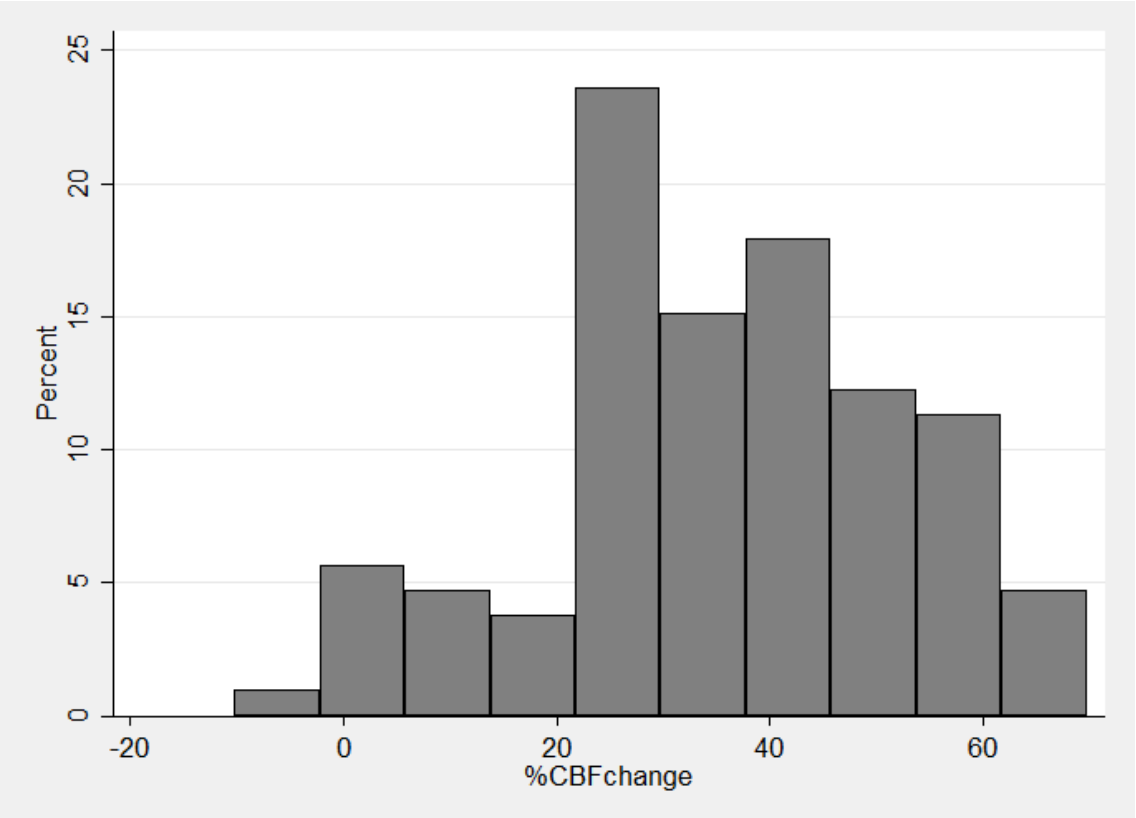

Figure 42: Histogram outlining the distribution of % change CBF_{GM} between normo- and hypercapnia in the hypercapnic challenge cohort.

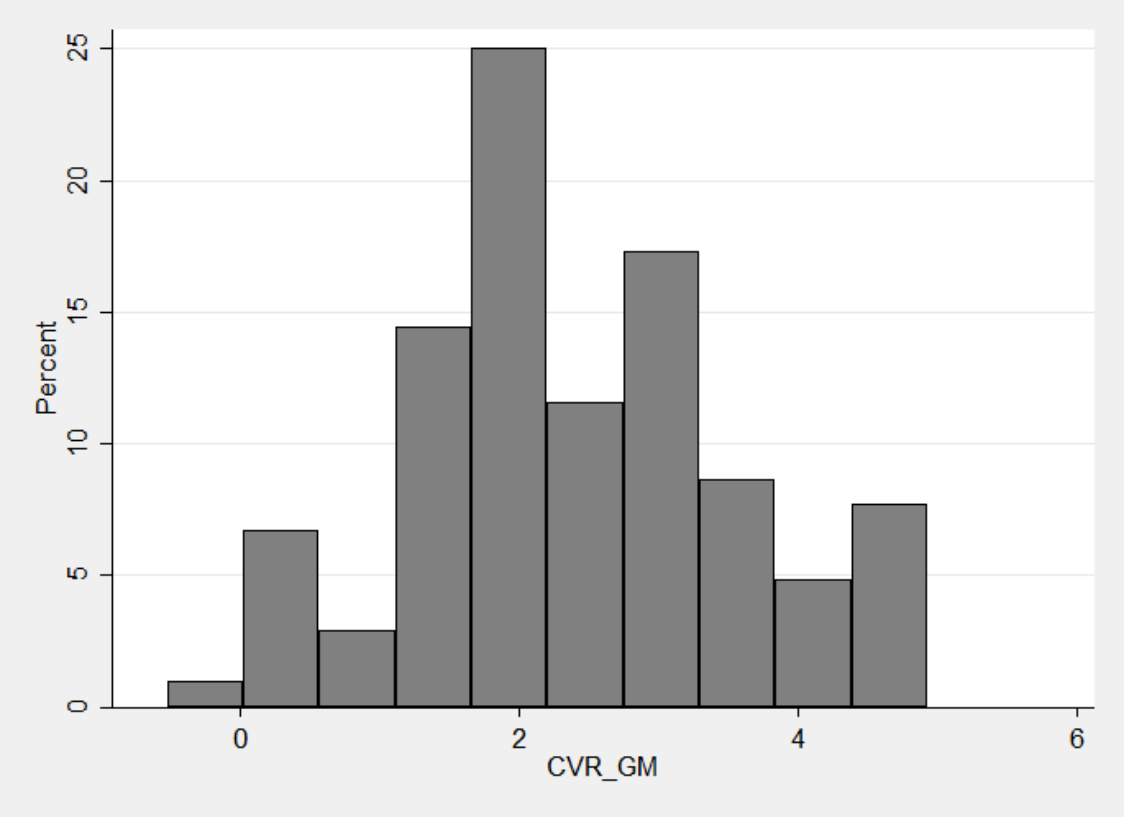

Figure 43: Histogram outlining the distribution of CVR_{GM} in the hypercapnic challenge cohort.

3.7 Effect of age on CVR_{GM}

There was no statistically significant relationship between grey matter cerebrovascular reactivity (CVR_{GM}) and age (p = 0.916; linear regression, model adjusted for sex).

3.8 Effect of sex on CVR_{GM}

There was no statistically significant relationship between grey matter cerebrovascular reactivity (CVR_{GM}) and sex (p = 0.574; linear regression, model adjusted for age).

3.9 Effect of cardiovascular risk factors on CVR_{GM}

Grey matter cerebrovascular reactivity (CVR_{GM}) increased by 0.1 per 1 unit increase in body mass index (BMI) (95% CI = 0.02, 0.12, p = 0.007; linear regression, model adjusted for age and sex). *See figure 44.*

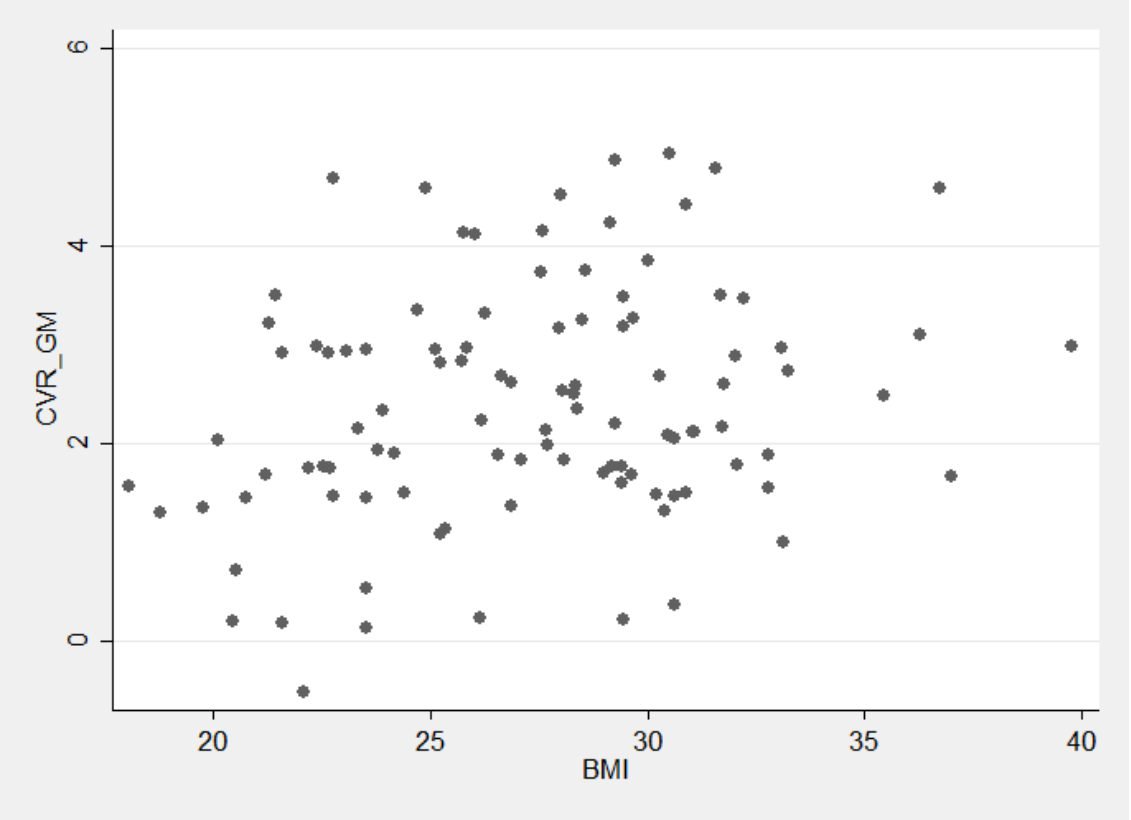

Figure 44: Scatterplot illustrating the positive correlation between CVR_{GM} and BMI.

There was no significant relationship between grey matter cerebrovascular reactivity (CVR_{GM}) and mean systolic blood pressure (MSBP) (p = 0.069), mean diastolic blood pressure (MDBP) (p = 0.522) or mean arterial blood pressure (MAP) (p = 0.201) (all linear regressions, all models adjusted for age and sex).

While prior transient ischaemic attack (TIA) was associated with decreased grey matter cerebrovascular reactivity (CVR_{GM}) (p = 0.038; linear regression, model adjusted for age and sex), there was no association between CVR_{GM} and self-reported type 2 Diabetes Mellitus (T2DM) (p = 0.220), high cholesterol (p = 0.437) or number of cardiovascular conditions (p = 0.618 [CVD=1]/0.706 [CVD≥2]) (all linear regressions, all models adjusted for age and sex).).

There was no significant association between grey matter cerebrovascular reactivity (CVR_{GM}) and antihypertensive medication(s) (p = 0.288; linear regression, model adjusted for age and sex).

Neither excess alcohol consumption (p = 0.975) nor prior/current smoking was significantly associated with grey matter cerebrovascular reactivity (CVR_{GM}) (p =

0.196 [prior smoking]/0.826 [current smoking]) (both linear regressions, models adjusted for age and sex).

There was no association between grey matter cerebrovascular reactivity (CVR_{GM}) and depressive ($p \leq 0.874$; linear regression, model adjusted for age and sex) or cognitive status ($p \leq 0.152$; linear regression, model adjusted for age, sex and educational level). *See table 7.*

	β (95% CI)	P Value
CVR_{GM} (n = 104)		
BMI[a] [per 1 kg/m^2]	0.1 (0.02 to 0.12)	**0.007**
T2DM[a] [Ref: No]		
Yes	0.6 (-0.39 to 1.68)	0.220
High Cholesterol[a] [Ref: No]		
Yes	0.2 (-0.27 to 0.63)	0.437
TIA[a] [Ref: No]		
Yes	-0.5 (-0.88 to -0.03)	**0.038**
Number of Cardiovascular Conditions [a, b] [Ref: 0]		
1	-0.1 (-0.64 to 0.38)	0.618
2+	-0.2 (-1.25 to 0.85)	0.706
MSBP [per 1 mmHg]	0.0 (-0.03 to 0.00)	0.069
MDBP [per 1 mmHg]	0.0 (-0.03 to 0.01)	0.522
MAP [per 1 mmHg]	0.0 (-0.03 to 0.01)	0.201
Antihypertensive Medication(s) [Ref: No]		
Yes	-0.3 (-0.79 to 0.24)	0.288
CAGE (alcohol screening) questionnaire[a] [Ref: CAGE < 2]		
CAGE ≥ 2	0.0 (-1.39 to 1.34)	0.975
Smoker[a] [Ref: Never]		
Past	-0.3 (-0.83 to 0.17)	0.196
Current	0.1 (-0.89 to 1.11)	0.826
CESD [Ref: CESD <9]		
Depressed (CESD ≥9)	0.1 (-0.70 to 0.82)	0.874
Mean MMSE[c]	-0.1 (-0.31 to 0.05)	0.152

[a]Self-reported; [b]Cardiovascular conditions: high cholesterol, high blood pressure, angina, heart attack, heart failure, murmur, cardiac arrhythmia, DM, stroke, TIA. [c]Adjusted for educational attainment.
Abbreviations: BMI, body mass index; T2DM, type 2 Diabetes Mellitus; TIA, transient ischaemic attack; MSBP, mean systolic blood pressure; MDBP, mean diastolic blood pressure; MAP, mean arterial (blood) pressure; CESD, Center for Epidemiologic Studies Depression scale; MMSE, Mini-Mental State Examination.

Table 7: Age and sex (and education for MMSE) adjusted associations of cardiovascular risk factors/measures, antihypertensive medication(s) and depressive/cognitive status with CVR_{GM}.

CHAPTER 4: DISCUSSION

4.1 Cerebral perfusion imaging

As outlined in *Chapter 1*, accurate measurement of cerebral perfusion has, to date, been challenging, due to the limitations associated with many of the imaging techniques traditionally used in the assessment of cerebral blood flow (CBF). [^{15}O]-H_2O positron emission tomography (PET) is currently considered the gold standard for cerebral blood flow (CBF) measurement.[38]

4.1.1 Positron emission tomography

Positron mission tomography (PET) perfusion imaging typically involves intravenous (IV) injection of radioactive [^{15}O]-H_2O, a freely diffusible tracer that enters the brain tissue and is not metabolized.[38] Once equilibrium is reached, the amount of radiotracer within the brain is proportional to blood flow i.e. the PET signal generated reflects cerebral perfusion.

PET, like arterial spin labeling (ASL) magnetic resonance imaging (MRI), quantitatively measures both total and region-specific CBF. It can also be used to calculate cerebral blood volume (CBV), cerebral metabolic rate of oxygen ($CMRO_2$), oxygen extraction fraction (OEF) and glucose metabolism. However, there are distinct disadvantages with PET. It is technically-complex and invasive - involving injection of radioactive pharmaceuticals, arterial blood sampling and ionizing radiation and is therefore poorly suited to repeated studies.[28] Additionally, it is costly, not as widely available as MRI and an on-site cyclotron is required to generate [^{15}O]-H_2O, because of its short half-life.[39]

4.1.2 Arterial spin labeling MRI

One of the main strengths of the present study is the use of arterial spin labeling (ASL) magnetic resonance imaging (MRI), which offers a promising alternative to PET in the assessment of cerebral perfusion. Similar to PET, ASL utilizes a tracer of sorts. However, the “tracer” is a physiological one, generated in-vivo by the magnetic labeling of arterial blood, thereby negating the need for exogenous contrast. Arterial blood is labeled magnetically using 180-degree radiofrequency pulses, which invert the net magnetization of blood water, generating an intravascular contrast i.e. the tag. This can be imaged as it flows into and

exchanges with brain tissue across the blood brain barrier (BBB). The inverted inflowing spins decrease total brain magnetization and thus signal intensity. The process is then repeated without arterial blood labeling to generate a control image. By subtracting two sets of images (tags and controls), a perfusion-weighted map is generated, in which image intensity is proportional to blood flow.[101]

Although there are many competing methods for tagging arterial blood, the optimal labeling technique recommended by the International Society for Magnetic Resonance in Medicine (ISMRM) is pseudocontinuous labeling (pcASL)[27] and it is this technique, which we used in our study.

Strengths of ASL MRI

ASL MRI offers distinct advantages over PET in that it is non-invasive, involving neither exogenous tracer nor ionizing radiation. It has higher spatial resolution than PET.[28] It can be performed as one of a number of sequences in a single MRI study, allowing co-registration of anatomical and functional data. It can be repeated as necessary. It demonstrates excellent intra- and inter-scanner reliability and reproducibility.[45] Its non-invasiveness and repeatability make it an ideal imaging modality for large, population-based and longitudinal studies.

Limitations of ASL MRI

There are some limitations of ASL MRI.

Signal to noise ratio

ASL has low signal to noise ratio (SNR) per unit time. Indeed, the difference in signal intensity between tag and control images is approximately 1%.[102] SNR is directly proportional to magnetic field strength. The strong magnetic field scanner (3 Tesla) used in this study optimized ASL signal. The higher field strength also lengthened the T1 relaxation time of blood, resulting in increased accumulation of labeled spins within the brain tissue and higher perfusion signal.[103] We also employed a 32 channel head coil, which ensured lower noise, higher SNR, higher contrast to noise ratio and improved image quality.[104]

Post labeling delay/arterial transit time

Another challenge in the acquisition of ASL data relates to selection of the post labeling delay (PLD), the time between the end of magnetic labeling and the start of image acquisition (*see Chapter 2, sections 3 & 5)*. Ideally, the PLD would be

sufficient to allow the entire labeled bolus to reach the capillaries and exchange with tissue in the region of interest before any images were acquired. This would maximize the amount of labeled blood contributing to ASL signal and ensure that the signal measured is approximately proportional to tissue perfusion.[31] However, the tracer is constantly decaying. Therefore, optimal PLD is a compromise between acceptable SNR and complete label delivery.[105] Too short a PLD may result in a very small perfusion signal, owing to insufficient time for the tagged spins to arrive at the region of interest. It may also result in unwanted ASL signal within large feeding arteries. Too long a PLD results in a very small ASL signal, indistinguishable from background noise, due to tracer decay.

Arterial transit time (ATT), the time required for blood to travel from the large arteries to the capillaries, increases with age and with cerebrovascular disease. Given that the mean age of our study cohort was 68.2 years, we used a PLD of 1,800 ms, as recommended in the ISMRM consensus paper for healthy subjects less than 70 years.[27] This PLD was chosen to maximise SNR and minimize large vessel arterial signal, in this ageing cohort in whom AATs were likely to be delayed.[26]

Our MRI parameters were modelled on ISMRM recommendations. We used 3T field strength, pseudocontinuous labeling, a label duration of 1.8 s and a PLD of 1.8 s, as well as background suppression, as recommended in the ASL "white paper", to ensure high quality data.[27]

Movement artefact

MRI studies are costly and time-consuming. Thus, for cost and time-effectiveness, MRI data obtained should be of the highest quality possible. Given the susceptibility of MRI to movement artefact, patient comfort and tolerability are key considerations. For this study, we ensured the head coil was tight-fitting in order to limit subject movement. A cushion was placed beneath the subject's head for increased comfort and all participants had noise-attenuating ear defenders.

The hypercapnic challenge, as illustrated in *Chapter 2, section 4,* required that a non-rebreather facemask be fitted to participating subjects, through which a hypercapnic air mixture was delivered. Participants were informed that the altered air composition could have temporary side effects such as increased rate of breathing and/or mild headache. Vital observations of participants were monitored throughout the study and subjects were encouraged to press the emergency call bell if experiencing discomfort. Prior research suggests that carbon dioxide (CO_2)-blood

oxygen level dependent (BOLD) MRI assessment of cerebrovascular reactivity (CVR) is safe, well tolerated and technically feasible in clinical cohorts.[106] The most common symptoms reported by participants are anxiety during hypercapnic breathing and discomfort due to the facemask.[20] At follow-up, most subjects in our study reported that the hypercapnic challenge was tolerable.[107] However, more participants had to be excluded from the smaller hypercapnic challenge cohort than the larger baseline/normocapnic cohort (n = 22 vs. 7) due to motion artefact, possibly secondary to patient discomfort and increased scan duration.

4. 2 Reported CBF values

Most neuroimaging studies have modest sample sizes, with less than 50 subjects.[108] This is primarily due to the financial costs and time associated with performing and analysing magnetic resonance imaging (MRI). Of previous arterial spin labeling (ASL) MRI studies that evaluated cerebral perfusion, there is significant variation in methodology. Not all ASL MRI studies followed the International Society for Magnetic Resonance in Medicine (ISMRM) consensus guidelines.[27] As a result of these discrepancies, as well as physiologic variations in cerebral blood flow (CBF) between individuals, reported cerebral perfusion values in the literature vary greatly. A consensus on normative CBF values has not been reached. Direct comparison between the present study and previous ones is limited, however, the cerebral perfusion values in the present research are in line with those where CBF was measured using 3T pseudocontinuous (pc)ASL MRI according to ISMRM recommendations.[27]

The largest population-based CBF study, the Rotterdam study, used 2D phase contrast (PC) MRI at 1.5T to assess cerebral perfusion. This group reported mean whole brain cerebral perfusion of 56.3 ml/100g/min. in 4759 subjects with a mean age 63.7 years.[52]

ASL MRI has a distinct advantage over PC MRI, as it directly measures CBF at a voxel level as opposed to indirectly measuring blood flow velocities through the internal carotid and vertebral arteries and using these velocities to calculate volumetric blood flow to the brain.[39]

PC MRI estimates of CBF tend to be higher and more variable than pcASL measurements.[109] In a study of 541 healthy, middle-aged subjects comparing pcASL and PC MRI at 3T, Dolui et al. reported CBF values of 47.7 ± 9.8 ml/100g/min. with pcASL vs. 55.8 ± 12.1 ml/100g/min. with PC MRI.[109]

Soni et al. used 3T pcASL MRI to assess cerebral perfusion in 160 volunteers from 6 to 72 years and reported mean global grey matter CBF values of 77.8, 65.4, 58.8 and 48.3ml/100g/min. in children (<12 years), adolescents (12-18 years), adults (18-60 years) and elderly subjects (>60 years) respectively.[58]

Chen et al., using 3T pulsed (p)ASL MRI, reported lower mean cortical grey matter CBF values of 52.6 ± 9.3, 52 ± 10.7 and 42.7 ± 8.8 ml/100g/min. in younger (mean age 30 ± 6 years [n = 11]), middle-aged (52 ± 6 years [n = 38]) and older adults (71 ± 10 years [n = 37]) respectively.[64]

Jefferson et al., who employed pcASL MRI at 3T in an older cohort, reported mean total whole brain grey matter CBF values of 37.3 ± 7.1 ml/100g/min. in 270 adults with a mean age of 73 ± 7 years.[110] These values are comparable to ours (36.5 ± 8.2 ml/100g/min.).

As outlined in *Chapter 1*, CBF and cerebrovascular reactivity (CVR) can be considered important measures of cerebrovascular health. However, the lack of reference values for CBF in the general population has hindered its acceptance as a biomarker of cerebrovascular integrity and has limited researchers and clinicians in distinguishing expected age-related decline from pathological reduction. That is why one of the main aims of this project was to obtain a set of normative values for grey matter CBF in ageing adults.

A major strength of the present work is that a robust statistical method i.e. GAMLSS was employed to model CBF according to age and sex. This was only possible due to the large sample size with a continuum of ages.

The normative values generated in this work are generalizable to the ageing population. We propose that our research, quantifying cerebral perfusion using ASL MRI, will enable improved interpretation of CBF values and advance the use of ASL MRI in clinical practice. By identifying subjects with compromised cerebrovascular

haemodynamics, interventions can potentially be introduced in those at risk of neurodegenerative and/or cerebrovascular diseases.

4.3 Age-related changes in CBF

Our research, consistent with multiple prior studies using different imaging techniques, demonstrates decreasing cerebral perfusion with advancing age.[52, 55-65] While the cross-sectional nature of our study prevents us from drawing conclusions regarding cause and effect, previous studies have suggested that this relationship is likely a consequence of multiple inter-related factors.

Cortical atrophy may play a role,[57] however, cerebral blood flow (CBF) reduction with age persists even when factors like brain atrophy and cortical thinning are accounted for.[64] The Rotterdam group demonstrated the bidirectional nature of the relationship between CBF and brain volume, reporting that smaller baseline brain volume results in steeper decline in CBF over time but also that lower CBF at baseline is associated with accelerated brain atrophy, only in subjects aged 65 years and older.[111] This finding suggests that the relationship between CBF and atrophy may be even more complex in the older population. In our study, we tried to limit the effects of cortical atrophy on CBF measurements by choosing a reasonably conservative threshold of 70% grey matter (GM) to reduce the partial volume effect on mean CBF_{GM} values *(see Chapter 2, section 5.3).*

There are likely multiple additional factors contributing to decreased CBF with age.

As outlined in *Chapter 1*, *section 2,* changes in neuronal/metabolic activity result in alterations in local perfusion, via a process known as neurovascular coupling. Therefore, factors such as neuronal loss, reduced neuronal size and/or synaptic density, diminished neuronal activity[53, 57] and decreased metabolic activity and/or reduced metabolic demand,[57, 61] all of which have been observed with ageing, likely contribute to declining CBF with age.

Furthermore, blood viscosity, which is one of the major determinants of blood flow (*see Chapter 1, section 2)*, is significantly higher in elderly subjects;[112] this may also contribute to the decline in CBF with age.

Additionally, both normal ageing and hypertension (HTN), and to a lesser extent other cardiovascular risk factors like obesity, are associated with arterial stiffening. In healthy young adults, the elastic proximal aorta is more compliant than the stiff, muscular carotid arteries. This impedance mismatch between vessels causes wave reflection and transforms intermittent, highly pulsatile cardiac energy into steady, minimally pulsatile cerebral blood flow. However, stiffening of the central arteries, as occurs with age and HTN, causes equalization of aortic and carotid rigidity. Loss of the protective impedance mismatch between vessels results in transmission of harmful high-pressure energy to the brain and damages the cerebral microvasculature.[113] Tarumi et al., using transcranial Doppler (TCD), demonstrated an association between increased CBF pulsatility and cerebral hypoperfusion in older adults.[114] Similarly, increased aortic pulse wave velocity (PWV), a marker for arterial stiffness, has been associated with decreased blood-flow-volume towards the brain and regional cerebral hypoperfusion in older adults using velocity-encoded and pseudocontinuous arterial spin labeling (pcASL) magnetic resonance imaging (MRI) respectively.[110, 115]

The Dallas Lifespan Brain Study demonstrated increased cerebral metabolic rate of oxygen ($CMRO_2$) despite decreased CBF with age. This disparity between increased demand and decreased supply further strengthens the argument that disruption of the brain's normal homeostasis occurs with ageing.[61]

Evidently, ageing itself is associated with dysregulation of the mechanisms that maintain adequate brain perfusion. The challenge lies in distinguishing expected age-related decline in cerebral perfusion from pathological reduction. The normative reference values outlined in this paper should aid in making that distinction.

4.4 Sex-related changes in CBF

This research, consistent with prior studies using arterial spin labeling (ASL) magnetic resonance imaging (MRI) and other perfusion imaging techniques, corroborates higher cerebral blood flow (CBF) in females compared to males.[52, 56, 57, 62, 65] While this cross-sectional study does not allow for causal inference, previous studies have suggested that this finding may reflect lower haematocrit and blood viscosity, increased oestrogen levels[57] and higher cerebral metabolic rates of glucose and oxygen in women.[116]

Lower haematocrit is associated with higher CBF for two reasons - reduced haematocrit results in decreased blood viscosity and hence increased CBF. Additionally, reduced haematocrit and therefore reduced blood oxygen carrying capacity may result in increased CBF in order meet cerebral oxygen demands.[65]

Oestrogen is known to have both vascular and neuroprotective effects.[56] However, as only 13 of the women in our baseline/normocapnic cohort were pre-menopausal, oestrogen is unlikely to be a contributing factor to sex-related differences in cerebral perfusion in our cohort.

Given the complex interactions between neuronal/metabolic activity and CBF via neurovascular coupling, higher cerebral metabolic rates of glucose and oxygen in women could result in increased CBF.

4.5 Cardiovascular determinants of CBF

Unsurprisingly, given that cerebral blood flow (CBF) is considered a measure of cerebrovascular health, various cardiovascular risk factors including body mass index (BMI), [55, 59, 62, 66] hypertension (HTN),[59, 67-69] hypercholesterolaemia,[52] type 2 Diabetes Mellitus (T2DM),[55, 70] metabolic syndrome[62, 71] and smoking[52, 59] have also been shown to reduce CBF. In this study, we sought to assess the effects of various modifiable risk factors, including BMI and blood pressure (BP) on cerebral perfusion.

4.5.1 Body mass index

We found, as with prior studies,[55, 59, 62, 66] that elevated body mass index (BMI) reduces CBF. While the cross-sectional nature of our study prevents us from drawing conclusions as to the cause of this finding, prior research suggests that obesity alters both cerebral artery function and structure.

Obesity is associated with defective endothelium dependent-dilatation, mainly due to decreased nitric oxide (NO) production and availability secondary to oxidative stress.[10] Additionally, impaired insulin-induced cerebral vasodilatation and compromised potassium channel function may play a role.[10]

Obesity may also cause cerebral artery remodelling. Animal studies report decreased middle cerebral artery luminal diameters in high-fat fed rats, as well as

increased wall thickness and increased wall to lumen ratio. These changes manifest as arterial stiffening[10] and ultimately decreased compliance of the cerebrovasculature.

4.5.2 Hypertension

Similar to prior studies, [59, 67-69] we found that hypertension (HTN) has adverse effects on cerebral perfusion.

Muller et al. in a large (n = 575), longitudinal phase contrast (PC) magnetic resonance imaging (MRI) study, demonstrated decreased cerebral blood flow (CBF) independent of other vascular risk factors, carotid atherosclerosis and established cerebrovascular pathology on MRI in patients with increased blood pressure (BP).[68]

Like obesity, HTN affects the structure and function of the cerebrovasculature and can also impair blood brain barrier (BBB) function.

Increased vascular resistance is the hallmark of HTN and occurs due to vascular remodelling. Increased tensile stress in the setting of HTN causes vascular smooth muscle hypertrophy/hyperplasia and increased collagen deposition in the tunica media of resistance arteries. These changes result in increased arterial wall thickness, decreased luminal diameter and increased vessel stiffness/decreased vessel elasticity.[11] The aim of vascular remodelling is to protect downstream vessels from the harmful effects of increased BP. However, as with obesity, vascular remodelling/arterial stiffening reduces the compliance of the cerebrovasculature and may increase the risk of cerebral hypoperfusion. While the haemodynamic effects of increased BP certainly contribute to vascular remodelling, other factors including alterations in the renin-angiotensin-aldosterone system may play a role.[11]

HTN is also associated with loss of cerebral arterioles and capillaries.[11]

Vascular function is also adversely affected by HTN. Regulation of myogenic reactivity (i.e. the ability of the vessels to alter their calibre in response to changes in intraluminal pressure) is impaired in subjects with HTN. This is a consequence of impaired endothelial function, involving nitric oxide (NO) and prostacyclin among other factors.[11] As with obesity, NO-dependent dilatation is also impaired by oxidative stress, a common finding in patients with HTN.[11]

Additionally, HTN increases the permeability of the BBB and its ability to regulate central nervous system homeostasis. This likely occurs due to physical damage to the BBB caused by high BP, vascular remodelling, oxidative stress and inflammation.[11]

As illustrated in *section 3* of this chapter, HTN also causes stiffening of the large arteries, which can result in transmission of harmful high-pressure pulsatility to the cerebral microvasculature.

HTN also results in the upper and lower limits of the autoregulatory system being displaced to higher BP levels.[117] This means that in subjects with HTN, cerebral hypoperfusion can occur at higher levels of mean arterial blood pressure (MABP) compared to normotensive subjects.

Evidently, HTN can have detrimental structural and functional effects on the cerebrovasculature with resultant negative impact on cerebral perfusion. It is unsurprising, therefore, that this research, as with prior studies, demonstrated reduced CBF in the context of elevated BP.
This study found no significant association between grey matter perfusion and self-reported type 2 Diabetes Mellitus (T2DM), high cholesterol, transient ischaemic attack (TIA), number of cardiovascular conditions or smoking, possibly due to the reasonably small numbers of participants with these conditions among our study sample.

4.6 Reported CO_2CBF, % change CBF and CVR values

There is a paucity of literature detailing reference hypercapnic cerebral blood flow (CO_2CBF), % change CBF (between normo- and hypercapnia) and cerebrovascular reactivity (CVR) values, especially in older adults. Indeed, a prior systematic review and meta-analysis failed to establish normative CVR values due to significant methodological and clinical diversity between studies.[20] There is no universally defined method for measuring CVR. Of prior magnetic resonance imaging (MRI) studies that assessed CVR, there is significant variation in imaging techniques employed, sample size and cohort characteristics.[63, 74, 110, 118] The vast majority of previous MRI studies that assessed CVR utilized blood oxygen level dependent (BOLD) as opposed to arterial spin labeling (ASL)[20] As outlined in *Chapter 1, section*

7, BOLD does not provide a direct measure of CBF/CVR,[48] whereas ASL exclusively and quantitatively measures CBF and therefore provides a superior measure of CVR.

As with CBF, the CVR study that is most comparable to ours is that by Jefferson et al.[110] This group used pseudocontinuous (pc)ASL MRI at 3T in a large, elderly sample (mean age 73 ± 7 years, n = 270) to assess mean total whole brain CVR and reported CVR values of 2.2 ± 1.6, which are similar to ours (2.4 ± 1.2, range -0.5 to 4.9). Unfortunately, Jefferson et al. do not report hypercapnic/CO_2CBF or % change CBF values in this paper.

Our CBF change and CVR values are similar to those reported by Gauthier et al.[63] This group, in a smaller cohort of 62 subjects (31 younger, mean age 23 ± 3 years age and 31 older, mean age 64 ± 5 years age) assessed CBF using hypercapnic pcASL and BOLD MRI at 3T. They observed average grey matter CBF increases of 14.3 ± 1 ml/100g/min. and 10 ± 1.2 ml/100g/min. in younger and older subjects respectively between normo- and hypercapnia. This compares to 12.7 ml/100g/min. in our study. They obtained mean ASL grey matter CVR values of 3 ± 0.2 and 2.1 ± 0.2 in younger and older cohorts respectively, the latter being comparable to ours (2.4).

We did not attempt to document normative CVR values in the hypercapnic challenge cohort, as the hypercapnic challenge sample (n = 104) was much smaller than the baseline/normocapnic sample (n = 468) and a large sample size with a continuum of ages is required to effectively model variables using GAMLSS.

4.7 Age-related changes in CVR

In our study, we observed no significant association between cerebrovascular reactivity (CVR) and age. However, as with cerebral blood flow (CBF), prior cross-sectional and longitudinal studies have reported significant differences in CVR between younger and older subjects. [60, 61, 63, 72, 73]

Importantly though, these studies varied greatly in terms of imaging techniques (^{133}Xenon single photon emission computed tomography (SPECT), arterial spin

labeling (ASL) and blood oxygen level dependent (BOLD) magnetic resonance imaging (MRI)) and vasoactive stimuli (100% oxygen, carbon dioxide (CO_2)) used.

The Dallas Lifespan Brain Study demonstrated faster CVR decline with age when compared with CBF.[61] This group assessed regional CBF using ASL MRI in 226 healthy adults and regional CVR using hypercapnic BOLD MRI in 152 healthy adults and reported an 18% decrease in average prefrontal CBF and a 54% decrease in average prefrontal CVR when subjects in their 80s were compared with those in their 20s.

Interestingly, de Vis et al., who used both pseudocontinuous (pc)ASL and BOLD MRI to measure CVR in 20 young (28 ± 13 years) and 45 older (66 ± 14 years) subjects, observed a significant difference in mean whole brain CVR between younger and older subjects using BOLD but not with ASL MRI.[60]

As illustrated in *Chapter 1, section 7,* ASL is superior to BOLD MRI in the assessment of CVR as it solely and quantitatively measures CBF and unlike BOLD, is not influenced by other factors such as cerebral blood volume (CBV), cerebral metabolic rate of oxygen ($CMRO_2$), oxygen extraction fraction (OEF) and haematocrit.[48] Therefore, it is unclear whether the decline in CVR observed in BOLD studies is a true finding or relates to other physiological changes associated with ageing.

As outlined in *sections 3 and 5* of this chapter*,* age and HTN are associated with increased aortic stiffness, which impairs vascular reactivity. The Framingham Heart study, using Doppler ultrasound (US), reported an association between increased aortic stiffness, increased pressure pulsatility and blunted reactivity of the peripheral microvasculature to ischemic stress.[119] Similarly, increased pulse wave velocity (PWV), a measure of arterial stiffness, has been associated with decreased cerebrovascular reserve using [^{15}O]-H_2O positron emission tomography (PET).[56] Jefferson et al., using ASL MRI, investigated the complex relationship between aortic stiffening and cerebral haemodynamics. In community-dwelling older adults with normal cognition but not those with impaired cognition, they observed lower CBF and higher CVR. They postulated that because age-related changes in vascular structure/resistance due to arterial stiffening occur over time, intact cerebrovasculature may adapt to preserve vasoreactivity, whereas in subjects with

cognitive impairment (CI) in whom cerebrovascular damage is already likely, CVR may be disturbed.[110]

The strength of the CVR response is related to the density of the cerebral arterioles. Cortical atrophy and neuronal loss that occurs with normal ageing is likely to be accompanied by loss of cerebral arterioles and capillaries, which could contribute to declining CVR with age.

Our research cohort, unlike earlier referenced studies,[60, 61, 63, 72, 73] consisted solely of older adults, without a younger cohort for comparison. It is likely that if there is an association between increasing age and declining CVR, that the relationship is non-linear. It may be that the mechanisms underpinning declining CVR with age have already taken effect by middle-age. This might explain the lack of significant association between CVR and age in our older cohort. In the Dallas Lifespan Brain Study, steep declines in CVR were observed at the extremes of age, with less severe decline in CVR in middle-aged adults. Therefore, in our cohort with a limited age range of between 54 and 83 years (mean 67.4), it is possible that the postulated decline in CVR with age was not detectable.

The fact that CVR appears to be impaired in certain middle to older-aged adults merits attention. It might indicate that while some adults have sufficient blood flow to maintain cerebral perfusion under normal resting conditions, the ability of the cerebrovasculature to increase CBF in response to a challenge is impaired, thereby predisposing to transient cerebral ischaemia.

Miller et al. demonstrated a greater mean arterial blood pressure (MAP) increase in older vs. younger adults during hypercapnia, despite similar blood pressure (BP) levels at rest.[120] This suggests that older adults may be more reliant on perfusion pressure to increase CBF in response to a vasoactive challenge, because of impaired vasodilatation to carbon dioxide (CO_2).

Clearly the relationship between CVR and ageing is complex and, as of yet, poorly understood. Further standardized research, ideally using ASL MRI, will aid in exploring this relationship further.

4.8 Sex-related changes in CVR

Cerebrovascular reactivity (CVR), unlike cerebral blood flow (CBF), does not appear to be influenced by sex. As in this study, prior researchers have demonstrated CBF reductions in men, without corresponding CVR decreases.[55, 61]

4.9 Cardiovascular determinants of CVR

4.9.1 Body mass index

In our study, we observed increasing cerebrovascular reactivity (CVR) with body mass index (BMI). This finding is consistent with that of Selim et al.[55] but is discrepant from other studies. [121, 122]

Obesity, as outlined in section *5.1* of this chapter, can alter both arterial function and structure. It is associated with defective vasodilation and arterial stiffening, which decreases vessel compliance.[10] Thus, it stands to reason that CVR may be impaired in patients with elevated BMI.

Selim et al. using transcranial Doppler (TCD) demonstrated decreased blood flow velocity and increased resistance in the middle cerebral arteries (MCA) of overweight and obese subjects, as well as increased CVR.[55] In our study, we observed similar findings of significantly decreased CBF and significantly increased CVR in the context of elevated BMI. Selim et al. do not postulate as to the mechanisms underpinning their findings. It may be that elevated CVR in the context of obesity represents a compensatory adaptation. Obesity induces functional and structural changes in the cerebrovasculature, which damage CBF. Consequently, the cerebrovasculature may adapt by becoming more reactive, to ensure adequate brain perfusion in the face of increased orthostatic stress. Prospective studies will assist in exploring this association further.

4.9.2 Hypertension

Prior studies have demonstrated impaired CVR in the context of hypertension (HTN),[35, 74, 75] however our research demonstrated no significant association between CVR and blood pressure (BP).

Like BMI, it stands to reason that HTN could negatively affect CVR. Elevated BP causes structural arterial changes, as illustrated in *section 5.2* of this chapter. Increased tensile stress within resistance arteries results in arterial wall thickening, decreased luminal diameter and increased wall to lumen ratio. Arterial wall thickening increases vessel rigidity/resistance and decreased vessel compliance/reactivity.[11]

HTN is also associated with rarefaction of cerebral arterioles and capillaries, which may blunt the CVR response.[11]

Impaired endothelial vasodilation is observed in the context of HTN.[11] HTN is associated with decreased levels of nitric oxide (NO), which is a key determinant in the ability of the cerebrovasculature to respond appropriately to carbon dioxide (CO_2).[35] HTN also promotes the release of vasoconstrictors from the vascular endothelium. Thus, when a vasodilator is administered, as in the assessment of CVR, the constrictive effects of HTN on the vascular endothelium must first be overcome before vasodilation can occur.[35]

In our study, there was no significant association between mean diastolic blood pressure (MDBP)/mean arterial blood pressure (MAP) and CVR but there was an association between increased mean systolic blood pressure (MSBP) and reduced CVR, which approached significance (p = 0.069). Among our cohort of community-dwelling ageing adults, MDBP, at 80.1 mmHg was well-controlled (normal MDBP < 80 mmHg), whereas MSBP was elevated at 134.4 mmHg (normal MSBP <120 mmHg). This may account for the negative trend observed between MSBP and CVR, without correspondent association between MDBP and CVR.

4.9.3 Transient ischaemia attack

While our research demonstrated a significant association between CVR and prior transient ischaemic attack (TIA) (p = 0.038), the very small sample size of the hypercapnic TIA cohort (n = 2) negates the significance of this finding. Future studies with larger cohorts can further explore this potential association. *See section 12 of this chapter for further detail on the relationship between CVR and TIA risk.*

Our research identified no significant association between grey matter cerebrovascular reactivity and self-reported type 2 Diabetes Mellitus (T2DM), high

cholesterol, number of cardiovascular condition(s) or smoking, possibly due to the small numbers of participants with these conditions in our hypercapnic challenge cohort.

4.10 Ageing, dementia and stroke

The world's older population is growing disproportionately. The global population aged 60 years and older is predicted to increase from 901 million to 2.1 billion between 2015 and 2050, with an anticipated greater than threefold increase in those aged 80 years and older.[50] In Ireland, 59% and 95% increases are expected in the ≥65 and ≥85 populations respectively between 2016-2031.[123]

Ageing is associated with increased morbidity and mortality from multiple causes, including dementia and stroke, for which it is among the most important risk factors.[51] Between 2010 and 2050, the incidence of dementia worldwide is expected to triple[124] and the number of incident strokes in the United States of America (USA) is predicted to double.[125]

Dementia is one of the top ten causes of disability in both men and women over the age of 60.[50] Stroke is the second most common cause of death worldwide and one of the leading causes of long-term disability.[126]

By 2030, the global cost of dementia will reach US$2 trillion[127] and the cost of stroke in the USA alone will average US$241 billion.[126] The significant financial costs associated with increased incidence of both dementia and stroke will pose a major economic challenge in Ireland, where our healthcare system is already poorly resourced.

Here in Ireland, overcrowding in acute hospitals is commonplace, long-term care and community-based services are inadequate and access to allied health professionals is limited. Increased incidence of dementia and stroke, amongst other chronic non-communicable diseases, over the coming decades, has the ability to overwhelm our health services.

Increased prevalence of both dementia and stroke will also have profound social and personal consequences. Because of the disability imposed by these conditions,

patients often require care and assistance with basic activities of daily living. This is particularly relevant in Ireland, where family members and friends often act as carers for loved ones, sometimes with little financial and social support. This can be onerous and distressing for carers, among whom depression is common.[128]

Because the treatments for dementia and stroke are limited, prevention is critical. As illustrated earlier, cerebral hypoperfusion and impaired cerebrovascular reactivity (CVR) are associated with increased risk of cognitive impairment (CI)/dementia and ischaemic stroke. However, lowering vascular risk factors can reduce the risk of certain types of dementia and of stroke.[51] This may prove an inexpensive and effective way of reducing the socioeconomic burden of both of these conditions.

4.11 Cerebral haemodynamics and cognitive impairment/dementia

A spectrum of impaired cognition can be seen in ageing adults, whereby normal cognition can progress to (mild) cognitive impairment ((M)CI) and ultimately dementia. There are various types of dementia, of which Alzheimer's disease (AlzD) is by far the most common subtype.[129] Dementia shares many risk factors with cerebrovascular disorders. Obesity, hypertension (HTN) and type 2 Diabetes Mellitus (T2DM) are known to predispose to both AlzD and vascular dementia (VaD).[130]

The pathophysiology of AlzD is complex and, to date, incompletely understood. It is thought that damage to the cerebral microcirculation occurs early in the disease process and results in blood brain barrier (BBB) dysfunction and cerebral hypoperfusion. There is resultant accumulation of toxins and β-amyloid, which ultimately leads to neuronal dysfunction and neurodegeneration.[130] *See figure 45.*

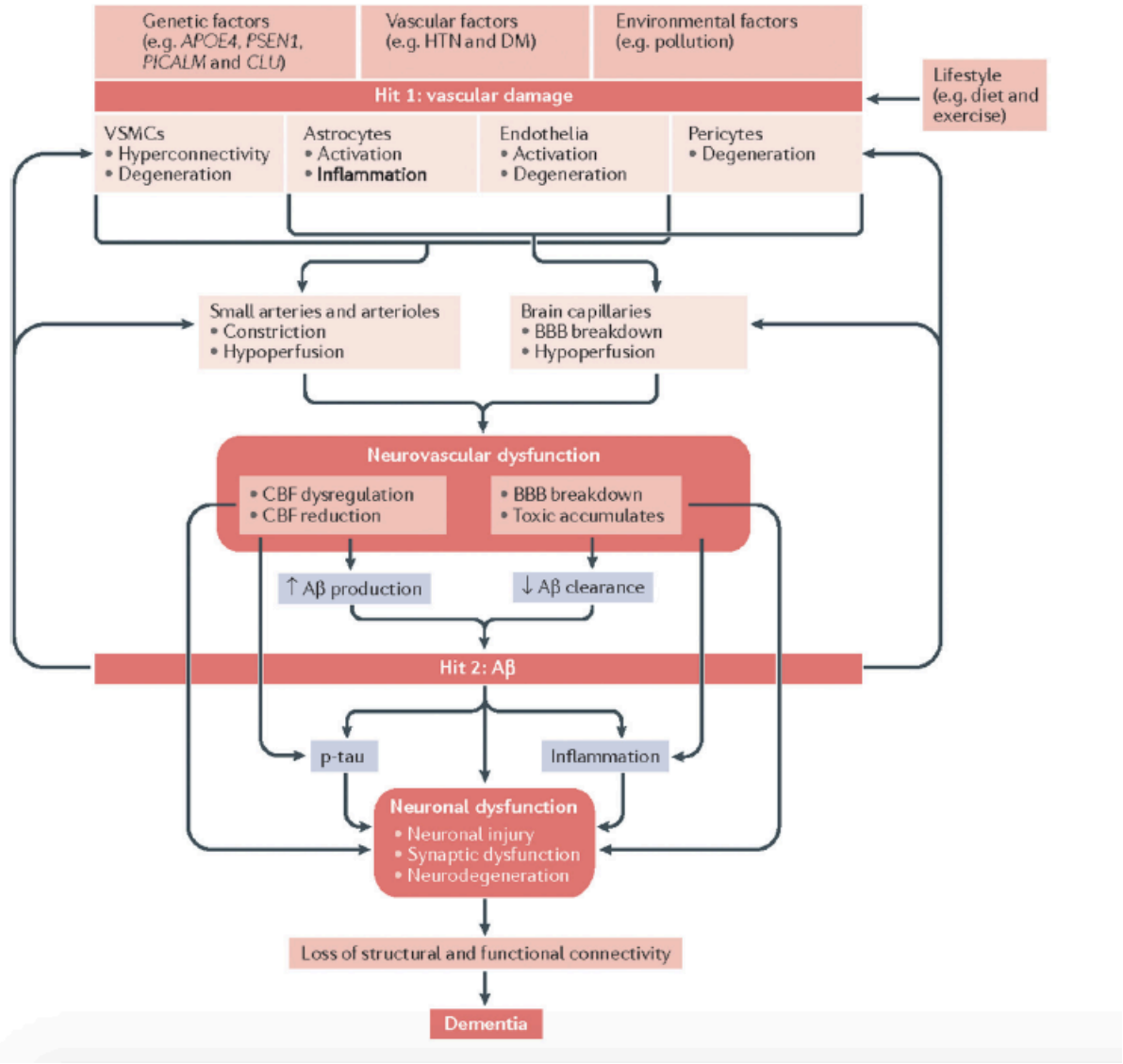

Figure 45 illustrates the pathophysiology of Alzheimer's disease. (From: Chen JJ. Cerebrovascular-Reactivity Mapping Using MRI: Considerations for Alzheimer's Disease. Front Aging Neurosci. 2018;10:170).

Like AlzD, endothelial dysfunction, BBB breakdown and cerebral hypoperfusion are thought to be key processes in the pathogenesis of VaD.[130]

Although studies assessing cerebral blood flow (CBF) and cerebrovascular reactivity (CVR) in patients with CI and dementia vary in terms of imaging methods employed, sample size and cohort characteristics, the majority of studies suggest that resting CBF is impaired in patients with cognitive impairment/AlzD[52] and VaD[131] and that CVR is impaired in patients with MCI and AlzD when compared with healthy controls.[19]

4.11.1 CBF and cognitive impairment/dementia

The largest population-based cerebral blood flow (CBF) study, the Rotterdam study, demonstrated an association between cerebral hypoperfusion (measured using 2D phase contrast (PC) magnetic resonance imaging (MRI)) and accelerated cognitive decline and increased risk of dementia over seven years of follow-up.[52]

Similarly, research employing arterial spin labeling (ASL) MRI demonstrates regional hypoperfusion in patients with both mild cognitive impairment (MCI) and Alzheimer's disease (AlzD), when compared with healthy controls. The most consistent finding in patients with AlzD is decreased blood flow to the precuneus and/or posterior cingulate cortex, the latter finding is also common among patients with MCI.[132] Research using both single photon emission computed tomography (SPECT)[133] and ASL MRI[134] suggests that perfusion abnormalities can predict conversion of MCI to AlzD.

Areas of hypoperfusion on ASL MRI in patients with MCI/AlzD correspond with areas of hypometabolism on fluorodeoxyglucose-positron emission tomography (FDG-PET).[135] This stands to reason given that perfusion and metabolism are tightly linked via neurovascular coupling. However, ASL MRI has distinct advantages over PET and could be considered the preferable imaging technique in patients with suspected CI/dementia.

Similarly in patients with vascular dementia (VaD), hypoperfusion of the frontal and parietal cortex has been documented using ASL MRI.[131]

Structural MRI is often performed as part of the routine work-up of patients with CI/dementia. Medial temporal lobe atrophy on structural MRI helps to distinguish AlzD from other dementia subtypes, as it is in the medial temporal lobes, particularly the hippocampus and entorhinal cortex, where AlzD typically begins and is most severe.[136]

As with AlzD, structural MRI may reveal typical findings in patients with VaD, including large vessel and watershed infarcts, lacunes and white matter hyperintensities (WMHs).[137]

ASL can be added to routine structural MRI protocols with little inconvenience to the patient, minimal additional scan time and negligible added cost. However, one of the limitations of neuroimaging in the workup/management of patients with cognitive decline is that image quality can be degraded by head movement artefact.[138]

Given its suitability to repeated studies, MRI can be used not only to aid the diagnosis of dementia but also for surveillance and in assessing effectiveness of and/or response to treatments.

The functional brain changes observed in patients with MCI/AlzD occur before structural changes, highlighting the ability of ASL MRI to detect abnormalities early in the disease course. Indeed, a reduction in CBF in high-risk subjects for AlzD has been reported to occur before the onset of cognitive decline, brain atrophy or amyloid-β accumulation,[53] suggesting that cerebral hypoperfusion may act as an early biomarker of AlzD.

Additionally, perfusion abnormalities have not just been observed in disease states but also in cognitively normal older adults, with prior research demonstrating regions of both increased and decreased perfusion in elderly subjects without CI/dementia. For example, decreased CBF has been observed in the parietal cortex and precuneus and increased CBF in the temporal lobe and posterior and anterior cingulate cortex (among other regions).[139-141] Regional hypoperfusion may indicate vulnerability to CI/AlzD in older adults, in whom cognition is still preserved, whereas hyperperfusion may represent a compensatory response before the onset of CI.

In cognitively normal subjects with vascular risk factors, regional decreases in blood flow to the putamen, globus pallidus and hippocampus have been observed,[69] areas that are crucial for executive function, learning and memory. These findings suggest that vascular risk factors may create a vulnerability state for the development of neurodegenerative disorders and emphasize the importance of reducing vascular risk in ageing populations in order to maintain CBF and ultimately cognition.

4.11.2 CVR and cognitive impairment/dementia

As with cerebral blood flow (CBF), prior research indicates that cerebrovascular reactivity (CVR) is altered in patients with mild cognitive impairment (MCI) and

Alzheimer's disease (AlzD). Two blood oxygen level dependent (BOLD) MRI studies report CVR reductions in patients with MCI and AlzD when compared with healthy controls.[142, 143]

Using ASL MRI, Glodzik et al. demonstrated decreased hippocampal CVR in patients with MCI vs. healthy elderly controls, an association that persisted after correction for age and vascular risk.[118] Indeed, impaired CVR was observed in patients with MCI despite preserved CBF, suggesting that CVR may detect abnormalities in cerebrovascular function even earlier than CBF.[118]

While CVR reductions have been described using transcranial Doppler in patients with vascular dementia (VaD),[144] this finding has yet to be replicated with ASL MRI.

As with CBF, cardiovascular risk factors correlate with impaired MRI-assessed CVR in the default network[75] and hippocampus,[118] areas that are integral to memory, re-iterating the importance of decreasing vascular risk in the prevention of CI/dementia.

4.12 Cerebral haemodynamics and stroke

In patients with significant stenosis/occlusion of the carotid arteries, there is increased resistance to blood flow at baseline. Because of this, vasodilation occurs to decrease arterial resistance and increase blood flow, thereby ensuring adequate cerebral perfusion. However, if compensatory vasodilation has reached its maximum and the cerebrovascular reserve is exhausted, further vasodilation is not possible, even in response to a vasoactive stimulus. Then blood flow becomes dependent on blood pressure. In this setting, hypotension with resultant cerebral hypoperfusion can result in transient ischaemic attack (TIA)/stroke.[145] Recruitment of blood flow via collateral pathways plays an important role in maintaining cerebral blood flow (CBF) in this setting.[146] However, in patients with exhausted cerebrovascular reserve, steal phenomena can occur, whereby blood flow is directed away from vascular territories that are maximally dilated i.e. those with exhausted cerebrovascular reserve to territories with preserved vasodilatory capacity, thereby further increasing the risk of ischaemia/infarction in at-risk brain tissue.[145]

Arterial spin labeling (ASL) magnetic resonance imaging (MRI) has previously demonstrated impaired CBF in patients with internal carotid artery occlusion.[147] However, in some cases, resting CBF may be preserved (especially in the supine

position as occurs during MRI) but the ability to augment flow in response to a vasoactive stimulus is compromised. Thus, an even more promising role for ASL may be in assessing cerebrovascular reserve in patients with chronic cerebrovascular disease.

Prior research suggests that patients with carotid stenosis/occlusion who have impaired cerebrovascular reactivity (CVR) are four times more likely to develop TIA/stroke.[54] This association between impaired CVR and increased risk of ischaemic events holds true regardless of imaging modality (transcranial Doppler (TCD), [^{15}O]-H_2O positron emission tomography (PET), ^{133}Xenon or 123I-IMP single photon emission computed tomography (SPECT) and vasodilatory stimulus (carbon dioxide (CO_2) or acetazolamide) used, and is observed in both symptomatic and asymptomatic patients with both high-grade carotid stenosis and occlusion.[54] These findings indicate that in combination with/in addition to the risk of embolic stroke secondary to carotid atherosclerotic plaque, patients with impaired CVR are also at risk of hypoperfusion/watershed stroke because of inability to compensate for sudden changes in CBF in vascular territories where vasoreactive capacity is already exhausted.[54]

In patients with symptomatic internal carotid artery (ICA) stenosis, ASL has demonstrated decreased cerebral vasodilatory capacity in brain tissue supplied by the affected ICA when compared with the contralateral ICA and healthy arteries.[148] ASL MRI has also revealed impaired CVR not only in the ipsilateral cerebral hemisphere, but also in the contralateral cerebral hemisphere of patients with symptomatic ICA occlusion when compared with healthy controls.[149] These findings are consistent with prior studies using TCD and nuclear medicine techniques, which demonstrate compromised CVR in the context of major arterial stenosis/occlusion.[150, 151]

Diagnosis of TIA, although challenging, offers significant benefit to patients, as early initiation of preventative treatments can reduce the risk of early/minor stroke by 80%.[152] Currently MRI with diffusion weighted imaging (DWI) is considered the preferred diagnostic test in the work-up of TIA,[153] however ASL may be more sensitive in detecting abnormalities than both DWI and magnetic resonance angiography.[154, 155] As indicated earlier, ASL can be added to standard clinical MRI protocols with little inconvenience to the patient, minimal additional scan time and negligible added cost and may play an important role in the future work-up/triage of patients with TIA.

ASL-assessed CVR may also help in effectively managing patients with steno-occlusive disease. Because revascularization interventions in this patient cohort are inherently high-risk, they should only be performed if anticipated benefits outweigh potential risks. Vascular challenges with ASL MRI can identify patients who are more likely to fail medical treatment and who may benefit from surgical intervention (endovascular stenting or carotid endarterectomy).[156]

The non-invasiveness of ASL and the ease with which it can be repeated make it the ideal imaging choice to monitor response to treatment. Prior studies using ASL MRI demonstrate improved CBF in both ipsilateral ICA/middle cerebral artery (MCA) and contralateral ICA territories following carotid artery stenting.[157] Similarly, BOLD MRI has shown significant improvement in ipsilateral CVR following revascularization with carotid endarterectomy.[158]

One limitation of ASL, however, which was alluded to earlier, is that the post labeling delay (PLD) must be sufficiently long to allowed tagged spins to reach the capillaries and exchange with brain tissue in the region of interest before image acquisition commences, otherwise CBF estimation proves inaccurate. This is of particular relevance in patients with chronic cerebrovascular disease, in whom arterial transit time (ATT) is delayed and there is slow blood flow through collateral pathways. In these patients, too short a PLD relative to the arrival time of the tagged spins results in underestimation of CBF or failure to detect flow through collateral pathways. For this reason, the International Society for Magnetic Resonance in Medicine (ISMRM) consensus guidelines recommend a PLD of 2,000 ms in adult clinical patients as a trade-off between ensuring near-complete delivery of tracer to the tissue of interest vs. tracer decay resulting in decreased signal to noise ratio (SNR).[27] By performing multiple ASL experiments at increasing PLDs, accuracy of perfusion quantification can be improved.[27] Novel techniques like perfusion-territory selective ASL may also help in imaging collateral pathways.[149]

Thus, with continued technological advancements, ASL is likely to become an increasingly important tool in the management of patients with chronic cerebrovascular disease.

4.13 Targets for intervention

As indicated earlier, lowering risk factors for vascular disease can significantly reduce the risk of dementia and stroke.[51] Interventions aimed at improving cerebral blood flow (CBF) and cerebrovascular reactivity (CVR) are likely to play a key role here.

4.13.1 Interventions targeting CBF

Physical training

Aerobic exercise in healthy, sedentary older adults has been shown not only to improve cardiovascular fitness but also resting regional cerebral blood flow (CBF) and immediate and delayed memory.[78] In a study by Chapman at al., participants began to reap benefits as early as 6 weeks after the introduction of a 3-hour per week exercise programme with sustained improvement at 12 weeks.[78] Rapid health gains so soon after commencing a training programme may prove a significant motivator for people.

Exercise training has also been shown to preferentially augment hippocampal blood flow,[159] to increase hippocampal volume and reverse age-related hippocampal volume loss[160] in older adults. Given the importance of the hippocampus in memory and executive function, it follows that increased hippocampal flow and volume are associated with improved memory performance in older adults.[160, 161]

Cognitive training

Cognitive training in healthy older adults has been shown to reverse some of the functional and structural brain changes that occur with normal ageing. In another study by Chapman et al., complex mental training in older adults was associated with increased global and regional blood flow, with resultant cognitive gains.[162]

Interventions targeting arterial stiffening/pulse wave velocity

As illustrated previously, normal ageing and hypertension (HTN) are associated with arterial stiffening and transmission of harmful high-pressure energy to the cerebral microvasculature. Increased arterial stiffness is linked to regional cerebral hypoperfusion in cognitively normal older adults, especially those with a genetic disposition towards Alzheimer's disease (AlzD).[110] Arterial stiffness contributes to

progressive decline in cognitive performance with increasing age,[163] a relationship, which may be mediated through the negative effects of arterial stiffness on CBF.

Pulse wave velocity (PWV), an indicator of arterial stiffness, is an important biomarker in predicting cardiovascular mortality.[164, 165] Aortic PWV is independently associated with cerebral white matter hyperintensities (WMHs), a manifestation of underlying cerebral small vessel disease.[166] Prior research demonstrates an association between lower CBF and higher volume of WMHs, particularly in association with HTN.[59] WMHs are associated with cognitive impairment (CI), double the risk of dementia and treble the risk of stroke.[167]

Thus, lifestyle modifications and pharmacological interventions aimed at improving PWV and increasing cerebral perfusion may halt the progression of chronic small vessel ischaemia and lower the risk of cognitive impairment/dementia and stroke. Exercise can improve central arterial stiffness in sedentary older adults free of major disease.[168] Certain antihypertensive medications have also been shown to effectively reduce PWV.[169]

Weight loss

Metabolic syndrome is associated with lower CBF and lower memory function.[71] However, long-term weight loss through intensive lifestyle modification has been shown to increase CBF in overweight and obese diabetics,[79] thereby providing a target for intervention.

Antihypertensives

The literature regarding the effects of antihypertensive medications on cerebral haemodynamics is conflicting, likely due to significant methodological variation between studies in terms of imaging techniques used, sample sizes, cohort characteristics.

As illustrated earlier, Muller et al. demonstrated decreased CBF in patients with elevated blood pressure (BP).[68] At four years of follow-up, they reported CBF stability in normotensive subjects and patients with controlled HTN but reduced CBF in untreated and poorly controlled hypertensives.[68] These findings suggest that optimal BP control can halt CBF decline in hypertensive patients.

Prior research demonstrates an association between antihypertensives, increased cerebral perfusion and improved cognitive function,[170] highlighting the potential role for antihypertensives in the prevention of CI/dementia.
Antihypertensives also significantly lower the risk of stroke, for which BP is the single most important risk factor.[171]

However, the class of antihypertensive medication is likely significant, with several studies indicating that angiotensin receptor blockers (ARBs) are especially protective of CBF compared with other antihypertensive agents.[68, 80, 172]

Other pharmacological interventions
Research by Chaudhary et al., using pseudocontinuous arterial spin labeling (pcASL) magnetic resonance imaging (MRI), demonstrated regional increases in cerebral perfusion (globally throughout the grey and in the anterior and posterior cingulate cortex) following 6 months of treatment with acetylcholinesterase inhibitors in patients with early AlzD.[173]

Multiple additional novel/experimental pharmacological agents have been proposed to increase cerebral perfusion for the prevention of AlzD. These include Rho kinase inhibitors, dimethyl sulfoxide, sirtuins, vascular growth factors and low-level laser therapy/photobiomodulation.[174] These interventions require further validation, but may prove promising in decreasing the risk of cognitive decline/dementia in ageing adults.

4.13.2 Interventions targeting CVR

Physical training
As with cerebral blood flow (CBF), aerobic exercise has been shown to improve cerebrovascular reactivity (CVR) in sedentary but otherwise healthy adults.[81] Exercise also positively influences CVR in the setting of vascular risk factors, with Meyer et al. reporting significantly improved intima-media thickness and flow-mediated vasodilation following 6 months of regular exercise in obese children.[175]

Antihypertensives
As with CBF, certain antihypertensives appear to positively influence CVR, with a prior study showing significantly increased CVR following 12 weeks of treatment with perindopril, beyond any effect on blood pressure (BP).[82]

Other pharmacological interventions

Similar to CBF, a prior study using transcranial Doppler (TCD) and carbon diode (CO_2) has revealed normalization of CVR in patients with Alzheimer's disease (AlzD) and vascular dementia (VaD) following treatment with galantamine, an acetylcholinesterase inhibitor.[176]

In conclusion, arterial spin labeling (ASL) magnetic resonance imaging (MRI), by non-invasively measuring CBF and CVR as early markers of cerebrovascular dysfunction, can help identify subjects with impaired cerebral haemodynamics for age. In those with modifiable risk factors, ASL parameters give a target for intervention, thereby preventing/delaying progression to established neurodegenerative/ cerebrovascular disease.

4.14 Study limitations

One of the major limitations of arterial spin labeling (ASL) is inaccurate quantification of cerebral blood flow (CBF) in the context of prolonged arterial transit times (ATT). This is of particular significance in elderly subjects and in those with cerebrovascular disease *(see section 4.12 of this chapter).* This issue can be addressed by increasing the label duration or by using multi-delay ASL.[27]

In our study, the same labeling duration and delay were used in the acquisition of all participants' data. However, inter-participant variations (both physiological and pathological) in cerebrovascular structure and function impact labeling estimates and affect flow measurements. This may have resulted in both under- and overestimation of CBF in certain subjects. As alluded to previously, the post labeling delay (PLD) used in this study, although in line with the International Society for Magnetic Resonance in Medicine (ISMRM) consensus guidelines,[27] may have been too short to account for prolonged ATTs in certain elderly subjects, especially those with cerebrovascular disease. However, a PLD of 1,800 ms was felt to be the optimal choice in our cohort amongst whom mean age was <70 years.

The ISMRM white paper recommends a slice thickness of 4-8 mm with no slice gap.[27] In our study, we used a slice thickness of 8 mm and a 1 mm slice gap. Due to partial volume effects associated with thick slices, this may have underestimated CBF.[102] The thick slices used in this study may also hinder direct comparison of our

results with those from other studies.

Another potential issue with ASL is imperfect labeling due to flow effects in the arteries, resulting in underestimation of CBF.

With regards to the hypercapnic challenge, the precise changes in end-tidal CO_2 ($EtCO_2$) following the administration of carbon dioxide (CO_2) depend on individual physiology and the efficacy with which the gas mixture is delivered.[39] Because of variations in anatomy, a tighter mask fit with a better air-seal might have resulted in more efficient CO_2 delivery in certain individuals.

In addition, while $EtCO_2$ is considered a marker for the partial pressure of arterial carbon dioxide ($PaCO_2$) (*see Chapter 2, section 6*), low cardiac output (as can be seen in certain elderly subjects) may increase the discrepancy between $PaCO_2$ and $EtCO_2$, leading to underestimation of $EtCO_2$-based cerebrovascular reactivity (CVR).[177]

Although this study validates the notion that age, sex and various modifiable vascular risk factors influence cerebral haemodynamics, the underlying mechanisms driving these changes cannot be determined in this cross-sectional study. Successive waves of The Irish Longitudinal Study on Ageing (TILDA) will allow us to further explore the effects of select variables on CBF and CVR.

Studies of ageing can be limited by the fact that some supposedly "healthy" participants might have, as of yet, occult or undiagnosed medical conditions. For example, it is unclear whether any of our cohort had pre-clinical neurodegenerative and/or cerebrovascular disease(s) at the time of imaging. Indeed, although we listed prior stroke and/or brain injury as exclusion criteria for this study, six subjects in the baseline/normocapnic cohort and one subject in the hypercapnic challenge cohort had MRI findings consistent with established large vessel infarct or haemorrhage/contusion. These insults were presumably clinically silent.

Thus, the normative results outlined in this research are not to be interpreted in the context of entirely "healthy" subjects, but rather in the context of nationally representative, neurologically asymptomatic, community dwelling, older adults, some of whom have chronic diseases.

CHAPTER 5: CONCLUSIONS

The maintenance of constant, disproportionally high blood flow to the brain is crucial because of its great metabolic demand and limited capacity for substrate storage/anaerobic metabolism. There are several integrated mechanisms involved in regulating cerebral blood flow (CBF). Among the most important are the partial pressure of arterial carbon dioxide, systemic blood pressure (via cerebral autoregulation), blood viscosity and neurovascular coupling. Failure of CBF regulatory mechanisms, as occurs with ageing, can negatively impact cerebrovascular function.

Cerebrovascular reactivity (CVR) i.e. the ability of the cerebral arteries and arterioles to alter their calibre and resistance in response to increased CBF requirements can be negatively affected by ageing and various risk factors/disease processes. Evaluation of CVR can be considered a “stress test” for the cerebrovasculature, identifying diseased, non-reactive vessels, usually before changes in CBF are evident.

Both CBF and CVR are considered important measures of cerebrovascular health. Impaired CBF and CVR have been implicated in various neurodegenerative and cerebrovascular diseases, including cognitive impairment/dementia and stroke.

Various techniques have been used to date in the evaluation of CBF and CVR. However, many of these imaging techniques have significant limitations. Positron emission tomography (PET), which is currently considered the gold standard for CBF measurement, is invasive, involving radioactive pharmaceuticals, arterial blood sampling and ionizing radiation. Blood oxygen level dependent (BOLD) magnetic resonance imaging (MRI), which is the most widely used technique in recent CVR research, does not directly measure CBF/CVR. Arterial spin labeling (ASL) MRI non-invasively and quantitatively assesses cerebral perfusion and offers a promising alternative to other perfusion techniques.

Prior MRI studies assessing cerebral perfusion have been limited by sample size. This research benefited from a large cohort of nationally representative, neurologically asymptomatic, community dwelling older Irish adults, enrolled in The Irish Longitudinal Study on Ageing (TILDA).

The large study cohort with a continuum of ages allowed us to generate, for the first time, normative values for grey matter cerebral perfusion in older adults. It is accepted that normal ageing is associated with declining CBF. However the lack of reference CBF values has, to date, limited researchers and clinicians from distinguishing age-expected CBF decline from pathological reduction. The normative values outlined in this paper represent a significant contribution to the literature and will help in establishing CBF/CVR as important clinical biomarkers of cerebrovascular integrity.

Consistent with prior studies, our research demonstrated higher CBF in women.

In our study, certain cardiovascular risk factors including body mass index (BMI) and blood pressure (BP) were also found to negatively affect CBF. Increased BMI was associated with increased CVR. The identification of BMI and BP as determinants of impaired CBF/CVR offers a target for intervention. Lifestyle modifications aimed at improving CBF and CVR i.e. exercise training, weight loss and BP control, may enhance brain integrity and decrease the risk of dementia and stroke in ageing adults.

One of the major limitations of ASL is underestimation of perfusion in the context of prolonged arterial transit times, a common finding in elderly subjects and in those with cerebrovascular disease. While all MRIs were performed in accordance with the International Society for Magnetic Resonance in Medicine (ISMRM) consensus guidelines, the post labeling delay (PLD) used in this study may have been too short for certain elderly participants, especially those with cerebrovascular disease. Continued improvements in MRI techniques, including the advent of multi-delay ASL, should help in ensuring optimal PLD for study samples going forward.

In conclusion, the present study defines ASL MRI as an optimal technique for CBF and CVR measurement. It presents normative reference values for grey matter cerebral perfusion measured using 3T pseudocontinuous (pc)ASL MRI in an ageing cohort. These values will aid in the clinical interpretation of CBF measurements. Given the significant effects of age and sex on CBF, these variables need to be taken into account when studying brain perfusion. This research also demonstrates significant negative associations between certain cardiovascular risk factors and CBF/CVR, thereby providing targets for intervention in those at risk of cognitive impairment/dementia and stroke due to altered cerebral haemodynamics.

REFERENCES

1. Gertz D. Liebman's Neuroanatomy Made Easy And Understandable, 6th Edition. *Aspen*. 1999.
2. Moore KL and Dalley AF. Clinically Oriented Anatomy, 5th Edition. *Lippincott Williams & Wilkins*. 2006.
3. Ellis H and Mahadevan V. Clinical Anatomy: Applied Anatomy for Students and Junior Doctors, 13th Edition. *Wiley-Blackwell*. 2013.
4. Waxman SG. Clinical Neuroanatomy, 28th Edition. *McGraw-Hill*. 2017.
5. Vanderah T and Gould D. Nolte's The Human Brain, 7th Edition. *Elsevier*. 2015.
6. Shah RS and Jeyaretna DS. Cerebral vascular anatomy and physiology. *Surgery (Oxford)*. 2018;36:606-612.
7. Hindenes LB, Haberg AK, Johnsen LH, Mathiesen EB, Robben D and Vangberg TR. Variations in the Circle of Willis in a large population sample using 3D TOF angiography: The Tromso Study. *PloS one*. 2020;15:e0241373.
8. Vrselja Z, Brkic H, Mrdenovic S, Radic R and Curic G. Function of circle of Willis. *Journal of Cerebral Blood Flow and Metabolism.* 2014;34:578-84.
9. Cipolla MJ. Chapter 2: Anatomy and Ultrastructure. The Cerebral Circulation. *Morgan & Claypool Life Sciences*. 2009.
10. Dorrance AM, Matin N and Pires PW. The effects of obesity on the cerebral vasculature. *Curr Vasc Pharmacol*. 2014;12:462-72.
11. Pires PW, Dams Ramos CM, Matin N and Dorrance AM. The effects of hypertension on the cerebral circulation. *Am J Physiol Heart Circ Physiol*. 2013;304:H1598-614.
12. Brown LS, Foster CG, Courtney JM, King NE, Howells DW and Sutherland BA. Pericytes and Neurovascular Function in the Healthy and Diseased Brain. *Front Cell Neurosci*. 2019;13:282.
13. Mastorakos P and McGavern D. The anatomy and immunology of vasculature in the central nervous system. *Sci Immunol*. 2019;4.
14. Torbey MT and Malkoff M. Neurocritical Care, 1 - Cerebral Blood Flow Physiology and Metabolism. *Cambridge University Press*. 2009.
15. Willie CK, Tzeng YC, Fisher JA and Ainslie PN. Integrative regulation of human brain blood flow. *The Journal of physiology*. 2014;592:841-59.
16. Lee J-M, Grabb MC, Zipfel GJ and Choi DW. Brain tissue responses to ischemia. *The Journal of Clinical Investigation*. 2000;106:723-731.
17. Fantini S, Sassaroli A, Tgavalekos KT and Kornbluth J. Cerebral blood flow and autoregulation: current measurement techniques and prospects for noninvasive optical methods. *Neurophotonics*. 2016;3:031411.
18. Lassen NA. Cerebral blood flow and oxygen consumption in man. *Physiological reviews*. 1959;39:183-238.
19. Glodzik L, Randall C, Rusinek H and de Leon MJ. Cerebrovascular reactivity to carbon dioxide in Alzheimer's disease. *J Alzheimers Dis*. 2013;35:427-40.
20. Smeeing DP, Hendrikse J, Petersen ET, Donahue MJ and de Vis JB. Arterial Spin Labeling and Blood Oxygen Level-Dependent MRI Cerebrovascular Reactivity in Cerebrovascular Disease: A Systematic Review and Meta-Analysis. *Cerebrovasc Dis*. 2016;42:288-307.
21. Schild HH. MRI made easy: (...well almost). *Berlex Laboratories*. 1994.
22. Pooley RA. AAPM/RSNA physics tutorial for residents: fundamental physics of MR imaging. *Radiographics*. 2005;25:1087-99.
23. Currie S, Hoggard N, Craven IJ, Hadjivassiliou M and Wilkinson ID. Understanding MRI: basic MR physics for physicians. *Postgrad Med J*. 2013;89:209-23.

24. Alvarez-Linera J. 3T MRI: advances in brain imaging. *Eur J Radiol*. 2008;67:415-26.
25. Williams DS, Detre JA, Leigh JS and Koretsky AP. Magnetic resonance imaging of perfusion using spin inversion of arterial water. *Proc Natl Acad Sci U S A*. 1992;89:212-6.
26. Haller S, Zaharchuk G, Thomas DL, Lovblad KO, Barkhof F and Golay X. Arterial Spin Labeling Perfusion of the Brain: Emerging Clinical Applications. *Radiology*. 2016;281:337-356.
27. Alsop DC, Detre JA, Golay X, Gunther M, Hendrikse J, Hernandez-Garcia L, Lu H, MacIntosh BJ, Parkes LM, Smits M, van Osch MJ, Wang DJ, Wong EC and Zaharchuk G. Recommended implementation of arterial spin-labeled perfusion MRI for clinical applications: A consensus of the ISMRM perfusion study group and the European consortium for ASL in dementia. *Magnetic resonance in medicine*. 2015;73:102-16.
28. Wintermark M, Sesay M, Barbier E, Borbely K, Dillon WP, Eastwood JD, Glenn TC, Grandin CB, Pedraza S, Soustiel JF, Nariai T, Zaharchuk G, Caille JM, Dousset V and Yonas H. Comparative overview of brain perfusion imaging techniques. *Journal of neuroradiology Journal de neuroradiologie*. 2005;32:294-314.
29. Gunther M. Perfusion imaging. *Journal of Magnetic Resonance Imaging*. 2014;40:269-79.
30. Buxton RB, Frank LR, Wong EC, Siewert B, Warach S and Edelman RR. A general kinetic model for quantitative perfusion imaging with arterial spin labeling. *Journal of Magnetic Resonance Imaging*. 1998;40:383-96.
31. Chappell M, MacIntosh B and Okell T. *Introduction to Perfusion Quantification using Arterial Spin Labelling*; 2017.
32. Meurée C. Arterial spin labelling : quality control and super-resolution. *Medical Imaging Université Rennes*. 2019.
33. Borogovac A and Asllani I. Arterial Spin Labeling (ASL) fMRI: advantages, theoretical constrains, and experimental challenges in neurosciences. *Int J Biomed Imaging*. 2012;2012:818456.
34. van Gelderen P, de Zwart JA and Duyn JH. Pittfalls of MRI measurement of white matter perfusion based on arterial spin labeling. *Magnetic resonance in medicine*. 2008;59:788-95.
35. Ficzere A, Valikovics A, Fulesdi B, Juhasz A, Czuriga I and Csiba L. Cerebrovascular reactivity in hypertensive patients: a transcranial Doppler study. *Journal of Clinical Ultrasound*. 1997;25:383-9.
36. Dorfler P, Puls I, Schliesser M, Maurer M and Becker G. Measurement of cerebral blood flow volume by extracranial sonography. *Journal of Cerebral Blood Flow and Metabolism.* 2000;20:269-71.
37. Venturelli PM, Brunser AM, Gaete J, Illanes S, Lopez J, Olavarria VV, Reccius A, Brinck P, Gonzalez F, Cavada G and Lavados PM. Reliability of Hand-Held Transcranial Doppler with M-mode Ultrasound in Middle Cerebral Artery Measurement. *J Med Ultrasound*. 2017;25:76-81.
38. Fan AP, Jahanian H, Holdsworth SJ and Zaharchuk G. Comparison of cerebral blood flow measurement with [15O]-water positron emission tomography and arterial spin labeling magnetic resonance imaging: A systematic review. *Journal of Cerebral Blood Flow and Metabolism.* 2016 May;36(5):842-61.
39. Juttukonda MR and Donahue MJ. Neuroimaging of vascular reserve in patients with cerebrovascular diseases. *Neuroimage*. 2019;187:192-208.
40. Wintermark M, Thiran JP, Maeder P, Schnyder P and Meuli R. Simultaneous measurement of regional cerebral blood flow by perfusion CT and stable xenon CT: a validation study. *AJNR American Journal of Neuroradiology*. 2001;22:905-14.
41. Johnson DW, Stringer WA, Marks MP, Yonas H, Good WF and Gur D. Stable xenon CT cerebral blood flow imaging: rationale for and role in clinical decision making. *AJNR American journal of neuroradiology*. 1991;12:201-13.

42. Davenport MS, Perazella MA, Yee J, Dillman JR, Fine D, McDonald RJ, Rodby RA, Wang CL and Weinreb JC. Use of Intravenous Iodinated Contrast Media in Patients with Kidney Disease: Consensus Statements from the American College of Radiology and the National Kidney Foundation. *Radiology*. 2020;294:660-668.
43. O'Connor JP, Tofts PS, Miles KA, Parkes LM, Thompson G and Jackson A. Dynamic contrast-enhanced imaging techniques: CT and MRI. *Br J Radiol*. 2011;84 Spec No 2:S112-20.
44. Liu P, Lu H, Filbey FM, Pinkham AE, McAdams CJ, Adinoff B, Daliparthi V and Cao Y. Automatic and reproducible positioning of phase-contrast MRI for the quantification of global cerebral blood flow. *PloS one*. 2014;9:e95721.
45. Wu B, Lou X, Wu X and Ma L. Intra- and interscanner reliability and reproducibility of 3D whole-brain pseudo-continuous arterial spin-labeling MR perfusion at 3T. *Journal of Magnetic Resonance Imaging*. 2014;39:402-9.
46. Heijtel DF, Mutsaerts HJ, Bakker E, Schober P, Stevens MF, Petersen ET, van Berckel BN, Majoie CB, Booij J, van Osch MJ, Vanbavel E, Boellaard R, Lammertsma AA and Nederveen AJ. Accuracy and precision of pseudo-continuous arterial spin labeling perfusion during baseline and hypercapnia: a head-to-head comparison with $^{15}OH_2O$ positron emission tomography. *Neuroimage*. 2014;92:182-92.
47. Leoni RF, Mazzetto-Betti KC, Silva AC, Dos Santos AC, de Araujo DB, Leite JP and Pontes-Neto OM. Assessing Cerebrovascular Reactivity in Carotid Steno-Occlusive Disease Using MRI BOLD and ASL Techniques. *Radiology research and practice*. 2012;2012:268483.
48. Blockley NP, Griffeth VE, Simon AB and Buxton RB. A review of calibrated blood oxygenation level-dependent (BOLD) methods for the measurement of task-induced changes in brain oxygen metabolism. *NMR in biomedicine*. 2013;26:987-1003.
49. Saito H, Ogasawara K, Suzuki T, Kuroda H, Kobayashi M, Yoshida K, Kubo Y and Ogawa A. Adverse effects of intravenous acetazolamide administration for evaluation of cerebrovascular reactivity using brain perfusion single-photon emission computed tomography in patients with major cerebral artery steno-occlusive diseases. *Neurol Med Chir (Tokyo)*. 2011;51:479-83.
50. United Nations, Department of Economic and Social Affairs, Population Division (2015). World Population Ageing 2015 (ST/ESA/SER.A/390).
51. Vijayan M and Reddy PH. Stroke, Vascular Dementia, and Alzheimer's Disease: Molecular Links. *J Alzheimers Dis*. 2016;54:427-43.
52. Wolters FJ, Zonneveld HI, Hofman A, van der Lugt A, Koudstaal PJ, Vernooij MW, Ikram MA and Heart-Brain Connection Collaborative Research G. Cerebral Perfusion and the Risk of Dementia: A Population-Based Study. *Circulation*. 2017;136:719-728.
53. Zhang N, Gordon ML and Goldberg TE. Cerebral blood flow measured by arterial spin labeling MRI at resting state in normal aging and Alzheimer's disease. *Neurosci Biobehav Rev*. 2017;72:168-175.
54. Gupta A, Chazen JL, Hartman M, Delgado D, Anumula N, Shao H, Mazumdar M, Segal AZ, Kamel H, Leifer D and Sanelli PC. Cerebrovascular reserve and stroke risk in patients with carotid stenosis or occlusion: a systematic review and meta-analysis. *Stroke; a journal of cerebral circulation*. 2012;43:2884-91.
55. Selim M, Jones R, Novak P, Zhao P and Novak V. The effects of body mass index on cerebral blood flow velocity. *Clinical Autonomic Research*. 2008;18:331-8.
56. DuBose LE, Boles Ponto LL, Moser DJ, Harlynn E, Reierson L and Pierce GL. Higher Aortic Stiffness Is Associated With Lower Global Cerebrovascular Reserve Among Older Humans. *Hypertension*. 2018;72:476-482.
57. Parkes LM, Rashid W, Chard DT and Tofts PS. Normal cerebral perfusion measurements using arterial spin labeling: reproducibility, stability, and age and gender effects. *Magnetic resonance in medicine*. 2004;51:736-43.

58. Soni N, Jain A, Kumar S, Pandey CM and Awasthi A. Arterial spin labeling magnetic resonance perfusion study to evaluate the effects of age and gender on normal cerebral blood flow. *Neurology India*. 2016;64 Suppl:S32-8.
59. Vernooij MW, van der Lugt A, Ikram MA, Wielopolski PA, Vrooman HA, Hofman A, Krestin GP and Breteler MM. Total cerebral blood flow and total brain perfusion in the general population: the Rotterdam Scan Study. *Journal of Cerebral Blood Flow and Metabolism*. 2008;28:412-9.
60. De Vis JB, Hendrikse J, Bhogal A, Adams A, Kappelle LJ and Petersen ET. Age-related changes in brain hemodynamics; a calibrated MRI study. *Human brain mapping*. 2015;36:3973-87.
61. Lu H, Xu F, Rodrigue KM, Kennedy KM, Cheng Y, Flicker B, Hebrank AC, Uh J and Park DC. Alterations in cerebral metabolic rate and blood supply across the adult lifespan. *Cerebral cortex*. 2011;21:1426-34.
62. Jennings JR, Heim AF, Kuan DC, Gianaros PJ, Muldoon MF and Manuck SB. Use of total cerebral blood flow as an imaging biomarker of known cardiovascular risks. *Stroke; a journal of cerebral circulation*. 2013;44:2480-5.
63. Gauthier CJ, Madjar C, Desjardins-Crepeau L, Bellec P, Bherer L and Hoge RD. Age dependence of hemodynamic response characteristics in human functional magnetic resonance imaging. *Neurobiology of aging*. 2013;34:1469-85.
64. Chen JJ, Rosas HD and Salat DH. Age-associated reductions in cerebral blood flow are independent from regional atrophy. *Neuroimage*. 2011;55:468-78.
65. Liu Y, Zhu X, Feinberg D, Guenther M, Gregori J, Weiner MW and Schuff N. Arterial spin labeling MRI study of age and gender effects on brain perfusion hemodynamics. *Magnetic resonance in medicine*. 2012;68:912-22.
66. Williamson W, Lewandowski AJ, Forkert ND, Griffanti L, Okell TW, Betts J, Boardman H, Siepmann T, McKean D, Huckstep O, Francis JM, Neubauer S, Phellan R, Jenkinson M, Doherty A, Dawes H, Frangou E, Malamateniou C, Foster C and Leeson P. Association of Cardiovascular Risk Factors With MRI Indices of Cerebrovascular Structure and Function and White Matter Hyperintensities in Young Adults. *JAMA*. 2018;320:665-673.
67. Beason-Held LL, Moghekar A, Zonderman AB, Kraut MA and Resnick SM. Longitudinal changes in cerebral blood flow in the older hypertensive brain. *Stroke; a journal of cerebral circulation*. 2007;38:1766-73.
68. Muller M, van der Graaf Y, Visseren FL, Mali WP, Geerlings MI and Group SS. Hypertension and longitudinal changes in cerebral blood flow: the SMART-MR study. *Ann Neurol*. 2012;71:825-33.
69. Dai W, Lopez OL, Carmichael OT, Becker JT, Kuller LH and Gach HM. Abnormal regional cerebral blood flow in cognitively normal elderly subjects with hypertension. *Stroke; a journal of cerebral circulation*. 2008;39:349-54.
70. Last D, Alsop DC, Abduljalil AM, Marquis RP, de Bazelaire C, Hu K, Cavallerano J and Novak V. Global and regional effects of type 2 diabetes on brain tissue volumes and cerebral vasoreactivity. *Diabetes care*. 2007;30:1193-9.
71. Birdsill AC, Carlsson CM, Willette AA, Okonkwo OC, Johnson SC, Xu G, Oh JM, Gallagher CL, Koscik RL, Jonaitis EM, Hermann BP, LaRue A, Rowley HA, Asthana S, Sager MA and Bendlin BB. Low cerebral blood flow is associated with lower memory function in metabolic syndrome. *Obesity*. 2013;21:1313-20.
72. Rogers RL, Meyer JS, Mortel KF, Mahurin RK and Thornby J. Age-related reductions in cerebral vasomotor reactivity and the law of initial value: a 4-year prospective longitudinal study. *Journal of Cerebral Blood Flow and Metabolism.* 1985;5:79-85.
73. Bhogal AA, De Vis JB, Siero JCW, Petersen ET, Luijten PR, Hendrikse J, Philippens MEP and Hoogduin H. The BOLD cerebrovascular reactivity response to progressive hypercapnia in young and elderly. *Neuroimage*. 2016;139:94-102.

74. Hajjar I, Zhao P, Alsop D and Novak V. Hypertension and cerebral vasoreactivity: a continuous arterial spin labeling magnetic resonance imaging study. *Hypertension*. 2010;56:859-64.
75. Haight TJ, Bryan RN, Erus G, Davatzikos C, Jacobs DR, D'Esposito M, Lewis CE and Launer LJ. Vascular risk factors, cerebrovascular reactivity, and the default-mode brain network. *Neuroimage*. 2015;115:7-16.
76. Novak V, Last D, Alsop DC, Abduljalil AM, Hu K, Lepicovsky L, Cavallerano J and Lipsitz LA. Cerebral blood flow velocity and periventricular white matter hyperintensities in type 2 diabetes. *Diabetes care*. 2006;29:1529-34.
77. Novak V, Zhao P, Manor B, Sejdic E, Alsop D, Abduljalil A, Roberson PK, Munshi M and Novak P. Adhesion molecules, altered vasoreactivity, and brain atrophy in type 2 diabetes. *Diabetes care*. 2011;34:2438-41.
78. Chapman SB, Aslan S, Spence JS, Defina LF, Keebler MW, Didehbani N and Lu H. Shorter term aerobic exercise improves brain, cognition, and cardiovascular fitness in aging. *Frontiers in aging neuroscience*. 2013;5:75.
79. Espeland MA, Luchsinger JA, Neiberg RH, Carmichael O, Laurienti PJ, Pi-Sunyer X, Wing RR, Cook D, Horton E, Casanova R, Erickson K, Nick Bryan R and Action for Health in Diabetes Brain Magnetic Resonance Imaging Research G. Long Term Effect of Intensive Lifestyle Intervention on Cerebral Blood Flow. *J Am Geriatr Soc*. 2018;66:120-126.
80. Nagata R, Kawabe K and Ikeda K. Olmesartan, an angiotensin II receptor blocker, restores cerebral hypoperfusion in elderly patients with hypertension. *J Stroke Cerebrovasc Dis*. 2010;19:236-40.
81. Murrell CJ, Cotter JD, Thomas KN, Lucas SJ, Williams MJ and Ainslie PN. Cerebral blood flow and cerebrovascular reactivity at rest and during sub-maximal exercise: effect of age and 12-week exercise training. *Age (Dordr)*. 2013;35:905-20.
82. Walters M, Muir S, Shah I and Lees K. Effect of perindopril on cerebral vasomotor reactivity in patients with lacunar infarction. *Stroke; a journal of cerebral circulation*. 2004;35:1899-902.
83. Whelan BJ and Savva GM. Design and methodology of the Irish Longitudinal Study on Ageing. *J Am Geriatr Soc*. 2013;61 Suppl 2:S265-8.
84. Kearney PM, Cronin H, O'Regan C, Kamiya Y, Savva GM, Whelan B and Kenny R. Cohort profile: the Irish Longitudinal Study on Ageing. *Int J Epidemiol*. 2011;40:877-84.
85. Cronin H, O'Regan C, Finucane C, Kearney P and Kenny RA. Health and aging: development of the Irish Longitudinal Study on Ageing health assessment. *J Am Geriatr Soc*. 2013;61 Suppl 2:S269-78.
86. Kenny RA, Coen RF, Frewen J, Donoghue OA, Cronin H and Savva GM. Normative values of cognitive and physical function in older adults: findings from the Irish Longitudinal Study on Ageing. *J Am Geriatr Soc*. 2013;61 Suppl 2:S279-90.
87. Ogg RJ, Kingsley PB and Taylor JS. WET, a T1- and B1-insensitive water-suppression method for in vivo localized 1H NMR spectroscopy. *J Magn Reson B*. 1994;104:1-10.
88. Lu H, Clingman C, Golay X and van Zijl PC. Determining the longitudinal relaxation time (T1) of blood at 3.0 Tesla. *Magnetic resonance in medicine*. 2004;52:679-82.
89. MP150 Systems Product Sheet. Biopac Systems. Available from: https://www.biopac.com/wp-content/uploads/MP150-Systems.pdf. [Accessed 11 December 2020].
90. Analysis of Functional NeuroImages (AFNI). Available from: afni.nimh.nih.gov/afni. [Accessed 11 December 2020].
91. Chappell MA GA, Whitcher B Woolrich MW. Variational Bayesian Inference for a Nonlinear Forward Model. *IEEE Transactions on Signal Processing*. 2009;57:223-236.

92. Groves AR, Chappell MA and Woolrich MW. Combined spatial and non-spatial prior for inference on MRI time-series. *Neuroimage*. 2009;April 15:795-809.
93. Woolrich MW, Jbabdi S, Patenaude B, Chappell M, Makni S, Behrens T, Beckmann C, Jenkinson M and Smith SM. Bayesian analysis of neuroimaging data in FSL. *Neuroimage*. 2009;March:(1 Suppl):S173-86.
94. BASIL - FSL. Oxford Centre for Functional MRI of the Brain, Oxford, UK. Available from: https://fsl.fmrib.ox.ac.uk/fsl/fslwiki/BASIL. [Accessed 11 December 2020].
95. Buxton RB. Quantifying CBF with arterial spin labeling. *Journal of Magnetic Resonance Imaging.* 2005;22:723-726.
96. Matlab Release R2015b. Mathworks. Available from: https://uk.mathworks.com/help/doc-archives.html. [Accessed 11 December 2020].
97. McFayden G. Respiratory gas analysis. *Updates in anaesthesia*. 2008.
98. Rigby RA and Stasinopoulos DM. Smooth centile curves for skew and kurtotic data modelled using the Box-Cox power exponential distribution. *Stat Med*. 2004;23:3053-76.
99. Rigby RA and Stasinopoulos DM. Generalized additive models for location, scale and shape. *Journal of the Royal Statistical Society: Series C (Applied Statistics)*. 2005;54:507-554.
100. STATA 12.1, StataCorp, TX, USA.
101. Hernandez-Garcia L. Arterial Spin Labeling. Functional MRI laboratory, University of Michigan. Available from: http://fmri.research.umich.edu/research/main_topics/ - artSpinLabel. [Accessed 09 December 2020].
102. Alsaedi A, Thomas D, Bisdas S and Golay X. Overview and Critical Appraisal of Arterial Spin Labelling Technique in Brain Perfusion Imaging. *Contrast Media Mol Imaging*. 2018;2018:5360375.
103. Wang J, Alsop DC, Li L, Listerud J, Gonzalez-At JB, Schnall MD and Detre JA. Comparison of quantitative perfusion imaging using arterial spin labeling at 1.5 and 4.0 Tesla. *Magnetic resonance in medicine*. 2002;48:242-54.
104. Ferre JC, Petr J, Bannier E, Barillot C and Gauvrit JY. Improving quality of arterial spin labeling MR imaging at 3 Tesla with a 32-channel coil and parallel imaging. *Journal of Magnetic Resonance Imaging*. 2012;35:1233-9.
105. Scarabino T, Pollice S and Popolizio T. High Field Brain MRI: Use in Clinical Practice. Chapter 10: ASL 30T Perfusion Studies. *Springer*. 2017.
106. Spano VR, Mandell DM, Poublanc J, Sam K, Battisti-Charbonney A, Pucci O, Han JS, Crawley AP, Fisher JA and Mikulis DJ. CO2 blood oxygen level-dependent MR mapping of cerebrovascular reserve in a clinical population: safety, tolerability, and technical feasibility. *Radiology*. 2013;266:592-8.
107. Donoghue OA, McGarrigle CA, Foley M, Fagan A, Meaney J and Kenny RA. Cohort Profile Update: The Irish Longitudinal Study on Ageing (TILDA). *Int J Epidemiol*. 2018;47:1398-1398l.
108. Smith SM and Nichols TE. Statistical Challenges in "Big Data" Human Neuroimaging. *Neuron*. 2018;97:263-268.
109. Dolui S, Wang Z, Wang DJJ, Mattay R, Finkel M, Elliott M, Desiderio L, Inglis B, Mueller B, Stafford RB, Launer LJ, Jacobs DR, Jr., Bryan RN and Detre JA. Comparison of non-invasive MRI measurements of cerebral blood flow in a large multisite cohort. *Journal of Cerebral Blood Flow and Metabolism*. 2016;36:1244-56.
110. Jefferson AL, Cambronero FE, Liu D, Moore EE, Neal JE, Terry JG, Nair S, Pechman KR, Rane S, Davis LT, Gifford KA, Hohman TJ, Bell SP, Wang TJ, Beckman JA and Carr JJ. Higher Aortic Stiffness Is Related to Lower Cerebral Blood Flow and Preserved Cerebrovascular Reactivity in Older Adults. *Circulation*. 2018;138:1951-1962.
111. Zonneveld HI, Loehrer EA, Hofman A, Niessen WJ, van der Lugt A, Krestin GP, Ikram MA and Vernooij MW. The bidirectional association between reduced

cerebral blood flow and brain atrophy in the general population. *Journal of Cerebral Blood Flow and Metabolism*. 2015;35:1882-7.
112. Santos-Galduroz RF, Bueno OF, Yamaga LI, Armani F and Galduroz JC. Influence of blood viscosity to cerebral blood flow in older humans compared to young subjects. *Clin Neurophysiol*. 2012;123:117-20.
113. de Roos A, van der Grond J, Mitchell G and Westenberg J. Magnetic Resonance Imaging of Cardiovascular Function and the Brain: Is Dementia a Cardiovascular-Driven Disease? *Circulation*. 2017;135:2178-2195.
114. Tarumi T, Ayaz Khan M, Liu J, Tseng BY, Parker R, Riley J, Tinajero C and Zhang R. Cerebral hemodynamics in normal aging: central artery stiffness, wave reflection, and pressure pulsatility. *Journal of Cerebral Blood Flow and Metabolism*. 2014;34:971-8.
115. Kroner ES, Lamb HJ, Siebelink HM, Cannegieter SC, van den Boogaard PJ, van der Wall EE, de Roos A and Westenberg JJ. Pulse wave velocity and flow in the carotid artery versus the aortic arch: effects of aging. *Journal of Magnetic Resonance Imaging*. 2014;40:287-93.
116. Tarumi T and Zhang R. Cerebral blood flow in normal aging adults: cardiovascular determinants, clinical implications, and aerobic fitness. *J Neurochem*. 2018;144:595-608.
117. Paulson OB, Strandgaard S and Edvinsson L. Cerebral autoregulation. *Cerebrovascular and brain metabolism reviews*. 1990;2:161-92.
118. Glodzik L, Rusinek H, Brys M, Tsui WH, Switalski R, Mosconi L, Mistur R, Pirraglia E, de Santi S, Li Y, Goldowsky A and de Leon MJ. Framingham cardiovascular risk profile correlates with impaired hippocampal and cortical vasoreactivity to hypercapnia. *Journal of Cerebral Blood Flow and Metabolism*. 2011;31:671-9.
119. Mitchell GF, Vita JA, Larson MG, Parise H, Keyes MJ, Warner E, Vasan RS, Levy D and Benjamin EJ. Cross-sectional relations of peripheral microvascular function, cardiovascular disease risk factors, and aortic stiffness: the Framingham Heart Study. *Circulation*. 2005;112:3722-8.
120. Miller KB, Howery AJ, Rivera-Rivera LA, Johnson SC, Rowley HA, Wieben O and Barnes JN. Age-Related Reductions in Cerebrovascular Reactivity Using 4D Flow MRI. *Frontiers in aging neuroscience*. 2019;11:281.
121. Rodriguez-Flores M, Garcia-Garcia E, Cano-Nigenda CV and Cantu-Brito C. Relationship of obesity and insulin resistance with the cerebrovascular reactivity: a case control study. *Cardiovasc Diabetol*. 2014;13:2.
122. Hurr C, Patik JC, Kim K and Brothers RM. Blunted cerebral vascular responsiveness to hypercapnia in obese individuals. *Exp Physiol*. 2017;102:1300-1308.
123. Health Service Capacity Review 2018 Executive Report. Review of Health Demand and Capacity Requirements in Ireland to 2031 - Findings and Recommendations. Available from: https://assets.gov.ie/10131/5bb5ff12463345bbac465aaf02a2333d.pdf. [Cited 2020 April 24].
124. World Health Organization. World Report on Ageing and Health. 2015. Available from: https://apps.who.int/iris/bitstream/handle/10665/186463/9789240694811_eng.pdf;jsessionid=C80C3691FF866B16A8F80CD06AC67DAA?sequence=1. [Cited 2020 April 24].
125. Howard G and Goff DC. Population shifts and the future of stroke: forecasts of the future burden of stroke. *Ann N Y Acad Sci*. 2012;1268:14-20.
126. Katan M and Luft A. Global Burden of Stroke. *Semin Neurol*. 2018;38:208-211.

127. Wimo A, Guerchet M, Ali GC, Wu YT, Prina AM, Winblad B, Jonsson L, Liu Z and Prince M. The worldwide costs of dementia 2015 and comparisons with 2010. *Alzheimers Dement*. 2017;13:1-7.
128. Han B and Haley WE. Family caregiving for patients with stroke. Review and analysis. *Stroke; a journal of cerebral circulation*. 1999;30:1478-85.
129. 2020 Alzheimer's disease facts and figures. *Alzheimers Dement*. 2020.
130. Zlokovic BV. Neurovascular pathways to neurodegeneration in Alzheimer's disease and other disorders. *Nat Rev Neurosci*. 2011;12:723-38.
131. Schuff N, Matsumoto S, Kmiecik J, Studholme C, Du A, Ezekiel F, Miller BL, Kramer JH, Jagust WJ, Chui HC and Weiner MW. Cerebral blood flow in ischemic vascular dementia and Alzheimer's disease, measured by arterial spin-labeling magnetic resonance imaging. *Alzheimers Dement*. 2009;5:454-62.
132. Alsop DC, Dai W, Grossman M and Detre JA. Arterial spin labeling blood flow MRI: its role in the early characterization of Alzheimer's disease. *J Alzheimers Dis*. 2010;20:871-80.
133. Caroli A, Testa C, Geroldi C, Nobili F, Barnden LR, Guerra UP, Bonetti M and Frisoni GB. Cerebral perfusion correlates of conversion to Alzheimer's disease in amnestic mild cognitive impairment. *J Neurol*. 2007;254:1698-707.
134. Kim SM, Kim MJ, Rhee HY, Ryu CW, Kim EJ, Petersen ET and Jahng GH. Regional cerebral perfusion in patients with Alzheimer's disease and mild cognitive impairment: effect of APOE epsilon4 allele. *Neuroradiology*. 2013;55:25-34.
135. Herholz K. PET studies in dementia. *Ann Nucl Med*. 2003;17:79-89.
136. Vemuri P and Jack CR, Jr. Role of structural MRI in Alzheimer's disease. *Alzheimers Res Ther*. 2010;2:23.
137. Guermazi A, Miaux Y, Rovira-Canellas A, Suhy J, Pauls J, Lopez R and Posner H. Neuroradiological findings in vascular dementia. *Neuroradiology*. 2007;49:1-22.
138. Haller S, Monsch AU, Richiardi J, Barkhof F, Kressig RW and Radue EW. Head motion parameters in fMRI differ between patients with mild cognitive impairment and Alzheimer disease versus elderly control subjects. *Brain Topogr*. 2014;27:801-7.
139. Preibisch C, Sorg C, Forschler A, Grimmer T, Sax I, Wohlschlager AM, Perneczky R, Forstl H, Kurz A, Zimmer C and Alexopoulos P. Age-related cerebral perfusion changes in the parietal and temporal lobes measured by pulsed arterial spin labeling. *Journal of Magnetic Resonance Imaging*. 2011;34:1295-302.
140. Lee C, Lopez OL, Becker JT, Raji C, Dai W, Kuller LH and Gach HM. Imaging cerebral blood flow in the cognitively normal aging brain with arterial spin labeling: implications for imaging of neurodegenerative disease. *J Neuroimaging*. 2009;19:344-52.
141. Zhang N, Gordon ML, Ma Y, Chi B, Gomar JJ, Peng S, Kingsley PB, Eidelberg D and Goldberg TE. The Age-Related Perfusion Pattern Measured With Arterial Spin Labeling MRI in Healthy Subjects. *Frontiers in aging neuroscience*. 2018;10:214.
142. Yezhuvath US, Uh J, Cheng Y, Martin-Cook K, Weiner M, Diaz-Arrastia R, van Osch M and Lu H. Forebrain-dominant deficit in cerebrovascular reactivity in Alzheimer's disease. *Neurobiology of aging*. 2012;33:75-82.
143. Cantin S, Villien M, Moreaud O, Tropres I, Keignart S, Chipon E, Le Bas JF, Warnking J and Krainik A. Impaired cerebral vasoreactivity to CO2 in Alzheimer's disease using BOLD fMRI. *Neuroimage*. 2011;58:579-87.
144. Vicenzini E, Ricciardi MC, Altieri M, Puccinelli F, Bonaffini N, Di Piero V and Lenzi GL. Cerebrovascular reactivity in degenerative and vascular dementia: a transcranial Doppler study. *Eur Neurol*. 2007;58:84-9.
145. Pillai JJ and Mikulis DJ. Cerebrovascular reactivity mapping: an evolving standard for clinical functional imaging. *AJNR American journal of neuroradiology*. 2015;36:7-13.

146. Romero JR, Pikula A, Nguyen TN, Nien YL, Norbash A and Babikian VL. Cerebral collateral circulation in carotid artery disease. *Curr Cardiol Rev*. 2009;5:279-88.
147. Hendrikse J, van Osch MJ, Rutgers DR, Bakker CJ, Kappelle LJ, Golay X and van der Grond J. Internal carotid artery occlusion assessed at pulsed arterial spin-labeling perfusion MR imaging at multiple delay times. *Radiology*. 2004;233:899-904.
148. Bokkers RP, van Osch MJ, van der Worp HB, de Borst GJ, Mali WP and Hendrikse J. Symptomatic carotid artery stenosis: impairment of cerebral autoregulation measured at the brain tissue level with arterial spin-labeling MR imaging. *Radiology*. 2010;256:201-8.
149. Bokkers RP, van Osch MJ, Klijn CJ, Kappelle LJ and Hendrikse J. Cerebrovascular reactivity within perfusion territories in patients with an internal carotid artery occlusion. *Journal of neurology, neurosurgery, and psychiatry*. 2011;82:1011-6.
150. Silvestrini M, Troisi E, Matteis M, Cupini LM and Caltagirone C. Transcranial Doppler assessment of cerebrovascular reactivity in symptomatic and asymptomatic severe carotid stenosis. *Stroke; a journal of cerebral circulation*. 1996;27:1970-3.
151. Oku N, Matsumoto M, Hashikawa K, Moriwaki H, Okazaki Y, Seike Y, Handa N, Uehara T, Kamada T and Nishimura T. Carbon dioxide reactivity by consecutive technetium-99m-HMPAO SPECT in patients with a chronically obstructed major cerebral artery. *J Nucl Med*. 1994;35:32-40.
152. Rothwell PM, Giles MF, Chandratheva A, Marquardt L, Geraghty O, Redgrave JN, Lovelock CE, Binney LE, Bull LM, Cuthbertson FC, Welch SJ, Bosch S, Alexander FC, Silver LE, Gutnikov SA, Mehta Z and Early use of Existing Preventive Strategies for Stroke s. Effect of urgent treatment of transient ischaemic attack and minor stroke on early recurrent stroke (EXPRESS study): a prospective population-based sequential comparison. *Lancet*. 2007;370:1432-42.
153. Easton JD, Saver JL, Albers GW, Alberts MJ, Chaturvedi S, Feldmann E, Hatsukami TS, Higashida RT, Johnston SC, Kidwell CS, Lutsep HL, Miller E, Sacco RL, American Heart A, American Stroke Association Stroke C, Council on Cardiovascular S, Anesthesia, Council on Cardiovascular R, Intervention, Council on Cardiovascular N and Interdisciplinary Council on Peripheral Vascular D. Definition and evaluation of transient ischemic attack: a scientific statement for healthcare professionals from the American Heart Association/American Stroke Association Stroke Council; Council on Cardiovascular Surgery and Anesthesia; Council on Cardiovascular Radiology and Intervention; Council on Cardiovascular Nursing; and the Interdisciplinary Council on Peripheral Vascular Disease. The American Academy of Neurology affirms the value of this statement as an educational tool for neurologists. *Stroke; a journal of cerebral circulation*. 2009;40:2276-93.
154. Zaharchuk G, Olivot JM, Fischbein NJ, Bammer R, Straka M, Kleinman JT and Albers GW. Arterial spin labeling imaging findings in transient ischemic attack patients: comparison with diffusion- and bolus perfusion-weighted imaging. *Cerebrovasc Dis*. 2012;34:221-8.
155. Qiao XJ, Salamon N, Wang DJ, He R, Linetsky M, Ellingson BM and Pope WB. Perfusion deficits detected by arterial spin-labeling in patients with TIA with negative diffusion and vascular imaging. *AJNR American Journal of Neuroradiology*. 2013;34:2125-30.
156. Krainik A, Villien M, Tropres I, Attye A, Lamalle L, Bouvier J, Pietras J, Grand S, Le Bas JF and Warnking J. Functional imaging of cerebral perfusion. *Diagnostic and interventional imaging*. 2013;94:1259-78.
157. Yun TJ, Sohn CH, Han MH, Yoon BW, Kang HS, Kim JE, Paeng JC, Choi SH, Kim JH and Chang KH. Effect of carotid artery stenting on cerebral blood flow:

evaluation of hemodynamic changes using arterial spin labeling. *Neuroradiology*. 2013;55:271-81.
158. Goode SD, Altaf N, Auer DP and MacSweeney ST. Carotid endarterectomy improves cerebrovascular reserve capacity preferentially in patients with preoperative impairment as indicated by asymmetric BOLD response to hypercapnia. *Eur J Vasc Endovasc Surg*. 2009;38:546-51.
159. Burdette JH, Laurienti PJ, Espeland MA, Morgan A, Telesford Q, Vechlekar CD, Hayasaka S, Jennings JM, Katula JA, Kraft RA and Rejeski WJ. Using network science to evaluate exercise-associated brain changes in older adults. *Frontiers in aging neuroscience*. 2010;2:23.
160. Erickson KI, Voss MW, Prakash RS, Basak C, Szabo A, Chaddock L, Kim JS, Heo S, Alves H, White SM, Wojcicki TR, Mailey E, Vieira VJ, Martin SA, Pence BD, Woods JA, McAuley E and Kramer AF. Exercise training increases size of hippocampus and improves memory. *Proc Natl Acad Sci U S A*. 2011;108:3017-22.
161. Heo S, Prakash RS, Voss MW, Erickson KI, Ouyang C, Sutton BP and Kramer AF. Resting hippocampal blood flow, spatial memory and aging. *Brain Res*. 2010;1315:119-27.
162. Chapman SB, Aslan S, Spence JS, Hart JJ, Jr., Bartz EK, Didehbani N, Keebler MW, Gardner CM, Strain JF, DeFina LF and Lu H. Neural mechanisms of brain plasticity with complex cognitive training in healthy seniors. *Cerebral Cortex*. 2015;25:396-405.
163. Elias MF, Robbins MA, Budge MM, Abhayaratna WP, Dore GA and Elias PK. Arterial pulse wave velocity and cognition with advancing age. *Hypertension*. 2009;53:668-73.
164. Laurent S, Boutouyrie P, Asmar R, Gautier I, Laloux B, Guize L, Ducimetiere P and Benetos A. Aortic stiffness is an independent predictor of all-cause and cardiovascular mortality in hypertensive patients. *Hypertension*. 2001;37:1236-41.
165. Laurent S, Katsahian S, Fassot C, Tropeano AI, Gautier I, Laloux B and Boutouyrie P. Aortic stiffness is an independent predictor of fatal stroke in essential hypertension. *Stroke; a journal of cerebral circulation*. 2003;34:1203-6.
166. van Elderen SG, Brandts A, Westenberg JJ, van der Grond J, Tamsma JT, van Buchem MA, Romijn JA, Kroft LJ, Smit JW and de Roos A. Aortic stiffness is associated with cardiac function and cerebral small vessel disease in patients with type 1 diabetes mellitus: assessment by magnetic resonance imaging. *Eur Radiol*. 2010;20:1132-8.
167. Wardlaw JM, Valdes Hernandez MC and Munoz-Maniega S. What are white matter hyperintensities made of? Relevance to vascular cognitive impairment. *J Am Heart Assoc*. 2015;4:001140.
168. Kim T, Richard Jennings J and Kim SG. Regional cerebral blood flow and arterial blood volume and their reactivity to hypercapnia in hypertensive and normotensive rats. *Journal of Cerebral Blood Flow and Metabolism.* 2014;34:408-14.
169. Liu M, Li GL, Li Y and Wang JG. Effects of Various Antihypertensive Drugs on Arterial Stiffness and Wave Reflections. *Pulse (Basel)*. 2013;1:97-107.
170. Efimova IY, Efimova NY, Triss SV and Lishmanov YB. Brain perfusion and cognitive function changes in hypertensive patients. *Hypertens Res*. 2008;31:673-8.
171. Li C, Engstrom G, Hedblad B, Berglund G and Janzon L. Blood pressure control and risk of stroke: a population-based prospective cohort study. *Stroke; a journal of cerebral circulation*. 2005;36:725-30.
172. Leenen FHH, Blaustein MP and Hamlyn JM. Update on angiotensin II: new endocrine connections between the brain, adrenal glands and the cardiovascular system. *Endocr Connect*. 2017;6:R131-R145.
173. Chaudhary S, Scouten A, Schwindt G, Janik R, Lee W, Sled JG, Black SE and Stefanovic B. Hemodynamic effects of cholinesterase inhibition in mild Alzheimer's disease. *Journal of Magnetic Resonance Imaging*. 2013;38:26-35.

174. de la Torre JC. Cerebral Perfusion Enhancing Interventions: A New Strategy for the Prevention of Alzheimer Dementia. *Brain Pathol*. 2016;26:618-31.
175. Meyer AA, Kundt G, Lenschow U, Schuff-Werner P and Kienast W. Improvement of early vascular changes and cardiovascular risk factors in obese children after a six-month exercise program. *J Am Coll Cardiol*. 2006;48:1865-70.
176. Bar KJ, Boettger MK, Seidler N, Mentzel HJ, Terborg C and Sauer H. Influence of galantamine on vasomotor reactivity in Alzheimer's disease and vascular dementia due to cerebral microangiopathy. *Stroke; a journal of cerebral circulation*. 2007;38:3186-92.
177. Chen JJ. Cerebrovascular-Reactivity Mapping Using MRI: Considerations for Alzheimer's Disease. *Frontiers in aging neuroscience*. 2018;10:170.